# Preparation of Functional Cellulose Particles

Omura, Taro

(Degree)
博士（工学）

(Date of Degree)
2020-03-25

(Date of Publication)
2021-03-01

(Resource Type)
doctoral thesis

(Report Number)
甲第7778号

(URL)
https://hdl.handle.net/20.500.14094/D1007778

博士論文

# Preparation of Functional Cellulose Particles

機能性セルロース粒子の創製

令和 2 年 1 月

神戸大学大学院工学研究科

大村　太朗

**Taro OMURA**

# Acknowledgement

This doctoral thesis is the research, which was carried out at *Soft Matter Interface Laboratory (SMIL:-)*, Department of Chemical Science and Engineering, Graduate School of Engineering, Kobe University.

I would like to express greatest gratitude to my supervisor Prof., Dr. Hideto Minami for sincere encouragement, in-depth and fruitful support to get more understanding of research subject from beginning to end, and giving me a lot of chances.

I would like to show deep appreciation to Assistant Prof., Dr. Toyoko Suzuki for tremendous and technical support, useful advices, and encouragement throughout this study.

I acknowledge their contribution to *The Cellulose Team*: Mr. Keigo Shimomura, Mr. Kyosuke Kono, Mr. Yasuhito Ihara, Ms. Kaori Imagawa, and Ms. Yuki Fujii for enormous suggestion and assistance of this study. Without their support, it would not have been possible to finish my doctoral dissertation.

I would like to offer my special thanks to Assistant Prof., Dr. Yukiya Kitayama, Dr. Keigo Kinoshita, Dr. Masayoshi Tokuda, and Dr. Wei Li for valuable discussions, advices, and constant encouragement.

I received generous support, valuable advice and discussion from Mr. Satoshi Ikubo, Mr. Ryuma Nakamura, Mr. Takuto Ouchi, Ms. Aya Kurozuka, and Mr. Hiroki Mitsui.

I appreciate to Ms. Chihiro Hayashi, Mr. Shuichiro Mizuhara, and Mr. Mitsuyoshi Yamane for their grateful friendship, continuous support and good times we shared.

I would like to thank for friendship and many supports to Mr. Hirotoshi Ienaga, Mr. Takanori Nakano, Mr. Junichi Tsukiji, Mr. Daiki Tsujita, Mr. Ken Mukai, Ms. Miku Onishi, Mr. Yuya Takeuchi, and Ms. Mana Fujii.

I also would like to express the deepest appreciation to Prof., Dr. Per B. Zetterlund. He gave me fruitful discussion and constant encouragement while I researched at Centre of Advanced Macromolecular Design (CAMD) in University of New South Wales.

I would like to express their gratitude to CAMD members, especially Mr. Eh Hau Pan, Dr. Florent Jasinski, Dr. Neomy Zaquen, Dr. Sivaprakash Shanmugam (Siva), Dr. Noor

Hadzuin Nik Hadzir (Awin), Dr. Victoria Teo, Dr. Ka Wai Fan, Dr. Jiangtao Xu (Jason), Dr. Fumi Ishizuka, Ms. Yasemin Fadil, Mr. Daniele Melodia and I really had a wonderful time for almost 1 year in Sydney thanks to everyone.

I would like to thank friends at *SUZUKI Daisuke Lab* in Shinshu University, Mr. Takumi Watanabe, Ms. Seina Hiroshige, Mr. Yuichiro Nishizawa, and Mr. Kenshiro Honda, for their friendship and encouragement.

I owe a very important debt to Research Fellowships of Japan Society for the Promotion of Science (JSPS) for Young Scientists and Scholarship of Japan Student Services Organization (JASSO) for their financial support.

Finally, I deeply express my appreciation to my parents Kiyotaka Omura and Yurie Omura, and my sister Asuka (Omura) Suzuki for their constant encouragement and affection.

January 2020

Taro OMURA

# Contents

# General introduction

Since the development of synthetic resins at the beginning of 20th century have made conditions of human life more abundant, synthetic organic polymers are absolutely necessary for human society. The synthetic resins are derived from natural organic materials — coals and natural gas, — and crude oil by produced by polymerization method, and they are used as diverse items, including bottles, straws, bags, and food packaging.

Polymer particles are particulate of resins, prepared by mainly heterogeneous polymerization systems.[1-3] The polymer particles have been used as film in many industrial fields as paints,[4] coating,[5, 6] and adhesives.[7] Nowadays, much attention has been focused on applying them directly as particulate materials for electronics,[3] cosmetics,[8] and biomedical[9] fields owing to their improvements in particle quality and functionality. However, such polymer particles are composed of persistent polymers, including polyethylene (PE),[10, 11] polypropylene (PP),[12, 13] polystyrene (PS),[14] and poly(methyl methacrylate) (PMMA),[15] with an estimated lifetime for degradation of hundreds of years, possibly leading to negative impact the marine environment, the food chain, and human health. Therefore, it is necessary for development of more environmentally sustainable alternatives to synthetic polymer particles.

Lignocellulosic biomass is the most abundant natural material on the Earth. It is mainly composed of cellulose, hemicellulose, which are carbohydrate polymers; lignin, a heterogeneous cross-linked aromatic polymer; and pectin along with minor amounts of small molecular weight chemicals.[16] The composition is up to the origin and the species of the lignocellulosic biomass: for instance, hard-wood stems are composed of 40–50% of cellulose,

24–40% hemicellulose, and 18–25% lignin, while soft-wood stems contain 45–50%, 25–35%, and 25–35%, respectively.[16] Thus, these components are often separated into individuals for desired materials.

As mentioned above, cellulose is one of the prime component of lignocellulosic biomass and the most abundant biopolymer on the planet with an estimated global production of $1.5 \times 10^{12}$ tons per year.[17] Moreover, it has many attractive properties such as thermal and chemically stability, nontoxicity, biocompatibility, and biodegradability.[18] Thus, there are a lot of cellulose-based products[19] by industry and used such as pulp,[20, 21] paper[22], food, and cosmetics.[23] Recently, cellulose particles have been recognized as functional materials[24] for use in many applications, such as removers for organic chemicals or metal, chromatography, protein immobilization, and drug delivery. owing to their excellent characteristics, including a low nonspecific adsorption of proteins[25] and the availability of surface modifications,[26, 27] in addition to the above-mentioned properties. Therefore, cellulose particles have a great potential for alternatives to conventional polymer particles and promising functional materials.

In the following sections, I will give overviews of *Cellulose*, *Dissolution of Cellulose*, and *Cellulose Particles*, and there I will explain why this doctoral dissertation's topic is morphology control and functionalization of cellulose particles and why it is important.

## *1. Cellulose*

### *1.1 Molecules*

Cellulose is a linearly polysaccharide homopolymer made of $\beta$-1,4-linked anhydro-D-glucopyranose unit (AGU), in which the 1st carbon on one glucose ring is linked the 4th carbon

on its neighbors by acetal linkage.[17] Owing to this *β*-linkage, each AGU unit is rotated 180° compared to the neighbor unit. The repeating unit, a dimer of glucose, are known as cellobiose. The chain length — The number of glucose unit or the degree of polymerization (*DP*) — of cellulose polymer varies and is up to $1.5 \times 10^4$,[28] which depend on its source and can change by the chemical pre-treatment: natural sources of cellulose typically have very high *DP*s, while isolated or treated cellulose sources shows lower *DP*s.[28, 29]

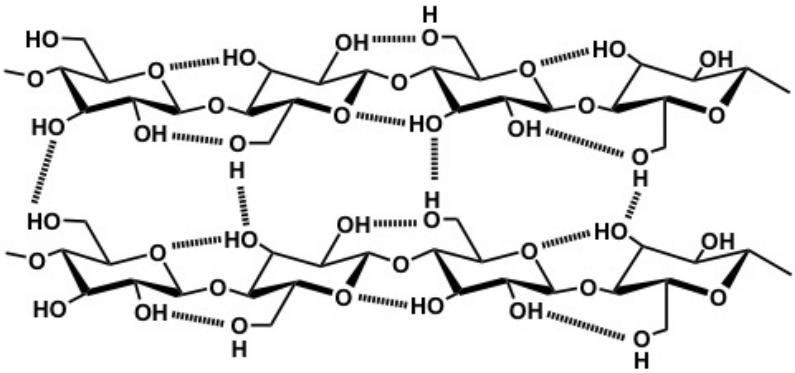

**Scheme 1.** Structure of cellulose molecules and hydrogen network (Cellulose I).

Each AGU possesses three hydroxyl groups: the primary hydroxyl group is present at C6 position and the secondary groups are at C2 and C3. Since all AGU has a $^4C_1$ chair conformation, all three available hydroxyl groups position in the equatorial direction while the carbon-hydrogen bonds lie in the axial direction.[30] Therefore, a cellulose molecule has a structural and chemical anisotropy, that is polar (hydrophilic) domain in the equatorial plane and non-polar (hydrophobic) domain in the axial plane, resulting in their amphiphilic character.[31, 32]

In cellulose molecules, there are two kinds of hydrogen bonds, intra- and intermolecular hydrogen bond, formed by hydroxyl groups.[30] Intramolecular hydrogen bond is

typically formed between C2 and C6 hydroxyl groups, and C3 hydroxyl group and hemiacetal oxygen, which is on horizontally adjacent AGU on the same polymer chain. On the other hand, C3 and C6 hydroxyl groups form an intermolecular hydrogen bond between laterally adjacent AGU in different cellulose chains. The intramolecular hydrogen bonds cause cellulose molecules relatively stiff and rigid, leading to a high tendency to crystallize and to form fibrils and fibers.

### *1.2 Structures*

Cellulose has four different polymorphs, cellulose I, II, III, and IV.[33] Natural cellulose is composed of crystalline and amorphous regions, and the crystalline region is cellulose I. The molecule chains in cellulose I lies in a parallel arrangement in a planer sheet-like structure. Intermolecular hydrogen bonds in the structure are parallel to pyranose rings. In addition, there are no hydrogen bonds, but hydrophobic interaction and van der Waals force between each sheet structure. Attalla and VanderHart[34-36] first analyzed native (*Valonia*) cellulose in detail using $^{13}C$ NMR with CP/MAS technique, which revealed that each native cellulose is a composite of two different crystalline polymorphs, Iα and Iβ. Moreover, they and other researchers showed that cellulose Iα is main component in bacterial[28] and algal[37] celluloses, whereas higher plants,[38] such as ramie and cotton, celluloses are dominated by Iβ. The cellulose Iα structure is metastable and can be converted irreversibly in the cellulose Iβ which is the more thermodynamically stable.[39] The major difference of two structure is cellulose Iα is a triclinic phase[40] while cellulose Iβ is a monoclinic phase.[41]

Upon mercerization[42, 43] or dissolution/regeneration[44] of cellulose I, cellulose II (which are called mercerized cellulose and regenerated cellulose, respectively) can be obtained. This

process is irreversible[39] and the chain arrangement changes from parallel packing to antiparallel packing.[43, 45] In cellulose II, there are not only intra- and intermolecular hydrogen bonds but also hydrogen bonds between cellulose chain sheets. Cellulose II has a zigzag sheet structure, which is different from that of cellulose I.

Cellulose I and II transform into cellulose $III_I$ and $III_{II}$, respectively, by liquid ammonia[46-49] or amine/diamine[50, 51] treatments with passing through ammonia–or (di)amine–cellulose complexes which are intermediates. Since both the cellulose III is metastable,[52] these conversions are reversible by hydrothermal[47] or thermal treatment[49], except for the transformation from cellulose Iα into cellulose $III_I$. The X-ray diffraction study suggests that cellulose $III_I$ and $III_{II}$ have the same unit cell containing two cellulose chain; however, the chains are packed in parallel for cellulose $III_I$ and in antiparallel for cellulose $III_{II}$.[52] Moreover, the conformation of the chains in cellulose $III_I$ has features, including zigzag sheet network, similar to that of the center chain in the highly stable cellulose II allomorph.[53]

Cellulose IV also has two types, cellulose $IV_I$ and $IV_{II}$, which are transformed from cellulose $III_I$ and cellulose $III_{II}$ by a heat treatment in glycerol at 260°C.[54] However, the reinvestigation of cellulose $IV_I$ structure reveals that cellulose $IV_I$ is analogous to cellulose $I_\beta$ structure and there it is concluded that cellulose $IV_I$ is cellulose $I_\beta$ which contains lateral disorder.[53] On the other hand, pure cellulose $IV_{II}$ can be obtained from a dilute solution of low-*DP* cellulose triacetate, followed by the deacetylation and precipitation at temperatures between 150 and 160°C.[55] However, the detailed structure of cellulose $IV_{II}$ has not been clear.

### *1.3 Morphology*

Native cellulose is known as a complex hierarchy which is composed of fibrillary elements. The elementally fibril (microfibril) composed of dozens of cellulose molecules is recognized as the smallest unit with size between ca. 3-30 nm depending on the source. The microfibril can be divided into crystalline and amorphous regions. The investigations of the *DP*s and the profiles of neutron small angle scattering of chemical treated cellulose shows that the crystal domain is composed of 200-300 residues, which decrease to an order of magnitude owing to dissolution/regeneration; on the other hand, the amorphous region is composed of 4 or 5 residues.

## *2. Dissolution of Cellulose*

In order to process cellulose into materials, cellulose must be dissolved to form a homogeneous solution; however, as mentioned above sections, owing to a strong intra- and intermolecular hydrogen bond network, cellulose is insoluble in most common solvents. The first attempts to dissolve cellulose or cellulose-containing materials were conducted in 1850s.[56]

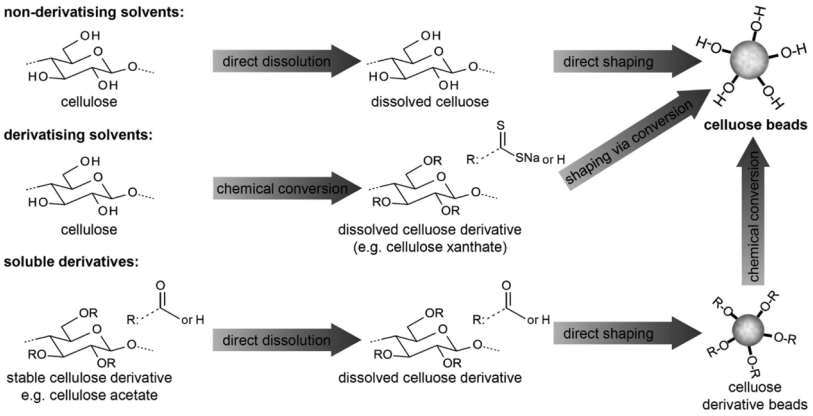


**Scheme 2.** General route for dissolution of cellulose and shaping into beads (particles). Adapted with permission form ref 24. Copyright 2013 American Chemical Society.

Since then various kinds of solvent for dissolving cellulose have been historically employed and discovered. In general, cellulose solvents are categorized as either derivatizing solvent and non-derivatizing solvent (**Scheme 2**). Derivatizing solvents are the solvents which chemically react with cellulose to form the soluble intermediate or stable derivative. On the other hand, non-derivatizing solvents are the class of solvents which can directly dissolve cellulose without any intermediates; however, both methods are correlated to the cleavage of hydrogen bonds, resulting in the dissolution of cellulose.

### *2.1 Derivatizing Solvents*

#### *2.1.1 $HNO_3/H_2SO_4$*

The first derivative cellulose for dissolving cellulose is cellulose (tri)nitrate which was unexpectedly obtained by the reaction of cotton and $HNO_3/H_2SO_4$, discovered by Christian Friedrich Schoenbein in 1845.[56] It is soluble in diethyl ether and ethanol. After that, John Wesley Hyatt invented *Celluloid*, which are consider to be the first man made plastic, prepared by mixing a solid cellulose nitrate and camphor. Moreover, Joseph Swan discovered how to de-nitrate the cellulose nitrate using ammonium bisulfate, and Frenchman Count Louis-Marie-Hilaire Berniguad, Comte de Chardonnet, developed the de-nitration further and produced the first artificial cellulose fibers.[56] However, this process has the drawbacks such as slow operation, difficulty in scale up safely due to its inflammability, and uneconomic.

#### *2.1.2 $N_2O_4$/DMF*

A mixture of *N,N*-dimethylformamide (DMF)/$N_2O_4$ is a solvent to prepare unstable cellulose nitrate, and subsequently it can be reacted with sulphur tri- or dioxide to eliminate

nitro groups and to form cellulose sulphates.[57] Though cellulose sulfate is soluble in water, DMF/$N_2O_4$ is highly toxic in nature.

### *2.1.3 NaOH/$CS_2$/$H_2O$ (Viscose process)*

In 1891, Charles Cross, Edward Bevan, and Clayton Beadle in England discovered the dissolution process for cotton or wood cellulose as cellulose xanthate: where cellulose is treated with sodium hydroxide (NaOH) dissolved in water, and then derivatizing the alkali-activated cellulose with carbon disulphide ($CS_2$) leading to a highly viscose sodium xanthogenate solution (called "viscose").[56] The solution is later treated with an acidic solution to convert back to pure cellulose. This is the most important and the oldest process, *viscose process*, currently used to produce cellulose fibers, and still now is a subject of research.[58] Since $CS_2$ is high toxic, *ca.* 70–75% $CS_2$ is recycled in this process. However, waste water, alkali, acid, and exhaust air containing hydrogen sulphide (that is also highly toxic) cause serious environment problems.

### *2.1.4 NaOH/molten urea/$H_2O$*

In order to reduce the environment impact of dissolving cellulose, an attractive alternative for viscose process, cellulose carbamate system, was exploited by Kemira Oy Saeteri and Neste Oy[59, 60]. This system is based on the original work discovered by Hill and Jacobsen: alkali-activated cellulose is mixed with urea at an elevated temperature, leading to decomposition of urea into isocyanic acid and ammonia. The isocyanic acid with high reactivity forms carbamate with hydroxyl groups of cellulose, and the formed cellulose carbamate is easily dissolved in dilute NaOH.[61]

*2.1.4 Others*

Cellulose acetate (CA) is one of the popular deirivative cellulose which was first prepared by Paul Schuetzenberger in 1865.[56] CA is obtained by esterification of cellulose with acetic acid and acetic anhydrate in the presence of sulfuric acid, resulting in substitution of acetyl groups for the hydroxyl groups of cellulose. The degree of substitution (DS) can be controlled and it changes the physical properties of CA such as hydrophobicity[62] and viscosity.[63] Compared with cellulose xanthate and cellulose carbamate, CA is rather stable derivative which can be isolated, purified, and stored after the preparation. However, if a pure cellulose material is necessary, an additional processing step (saponification) is required to convert CA into pure cellulose using an aqueous NaOH.

Concentrated phosphoric acid ($H_3PO_4$), phosphorous oxychloride/pyridine, and urea/ $H_3PO_4$ are solvents for cellulose where the hydroxyl groups at the C6 position is selectively converted into phosphate groups.[64-66] Cellulose phosphate is the attractive derivative due to their inherent flame resistance and ion exchange capability.

It is well known that cellulose reacts with formic acid at room temperature (*r.t.*), resulting in formation of cellulose formate (CF) during dissolution. The reaction is promoted using catalysis such as sulphuric acid and zinc chloride ($ZnCl_2$). The solubility of CF depends on the DS: CF with a DS of about 0.6 and 1.2 can be soluble in DMSO, and DMF and DMA, respectively.[67, 68]

## *2.2 Non-derivatizing Solvents*

*2.2.1 Schweizer's Reagent*

In 1857, Matthias Eduard Schweizer discovered that cotton can be dissolved in a solution of copper salts and ammonia (an aqueous solution of cuprammonium hydrxide), and

subsequently regenerated in an acidic coagulation bath.[69] The reagent is the chemical complex of tetraaminediaquacopper dihydroxide, $[Cu(NH_3)_4(H_2O)_2](OH)_2$, of which aqueous solution is often called cuoxam. The cuoxam dissolve cellulose by deprotonating and coordinately binding the deprotonated hydroxyl groups at the C2 and C3 positions of AGU.[70] Today there are also other metal complexing agent,[71] containing mainly a transition metal and an amine or ammonium component such as Cuen,[72] Nioxam (Ni ion)[71] and Cadoxen (Cd ion).[73] These are very useful tool for the analysis of cellulose, contributing the Nobel Prize in 1953 won by Hermann Staudinger.

### *2.2.2 NaOH/$H_2O$*

Aqueous alkali (base) solutions, such as an aqueous solution of NaOH, have long been known as mercerization agents and as dissolution solvents. Sobue et al.[74] established the ternary phase diagram for cellulose/NaOH/$H_2O$, and they suggested that that there is a cellulose soluble region in the phase diagram where NaOH concentration is 7 – 10 wt% below 268 K. Dissolution capability depends on molecular weight, crystalline polymorph, and degree of crystallinity of cellulose. Isogai et al.[75] reported that low *DP* (up to 200) celluloses (microcrystalline cellulose), prepared by hydrolysis of linter celluloses and kraft pulps, can be completely dissolved in cold aqueous solutions of NaOH. On the other hand, native linter celluloses and kraft pulps with high DPs have limited solubility value (ca. 30 wt%); however, the regenerated celluloses from the linter and kraft celluloses can be completely dissolved regardless of their *DP*s and degree of crystalline. This solution system of NaOH/$H_2O$ have developed the shape control of cellulose materials, although it has limited for dissolving cellulose above described.

*2.2.3 NaOH (LiOH)/urea/$H_2O$*

Recently, a number of reports on mixtures of an aqueous base solution and (thio)urea has been submitted. In 2000, Zhang et al.[76] discovered that only the addition of 2 – 4 wt% of urea remarkably improved the solubility of cellulose in 6 – 8 wt% aqueous solutions of NaOH without the cellulose gels. Moreover, the transparent solution dissolving cellulose completely were obtained within 2 min when the aqueous solution of 7.5 wt% NaOH/11 wt% urea was precooled to –10°C.[77, 78] Nowadays, to overcome their disadvantages[79, 80] such as unstable and sensitive to temperature, polymer concentration, and storage time, LiOH/urea[81, 82] and NaOH/thiourea[83] system have been exploited.

*2.2.4 $LiX \cdot nH_2O$ ($X = I^-, NO_3^-, CH_3CO_2^-, ClO_4^-$)*

In 1912, Weimarn[84] reported on the dissolution ability of concentrated aqueous solutions of inorganic salts. Later, in 1932, Letters described that cellulose swelling occurred in aqueous solution of 55 wt% $ZnCl_2$, and that cellulose dissolved in 63 wt% solutions.[85] After these reports, many researchers developed the inorganic salt solution system,[86-88] including $Ca(SCN)_2/H_2O$, $LiSCN/H_2O$, and melt NaSCN/KSCN with additives. In recent years, such inorganic molten salt hydrate or mixtures with these compounds have been reinvestigated and regarded as new efficient solvents for cellulose:[89-91] $Ca(SCN)_2 \cdot 3H_2O$ could dissolve cellulose in the temperature range from 120 to 140°C within 40 min.[87] Among them, the low molten compounds of the general formula $LiX \cdot nH_2O$ ($X = I^-, NO_3^-, CH_3CO_2^-, ClO_4^-$) were also investigated, and especially $LiClO_4 \cdot 3H_2O$ and $LiI \cdot 2H_2O$ are the sufficient solvents which did not lead to a decomposition of cellulose but to a decrease in *DP*.[89, 90] However, it was found

that a high excess of reagent is necessary for cellulose dissolution due to the water promoting side reactions.

### *2.2.5 LiCl/DMAc*

As mentioned above, it has been proven that Li cations play a specific role for dissolution for cellulose in aqueous solution systems; however, Li cations can be applied to non-aqueous solution systems. In 1979, Charles McCormick et al.[92] discovered LiCl/*N,N*-dimethylacetamide (DMAc), which can dissolve cellulose without or at least with negligible degradation resulting a colorless solution.[93] Therefore, it is used still widely as a solvent for the analysis of cellulose by $^{13}$C-nuclear magnetic resonance (NMR) spectroscopy,[94] gel permeation chromatography (GPC),[95] electrospray mass spectroscopy (ESI-MS),[96] and static light scattering (SLS).[97] Cellulose can be dissolved up to 16 wt% with minimum tine (4 – 6 h) and temperature (85°C) by the optimized process. The dissolution mechanism is still research topic and different solvent-cellulose structures have been proposed: $^{13}$C NMR results of cellulose dissolved in LiCl/DMAc by El-Kafrawy[94] pointed the exsistance of a cellulose–LiCl–DMAc complex where the Li cations is strongly bound to the DMAc carboxyl oxygen and where the Cl anion breaks the hydrogen bond network of cellulose molecules; while Balasubramanian et al.[98] showed the existence of Li–DMAc macro cations acting as the counter ion of Cl anions which get accumulated along the cellulose chain. Then, the cellulose molecules result in aniocally charged polymer, causing the polymer forced apart from each other due to charge repulsion. However, the disadvantage of the LiCl/DMAc process is that, cellulose should be activated before being dissolved, which makes it expensive and time-consuming.[99] Additionally,

DMAc combining with LiCl is highly toxic, corrosive, and volatile, causing health and environment damages. Thus, the LiCl/DMAc process has not been commercialized.[58]

### *2.2.6 NMMO·$H_2O$ (Lyocell Process)*

Monohydrated *N*-methylmorpholine-*N*-oxide (NMMO) is currently the most used solvent for cellulose in industry.[58] The optimized process using this solvent for manufacturing cellulosic fibers is called Lyocell process. The first attempt to dissolve cellulose was conducted using different tertiary amine oxide in 1936 and 1939 by Gränacher and Sallmann.[100] Later, in 1980s, Chanzy et al.[101, 102] investigated the crystallization and melting behavior of the cellulose/NMMO·$H_2O$ system by differential scanning calorimetry, optical and electron microscopy, and x-ray scattering. This work contributed the development of NMMO·$H_2O$ system and is basis of the Lyocell process. In cellulose/NMMO solution, the hydrogen bond network of cellulose molecules is disrupted and there are strong donate-accepter interactions between the N→O dipole and the hydroxyl groups of the cellulose.[103] The dissolution behavior of cellulose in NMMO·$H_2O$ changes with initial water content;[104] the dissolution ability of NMMO decreases with increase in water content (two or more water molecules).[105] However, the disadvantage of this solvent system is that: there is a probability of dangerous run-away reaction at high temperature owing to its chemical instability.[100]

### *2.2.9 Ionic Liquid*

Ionic liquids (ILs) are defined as the salts composed of organic cations and (in)organic anions with melting points (m.p.) around or below 100°C.[106] The first IL is ethylammonium nitrate (m.p. 13–14°C), which were observed and characterized by Paul Walden in 1914;[107]

however, at the time, this report did not attract attentions. By 1980s, the various ILs, composed of alkylpyridinium or alkylimidazolium cations with halide or aluminium(III) chloride[108] anions were synthesized and utilized as electrodepositions[109, 110] and battery electrolytes.[111] However, all choloroaluminate(III) IL have a disadvantage; that is their instability under air and humid condition. In 1992, Wilkes and Zawarotko[112] reported the air and water stable ILs under ambient condition, 1-ethyl-3-methylimidazolium tetrafluoroborate or acetate ([Emim]$BF_4$ or [Emim]Ac). Since then, ILs have been attracting attentions and a large number of ILs have reported.[113-117]

Among these history, the first ILs as cellulose solvent was reported in 1934. The ILs, which were halides salt of nitrogen-containing bases such as benzylpyridinium chloride, were mixed with cellulose at 110–115°C, and the cellulose solution obtained. However, the cellulose solutions contained the cellulose having very reactive forms. In 2002, Rogers et al.[118] firstly reported that the ionic liquid, 1-butyl-3-methylimidazolium chloride ([Bmim]Cl) can dissolve cellulose under mild heat treatment without any activation or pretreatment. They also reported the dissolution mechanism of cellulose in [Bmim]Cl by using $^{13}C$ and $^{35/37}Cl$ NMR relaxation technique:[119] there are stoichiometric hydrogen bonding between the hydroxyl protons of cellulose and the chloride anions of the IL. Thereafter, ILs have been recognized as new cellulose solvents and various ILs have been used such as 1-ethyl-3-methylimidazolium acetate ([Emim]Ac) and 1-allyl-3-methylimidazolium chloride ([Amim]Cl).[120-123]

Recently, dissolution mechanism using imdazolium-type IL have been clarified by various equipment. By using molecular dynamic simulations and NMR, IL anions associates with the hydroxyl groups of cellulose strongly by hydrogen bonds becaue IL anion has high accepting capablity of hydrogen bonds. This anion–hydroxyl group interactions may be leaded

by the van der Waals interactions of the imdazolium rings of IL cations with suger ring of cellulose molecule; IL cations may work donor in hydrogen bonds.

One of the benefits of substituting traditional solvents, most of which are composed of volatile organic compounds (VOCs) or harmful inorganic chemicals, with ILs is their non-volatility, preventing the emission of VOCs and the toxic inorganic chemicals. Moreover, because of the property, ILs would be recycled.

## *3. Cellulose Particles*

Cellulose-based materials have interested in many scientists working in the various fields, including chemistry, chemical engineering, biochemistry, and medicine, due to its excellent properties.[124] Cellulose particles have also been focused on because they have the properties derived from particulate form, such as high specific surface area, availability of surface modifications, and ease of handling in emulsion state. The first report about preparation of cellulose particle was described by O'Neil et al. in 1951.[125] They dropped a viscose solution into an aqueous coagulating bath to obtain cellulose materials, named cellulose pellets. Since this report, various methods for preparation of cellulose particles have been developed.[24]

### *3.1 Preparation of Cellulose Particles*

All methods are composed of three common steps (**Scheme 3**): (i) dissolution of cellulose (or derivatization of cellulose), (ii) shaping the solution into particle form, (iii) solidification of the drops (or droplets) into the particles. In my best knowledge, the preparation methods can be divided into three classes.

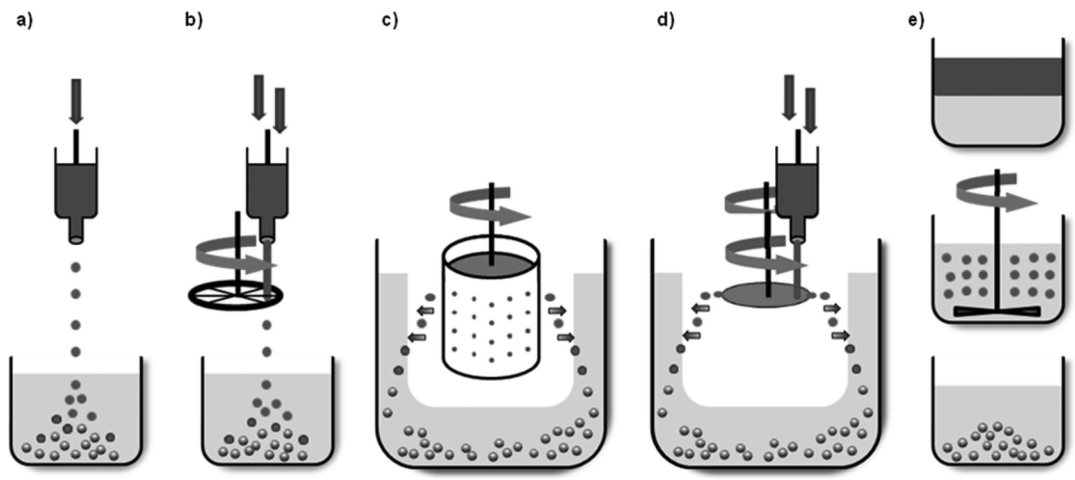


**Scheme 3.** Schematic drawings of different procedures for the preparation of cellulose beads (particles) by different techniques: dropping (a), jet cutting (b), spinning drop atomization (c), spinning disc atomization (d), and dispersion (e). Adapted with permission form ref 24. Copyright 2013 American Chemical Society.

*3.1.1 Dropping Methods*

In this method, cellulose particles are prepared by ejecting a cellulose solution in spherical shape with a thin opening, such as a capillary tube or a syringe nozzle,[126, 127] into a coagulation bath. A spherical shape droplet is formed before contacting the coagulation bath when the combined force of gravity and ejection pressure exceeds a certain value which is determined by the surface tension of cellulose solution and the capillary force at the outlet;[128] however, the particle become a flat shape when the mechanical stability of the droplets is lower than the force acting the droplets at the time of hitting the surface of the coagulation bath. In fact, particles shapes obtained by this method are effected by various factor, including ejection pressure (speed), viscosity of cellulose solution, falling height.[129] Thus, the preparation condition should be optimized to obtain the particles in a planned shape. Moreover, the size range of particle diameter is approximately from 0.5–3 mm which is depended on an inner

diameter of a capillary tube, viscosity of cellulose solution, and dropping device (syringes, vibrating nozzles or air jets).[129-131]

### *3.1.2 Dispersion Methods*

There are two steps in dispersion methods, emulsification and solidification:[24] a cellulose solution is dispersed in an immiscible solvent containing a stabilizer for droplets by using a homogenizer or a ultrasonication, resulting in the formation of emulsion. The droplets of the solution containing dissolved cellulose can be solidified to be the particles of the same size when the emulsion is mixed with a solvent (precipitant) which can dissolve the components except for cellulose. In this solidification step, the solvent in the droplets diffuses out and the precipitant goes into the droplets, resulting in the phase separation of cellulose and cellulose solvent; thus, cellulose precipitated in the droplets to form the cellulose particles. However, in general, the droplets tend to become spherical shape because the interfacial tension between droplets and medium should be minimize.[132] A spherical shape has the smallest interfacial free energy, resulting in formation of spherical particles. Therefore, it is difficult to prepare non-spherical cellulose particles in this method. In general, the particle diameter within approximately from several μm to several hundred μm is controlled by mixing speed, type and amount of stabilizer, viscosity of the cellulose solution, and the interfacial tension between the droplet and the emulsion medium.[133-135] Recently, taking environment problems into consideration, Minami et al. reported the successful preparation of cellulose particles by the Solvent-Releasing Method (SRM) using an ionic liquid as a cellulose solvent.[126]

### *3.1.2 Microfluidic Techniques*

Recently, microfluidic techniques have been recognized as powerful tools to produce monodisperse emulsions continuously.[136] Moreover, All the methods and tools, such as cross-flow,[137] flow focusing,[138] and co-flow geometry,[139] have been readily available, and some commercial company exist. More recently, the microfluidic technique has been applied for preparation of cellulose particles, and monodispersed cellulose particles could be obtained;[140, 141] however, in this technique, cellulose concentration should be low because the viscosity of cellulose solution is relatively high, resulting in clogging with the solution.

## ***3.2 Applications of Cellulose Particles***

Cellulose particles are expected to be applied to various functional materials owing to their properties.[142] In this section, the possibility of applications of cellulose particles will be introduced.

### *3.2.1 Chromatography*

As well as traditional polymer particles,[143, 144] cellulose particles are also suitable materials for chromatographic applications because they are easy to handle and to pack into columns owing to their spherical shape. Moreover, since cellulose have excellent properties such as high physical/chemical resistances, surface modification capability, and low non-specific adsorption of protein, cellulose particles can be used in fast flow without cross-linking treatment[145] and can be applied for various chromatography including size exclusion chromatography (SEC),[130, 146] ion exchange chromatography,[147, 148] and affinity chromatography.[149]

*3.2.2 Adsorbents for Water Treatment*

Heavy metal ions (aqueous solutions) have been widely used in metal finishing, painting, electroplating, and photography; however, most of them are toxic and carcinogenic even at low concentrations, thus, the presence of heavy metals in aquatic environment has serious negative impact on the global environment.[150] Since cellulose is the most abundant renewable polymer and is biocompatible and biodegradable, it has been considered as more suitable remover (adsorbent). Therefore, cellulose particles have become promising materials due to their eases of handling besides above-mentioned their intrinsic properties. In most research, cellulose is introduced functional groups, including sulfohydroxypropyl-, phosphate-, carboxylate-, and carboxymethyl groups,[151, 152] or it represented the matrices of composite particles with chitin,[153] chitosan,[154] magnetite,[155] or alginic acid[156] which provided the capability of metal adsorption via ionic or metal–ligand interactions.

*3.2.3 Supports and Scaffolds for Organic Synthesis*

Cellulose particles have been used as solid-phase synthesis supports.[24, 157-159] They can be used in various media including polar-, non-polar media, and acidic medium; whereas, generally, the conventional resin particles such as PS particles cross-linked by poly(divinylbenzen) are limited in use only in polar media.[160] Moreover, the cellulose particles can be used in high temperature owing to their thermal stability.[161] For a catalysis scaffold, porous cellulose particles with silver nanoparticles (AgNPs) were prepared by a sol-gel transition process, followed by the reduction of Ag in $AgNO_3$ aqueous solution.[162] The cellulose particles were scaffolds for AgNPs and contributed their good catalytic activity due to the high

specific surface area of porous structure. This report exhibits that cellulose particles have potential application for scaffolds of catalysis.

### *3.2.4 Loading and Releasing*

Recently, microcapsules have been attracted attention and rapidly developed for use in controlled delivery of drug.[163-165] Since cellulose has biocompatibility with human tissue[166, 167] and does not decompose enzymatically *in vivo*, cellulose has been recognized as a promising material for drug delivery matrix.[165, 168] Until now, various kind of cellulose capsules are reported, including regenerated cellulose particles prepared by microfluidic flow focusing,[140] carboxymethyl cellulose particles with layered double hydroxides,[169] cellulose/resins composite hollow particles,[170] and cellulose-core/carboxylmethyl cellulose-shell particles,[171] which were all pH sensitive carrier.

## *4. Object and Outline of This Dissertation*

As above-mentioned, cellulose particles have been prepared by various methods and are useful in wide range of applications. However, most of the cellulose particles were spherical and had rigid or porous structures; until now, the particles morphology has not been controlled precisely. *What are the root causes for this situation?* There is a big problem: that is the complicated process for dissolving cellulose. To dissolve cellulose in a solvent, it is necessary to use multistep process, some chemicals, or drastic conditions. This have made the fabrication of cellulose particles complicated, resulting that few researchers design and prepare cellulose particles from the point of view of interface chemistry.[24]

The primary aim of this dissertation is to establish the concept of morphology control of cellulose particles prepared by phase separation using ionic liquids in dispersed system, and to functionalize the cellulose particles. This dissertation consists of two main parts which have been subdivided into seven chapters to fulfill the above aim. **PART 1** covers the morphology control of cellulose particles prepared by the SRM. In ***Chapter 1***, the simple morphology control of porous cellulose particles in a dry state was demonstrated by focusing on a surface tension of medium at drying. In ***Chapter 2***, disk-like cellulose particles were prepared by stirring a dispersion of porous cellulose particles with a magnetic stir bar. ***Chapter 3*** shows that the effect of precipitation solvent on morphology of cellulose particles prepared by the SRM and that the important factor to control the morphology. **PART 2** concerns the application of the porous cellulose particles. In ***Chapter 4***, the application of porous cellulose particles to a capsule material was demonstrated. ***Chapter 5*** is aimed to prepare the composite cellulose/silver particles by TEMPO-mediated oxidation and to investigate their catalytic ability. In ***Chapter 6***, the synthesis of amine-functionalized porous cellulose particles was

conducted and composite cellulose/silver particles having recyclable catalytic property without chemical cross-linking to silver nanoparticles were successfully prepared through a one step. ***Chapter 7*** is aimed to prepare the composite cellulose/silica particles using amine-functionalized cellulose particles.

## References


1. S. Kawaguchi and K. Ito, in *Polymer Particles: -/-*, ed. M. Okubo, Springer Berlin Heidelberg, Berlin, Heidelberg, 2005, DOI: 10.1007/b100118, pp. 299-328.
2. G. L. Li, H. Möhwald and D. G. Shchukin, *Chemical Society Reviews*, 2013, **42**, 3628-3646.
3. S. Srivastava, J. L. Schaefer, Z. Yang, Z. Tu and L. A. Archer, *Adv. Mater. (Weinheim, Ger.)*, 2014, **26**, 201-234.
4. R. F. G. Brown, C. Carr and M. E. Taylor, *Progress in Organic Coatings*, 1997, **30**, 185-194.
5. C. J. McDonald and M. J. Devon, *Advances in Colloid and Interface Science*, 2002, **99**, 181-213.
6. J. C. Padget, *J. Coat. Technol.*, 1994, **66**, 89-105.
7. B. Pukánszky and E. Fekete, in *Mineral Fillers in Thermoplastics I: Raw Materials and Processing*, eds. J. Jancar, E. Fekete, P. R. Hornsby, J. Jancar, B. Pukánszky and R. N. Rothon, Springer Berlin Heidelberg, Berlin, Heidelberg, 1999, DOI: 10.1007/3-540-69220-7_3, pp. 109-153.
8. D. L. Wilcox and M. Berg, *MRS Proceedings*, 1994, **372**, 3.
9. J.-W. Yoo, D. J. Irvine, D. E. Discher and S. Mitragotri, *Nature Reviews Drug Discovery*, 2011, **10**, 521-535.
10. T. R. Green, J. Fisher, M. Stone, B. M. Wroblewski and E. Ingham, *Biomaterials*, 1998, **19**, 2297-2302.
11. G. J. Atkins, D. R. Haynes, D. W. Howie and D. M. Findlay, *World journal of orthopedics*, 2011, **2**, 93-101.
12. I. Urdampilleta, A. González, J. J. Iruin, J. C. de la Cal and J. M. Asua, *Macromolecules*, 2005, **38**, 2795-2801.
13. H. Matsuyama, M. Teramoto, M. Kuwana and Y. Kitamura, *Polymer*, 2000, **41**, 8673-8679.
14. J.-S. Song and M. A. Winnik, *Macromolecules*, 2005, **38**, 8300-8307.
15. A. Bettencourt and A. J. Almeida, *J. Microencapsulation*, 2012, **29**, 353-367.
16. Y. Sun and J. Cheng, *Bioresource Technology*, 2002, **83**, 1-11.
17. D. Klemm, B. Heublein, H.-P. Fink and A. Bohn, *Angewandte Chemie International Edition*, 2005, **44**, 3358-3393.
18. J. Perez, J. Munoz-Dorado, T. de la Rubia and J. Martinez, *Int. Microbiol.*, 2002, **5**, 53-63.
19. K. Jedvert and T. Heinze, *Journal*, 2017, **37**, 845.
20. D. Pokhrel and T. Viraraghavan, *Sci. Total Environ.*, 2004, **333**, 37-58.
21. D. Ciechańska, D. Wawro, W. Steplewski, J. Kazimierczak and H. Struszczyk, 2005, **13**, 19-23.
22. M. Nogi, S. Iwamoto, A. N. Nakagaito and H. Yano, *Advanced Materials*, 2009, **21**, 1595-1598.
23. H. Ullah, H. A. Santos and T. Khan, *Cellulose (Dordrecht, Neth.)*, 2016, **23**, 2291-2314.
24. M. Gericke, J. Trygg and P. Fardim, *Chemical Reviews*, 2013, **113**, 4812-4836.
25. D. J. Gardner, G. S. Oporto, R. Mills and M. A. S. A. Samir, *Journal of Adhesion Science and Technology*, 2008, **22**, 545-567.
26. D. Roy, M. Semsarilar, J. T. Guthrie and S. Perrier, *Chemical Society Reviews*, 2009, **38**, 2046-2064.
27. S. Eyley and W. Thielemans, *Nanoscale*, 2014, **6**, 7764-7779.

28. K. Watanabe, M. Tabuchi, M. Yasushi and F. Yoshinaga, *Cellulose (London)*, 1998, **5**, 187-200.
29. J. F. Kennedy and L. A. Quinton, *Carbohydr. Polym.*, 2000, **43**, 206-207.
30. Y. Habibi, L. A. Lucia and O. J. Rojas, *Chemical Reviews*, 2010, **110**, 3479-3500.
31. W. G. Glasser, R. H. Atalla, J. Blackwell, R. Malcolm Brown, W. Burchard, A. D. French, D. O. Klemm and Y. Nishiyama, *Cellulose*, 2012, **19**, 589-598.
32. B. Lindman, B. Medronho, L. Alves, C. Costa, H. Edlund and M. Norgren, *Physical Chemistry Chemical Physics*, 2017, **19**, 23704-23718.
33. P. Zugenmaier, *Progress in Polymer Science*, 2001, **26**, 1341-1417.
34. R. H. Atalla, J. C. Gast, D. W. Sindorf, V. J. Bartuska and G. E. Maciel, *Journal of the American Chemical Society*, 1980, **102**, 3249-3251.
35. R. H. Atalla and D. L. VanderHart, *Science (Washington, D. C., 1883-)*, 1984, **223**, 283-285.
36. D. L. VanderHart and R. H. Atalla, *Macromolecules*, 1984, **17**, 1465-1472.
37. P. S. Belton, S. F. Tanner, N. Cartier and H. Chanzy, *Macromolecules*, 1989, **22**, 1615-1617.
38. M. Wada, T. Okano and J. Sugiyama, *Cellulose (London)*, 1997, **4**, 221-232.
39. H. Yamamoto, F. Horii and H. Odani, *Macromolecules*, 1989, **22**, 4130-4132.
40. Y. Nishiyama, J. Sugiyama, H. Chanzy and P. Langan, *Journal of the American Chemical Society*, 2003, **125**, 14300-14306.
41. Y. Nishiyama, P. Langan and H. Chanzy, *Journal of the American Chemical Society*, 2002, **124**, 9074-9082.
42. F. J. Kolpak, M. Weih and J. Blackwell, *Polymer*, 1978, **19**, 123-131.
43. H. Nishimura, T. Okano and A. Sarko, *Macromolecules*, 1991, **24**, 759-770.
44. F. J. Kolpak and J. Blackwell, *Macromolecules*, 1976, **9**, 273-278.
45. P. Langan, Y. Nishiyama and H. Chanzy, *Journal of the American Chemical Society*, 1999, **121**, 9940-9946.
46. A. J. Barry, F. C. Peterson and A. J. King, *Journal of the American Chemical Society*, 1936, **58**, 333-337.
47. M. Wada, H. Chanzy, Y. Nishiyama and P. Langan, *Macromolecules*, 2004, **37**, 8548-8555.
48. M. Wada, Y. Nishiyama and P. Langan, *Macromolecules*, 2006, **39**, 2947-2952.
49. G. L. Clark and E. A. Parker, *The Journal of Physical Chemistry*, 1937, **41**, 777-786.
50. L. Segal, *Journal of Polymer Science Part A: General Papers*, 1964, **2**, 2951-2961.
51. L. Segal and J. J. Creely, *Journal of Polymer Science*, 1961, **50**, 451-465.
52. A. Sarko, J. Southwick and J. Hayashi, *Macromolecules*, 1976, **9**, 857-863.
53. M. Wada, L. Heux and J. Sugiyama, *Biomacromolecules*, 2004, **5**, 1385-1391.
54. K. Hutino and I. Sakurada, *Naturwissenschaften*, 1940, **28**, 577-578.
55. A. Buleon and H. Chanzy, *Journal of Polymer Science: Polymer Physics Edition*, 1980, **18**, 1209-1217.
56. T. Liebert, in *Cellulose Solvents: For Analysis, Shaping and Chemical Modification*, American Chemical Society, 2010, vol. 1033, ch. 1, pp. 3-54.
57. B. Philipp, I. Nehls, W. Wagenknecht and M. Schnabelrauch, *Carbohydrate Research*, 1987, **164**, 107-116.
58. A. J. Sayyed, N. A. Deshmukh and D. V. Pinjari, *Cellulose (Dordrecht, Neth.)*, 2019, **26**, 2913-2940.
59. A. G. Wilkes, in *Regenerated Cellulose Fibres*, ed. C. Woodings, Woodhead Publishing, 2001, DOI: https://doi.org/10.1533/9781855737587.37, pp. 37-61.

60. F. Fu, Q. Yang, J. Zhou, H. Hu, B. Jia and L. Zhang, *ACS Sustainable Chemistry & Engineering*, 2014, **2**, 2604-2612.
61. S. Paunonen, T. Kamppuri, L. Katajainen, C. Hohenthal, P. Heikkilä and A. Harlin, *Journal of Cleaner Production*, 2019, **222**, 871-881.
62. X. Zhou, X. Lin, K. L. White, S. Lin, H. Wu, S. Cao, L. Huang and L. Chen, *Cellulose (Dordrecht, Neth.)*, 2016, **23**, 811-821.
63. E. Samios, R. K. Dart and J. V. Dawkins, *Polymer*, 1997, **38**, 3045-3054.
64. J. D. Reid and L. W. Mazzeno, *Industrial & Engineering Chemistry*, 1949, **41**, 2828-2831.
65. J. D. Reid, L. W. Mazzeno and E. M. Buras, *Industrial & Engineering Chemistry*, 1949, **41**, 2831-2834.
66. F. Rol, C. Sillard, M. Bardet, J. R. Yarava, L. Emsley, C. Gablin, D. Léonard, N. Belgacem and J. Bras, *Carbohydrate Polymers*, 2019, DOI: https://doi.org/10.1016/j.carbpol.2019.115294, 115294.
67. T. Fujimoto, S.-i. Takahashi, M. Tsuji, T. Miyamoto and H. Inagaki, *Journal of Polymer Science Part C: Polymer Letters*, 1986, **24**, 495-501.
68. M. Schnabelrauch, S. Vogt, D. Klemm, I. Nehls and B. Philipp, *Die Angewandte Makromolekulare Chemie*, 1992, **198**, 155-164.
69. E. Schweizer, *Journal für Praktische Chemie*, 1857, **72**, 109-111.
70. W. Burchard, N. Habermann, P. Klüfers, B. Seger and U. Wilhelm, *Angewandte Chemie International Edition in English*, 1994, **33**, 884-887.
71. K. Saalwächter, W. Burchard, P. Klüfers, G. Kettenbach, P. Mayer, D. Klemm and S. Dugarmaa, *Macromolecules*, 2000, **33**, 4094-4107.
72. W. Traube, *Berichte der deutschen chemischen Gesellschaft (A and B Series)*, 1921, **54**, 3220-3232.
73. V. G. Jayme and K. Neuschäffer, *Die Makromolekulare Chemie*, 1957, **23**, 71-83.
74. H. Sobue, H. Kiessig and K. Hess, *Journal*, 1939, **43B**, 309.
75. A. Isogai and R. H. Atalla, *Cellulose*, 1998, **5**, 309-319.
76. J. Zhou and L. Zhang, *Polymer Journal*, 2000, **32**, 866-870.
77. L. Zhang, J. Cai and J. Zhou, *Journal*, 2005.
78. *Macromolecular Bioscience*, 2005, **5**, 539-548.
79. J. Cai and L. Zhang, *Biomacromolecules*, 2006, **7**, 183-189.
80. H. Qi, C. Chang and L. Zhang, *Cellulose*, 2008, **15**, 779-787.
81. J. Cai, Y. Liu and L. Zhang, *Journal of Polymer Science Part B: Polymer Physics*, 2006, **44**, 3093-3101.
82. S. Liu and L. Zhang, *Cellulose*, 2009, **16**, 189-198.
83. D. Ruan, A. Lue and L. Zhang, *Polymer*, 2008, **49**, 1027-1036.
84. P. P. von Weimarn, *Zeitschrift für Chemie und Industrie der Kolloide*, 1912, **11**, 41-43.
85. K. Letters, *Kolloid-Zeitschrift*, 1932, **58**, 229-239.
86. J. O. Warwicker, S. Cotton and A. Man-made Fibres Research, *A Review of the literature on the effect of caustic soda and other swelling agents on the fine structure of cotton*, Cotton, Silk and Man-Made Fibres Research Association, Manchester, 1966.
87. S. Kuga, *Journal of Colloid and Interface Science*, 1980, **77**, 413-417.
88. J. R. Katz and J. C. Derksen, *Recueil des Travaux Chimiques des Pays-Bas*, 1931, **50**, 149-152.
89. S. Fischer, W. Voigt and K. Fischer, *Cellulose*, 1999, **6**, 213-219.
90. H. Leipner, S. Fischer, E. Brendler and W. Voigt, *Macromolecular Chemistry and Physics*, 2000, **201**, 2041-2049.

91. S. Fischer, H. Leipner, K. Thümmler, E. Brendler and J. Peters, *Cellulose*, 2003, **10**, 227-236.
92. C. L. McCormick and D. K. Lichatowich, *Journal of Polymer Science: Polymer Letters Edition*, 1979, **17**, 479-484.
93. T. Bikova and A. Treimanis, *Carbohydrate Polymers*, 2002, **48**, 23-28.
94. A. El-Kafrawy, *Journal of Applied Polymer Science*, 1982, **27**, 2435-2443.
95. A. Striegel and J. D. Timpa, *Carbohydrate Research*, 1995, **267**, 271-290.
96. A. M. Striegel, J. D. Timpa, P. Piotrowiak and R. B. Cole, *International Journal of Mass Spectrometry and Ion Processes*, 1997, **162**, 45-53.
97. E. Sjöholm, K. Gustafsson, B. Eriksson, W. Brown and A. Colmsjö, *Carbohydrate Polymers*, 2000, **41**, 153-161.
98. D. Balasubramanian and R. Shaikh, *Biopolymers*, 1973, **12**, 1639-1650.
99. T. Huber, J. Müssig, O. Curnow, S. Pang, S. Bickerton and M. P. Staiger, *Journal of Materials Science*, 2012, **47**, 1171-1186.
100. T. Rosenau, A. Potthast, H. Sixta and P. Kosma, *Progress in Polymer Science*, 2001, **26**, 1763-1837.
101. H. Chanzy, A. Peguy, S. Chaunis and P. Monzie, *Journal of Polymer Science: Polymer Physics Edition*, 1980, **18**, 1137-1144.
102. H. Chanzy, S. Nawrot, A. Peguy, P. Smith and J. Chevalier, *Journal of Polymer Science: Polymer Physics Edition*, 1982, **20**, 1909-1924.
103. H. P. Fink, P. Weigel, H. J. Purz and J. Ganster, *Progress in Polymer Science*, 2001, **26**, 1473-1524.
104. C. Cuissinat and P. Navard, *Macromolecular Symposia*, 2006, **244**, 1-18.
105. E. Maia, A. Peguy and S. Perez, *Acta Crystallogr., Sect. B*, 1981, **B37**, 1858-1862.
106. J. S. Wilkes, P. Wasserscheid and T. Welton, *Ionic Liquids in Synthesis*, 2007, DOI: doi:10.1002/9783527621194.ch1

10.1002/9783527621194.ch1, 1-6.

107. P. Walden, *Bull. Acad. Imp. Sci. St.-Petersbourg*, 1914, 405-422.
108. J. C. Nardi, C. L. Hussey, L. A. King and J. K. Erbacher, *The electrolytic removal of aluminum from a two-phase aluminum-trialuminum nickelide matrix*, U. S. Air Force Acad., 1976.
109. US2446331, 1948.
110. US2446349, 1948.
111. US4100044A, 1978.
112. J. S. Wilkes and M. J. Zaworotko, *Journal of the Chemical Society, Chemical Communications*, 1992, DOI: 10.1039/C39920000965, 965-967.
113. R. D. Rogers and K. R. Seddon, *Science*, 2003, **302**, 792.
114. T. Welton, *Chemical Reviews*, 1999, **99**, 2071-2084.
115. P. Wasserscheid and W. Keim, *Angew. Chem., Int. Ed.*, 2000, **39**, 3772-3789.
116. M. Armand, F. Endres, D. R. MacFarlane, H. Ohno and B. Scrosati, *Nat. Mater.*, 2009, **8**, 621-629.
117. J. P. Hallett and T. Welton, *Chem. Rev. (Washington, DC, U. S.)*, 2011, **111**, 3508-3576.
118. R. P. Swatloski, S. K. Spear, J. D. Holbrey and R. D. Rogers, *Journal of the American Chemical Society*, 2002, **124**, 4974-4975.
119. R. C. Remsing, R. P. Swatloski, R. D. Rogers and G. Moyna, *Chemical Communications*, 2006, DOI: 10.1039/B600586C, 1271-1273.
120. A. Pinkert, K. N. Marsh, S. Pang and M. P. Staiger, *Chemical Reviews*, 2009, **109**, 6712-6728.

121. C. Verma, A. Mishra, S. Chauhan, P. Verma, V. Srivastava, M. A. Quraishi and E. E. Ebenso, *Sustainable Chemistry and Pharmacy*, 2019, **13**, 100162.
122. Y. Li, J. Wang, X. Liu and S. Zhang, *Chemical Science*, 2018, **9**, 4027-4043.
123. H. Wang, G. Gurau and R. D. Rogers, *Chemical Society Reviews*, 2012, **41**, 1519-1537.
124. X. Shen, J. L. Shamshina, P. Berton, G. Gurau and R. D. Rogers, *Green Chemistry*, 2016, **18**, 53-75.
125. US2543928, 1951.
126. T. Suzuki, K. Kono, K. Shimomura and H. Minami, *Journal of Colloid and Interface Science*, 2014, **418**, 126-131.
127. T. Omura, K. Imagawa, K. Kono, T. Suzuki and H. Minami, *ACS Applied Materials & Interfaces*, 2017, **9**, 944-949.
128. E. D. Wilkes, S. D. Phillips and O. A. Basaran, *Physics of Fluids*, 1999, **11**, 3577-3598.
129. R. Sescousse, R. Gavillon and T. Budtova, *Journal of Materials Science*, 2011, **46**, 759-765.
130. W. D. Oliveira and W. G. Glasser, *Journal of Applied Polymer Science*, 1996, **60**, 63-73.
131. D. Ishimura, Y. Morimoto and H. Saito, *Cellulose*, 1998, **5**, 135-151.
132. H.-J. Butt, K. Graf and M. Kappl, *Physics and Chemistry of Interfaces, Third Edition*, Wiley-VCH, 2013.
133. K. Thümmler, S. Fischer, A. Feldner, V. Weber, M. Ettenauer, F. Loth and D. Falkenhagen, *Cellulose*, 2011, **18**, 135-142.
134. M. Liu, J. Huang and Y. Deng, *Bioresource Technology*, 2007, **98**, 1144-1148.
135. X. Luo and L. Zhang, *Journal of Chromatography A*, 2010, **1217**, 5922-5929.
136. B. Wang, P. Prinsen, H. Wang, Z. Bai, H. Wang, R. Luque and J. Xuan, *Chemical Society Reviews*, 2017, **46**, 855-914.
137. J. Wan, A. Bick, M. Sullivan and H. A. Stone, *Advanced Materials*, 2008, **20**, 3314-3318.
138. A. S. Utada, L. Y. Chu, A. Fernandez-Nieves, D. R. Link, C. Holtze and D. A. Weitz, *MRS Bulletin*, 2007, **32**, 702-708.
139. W. H. Tan and S. Takeuchi, *Advanced Materials*, 2007, **19**, 2696-2701.
140. C. Carrick, P. A. Larsson, H. Brismar, C. Aidun and L. Wågberg, *RSC Advances*, 2014, **4**, 19061-19067.
141. J. Coombs Obrien, L. Torrente-Murciano, D. Mattia and J. L. Scott, *ACS Sustainable Chemistry & Engineering*, 2017, **5**, 5931-5939.
142. S. Wang, A. Lu and L. Zhang, *Progress in Polymer Science*, 2016, **53**, 169-206.
143. R. Perrier-Cornet, V. Héroguez, A. Thienpont, O. Babot and T. Toupance, *Journal of Chromatography A*, 2008, **1179**, 2-8.
144. J. Ugelstad, L. Söderberg, A. Berge and J. Bergström, *Nature*, 1983, **303**, 95-96.
145. J. A. Kaster, W. de Oliveira, W. G. Glasser and W. H. Velander, *Journal of Chromatography A*, 1993, **648**, 79-90.
146. P. Vincent, J.-P. Compoint, V. Fitton and X. Santarelli, *Journal of Biochemical and Biophysical Methods*, 2003, **56**, 69-78.
147. K.-F. Du, M. Yan, Q.-Y. Wang and H. Song, *Journal of Chromatography A*, 2010, **1217**, 1298-1304.
148. Y. Motozato and C. Hirayama, *Journal of Chromatography A*, 1984, **298**, 499-507.
149. P. Gemeiner, M. Polakovič, D. Mislovičová and V. Štefuca, *Journal of Chromatography B: Biomedical Sciences and Applications*, 1998, **715**, 245-271.

150. R. Kumar Sharma, M. Agrawal and F. Marshall, *Ecotoxicology and Environmental Safety*, 2007, **66**, 258-266.
151. Mat and Bene, *Reactive Polymers, Ion Exchangers, Sorbents*, 1984, **3**, 33-36.
152. M. Hirota, N. Tamura, T. Saito and A. Isogai, *Cellulose*, 2009, **16**, 841-851.
153. D. Zhou, L. Zhang, J. Zhou and S. Guo, *Water Research*, 2004, **38**, 2643-2650.
154. S. Peng, H. Meng, Y. Ouyang and J. Chang, *Industrial & Engineering Chemistry Research*, 2014, **53**, 2106-2113.
155. X. Luo, X. Lei, N. Cai, X. Xie, Y. Xue and F. Yu, *ACS Sustainable Chemistry & Engineering*, 2016, **4**, 3960-3969.
156. L. Zhang, J. Cai, J. Zhou and Y. Tang, *Separation Science and Technology*, 2005, **39**, 1203-1219.
157. A. Chesney, P. Barnwell, D. F. Stonehouse and P. G. Steel, *Green Chemistry*, 2000, **2**, 57-62.
158. D. R. Englebretsen and D. R. K. Harding, *International Journal of Peptide and Protein Research*, 1992, **40**, 487-496.
159. A. Chesney, P. G. Steel and D. F. Stonehouse, *Journal of Combinatorial Chemistry*, 2000, **2**, 434-437.
160. F. Guillier, D. Orain and M. Bradley, *Chemical Reviews*, 2000, **100**, 2091-2158.
161. H. P. L. Willems, D. F. Berry, G. Samaranayake and W. G. Glasser, *Environmental Science & Technology*, 1996, **30**, 2148-2154.
162. J. Wu, N. Zhao, X. Zhang and J. Xu, *Cellulose*, 2012, **19**, 1239-1249.
163. C. E. Mora-Huertas, H. Fessi and A. Elaissari, *Int. J. Pharm.*, 2010, **385**, 113-142.
164. M. N. Singh, K. S. Y. Hemant, M. Ram and H. G. Shivakumar, *Res Pharm Sci*, 2010, **5**, 65-77.
165. A. Kumari, S. K. Yadav and S. C. Yadav, *Colloids and Surfaces B: Biointerfaces*, 2010, **75**, 1-18.
166. A. Sannino, C. Demitri and M. Madaghiele, *Materials*, 2009, **2**, 353-373.
167. T. Miyamoto, S.-i. Takahashi, H. Ito, H. Inagaki and Y. Noishiki, *Journal of Biomedical Materials Research*, 1989, **23**, 125-133.
168. M. Märtson, J. Viljanto, T. Hurme, P. Laippala and P. Saukko, *Biomaterials*, 1999, **20**, 1989-1995.
169. S. Barkhordari and M. Yadollahi, *Applied Clay Science*, 2016, **121-122**, 77-85.
170. A.-F. Metaxa, E. K. Efthimiadou, N. Boukos and G. Kordas, *Journal of Colloid and Interface Science*, 2012, **384**, 198-206.
171. M. Ma, L. Tan, Y. Dai and J. Zhou, *Iranian Polymer Journal*, 2013, **22**, 689-695.

# *Chapter 1*

## Morphology Control of Porous Cellulose Particles by Tuning the Surface Tension of Media During Drying

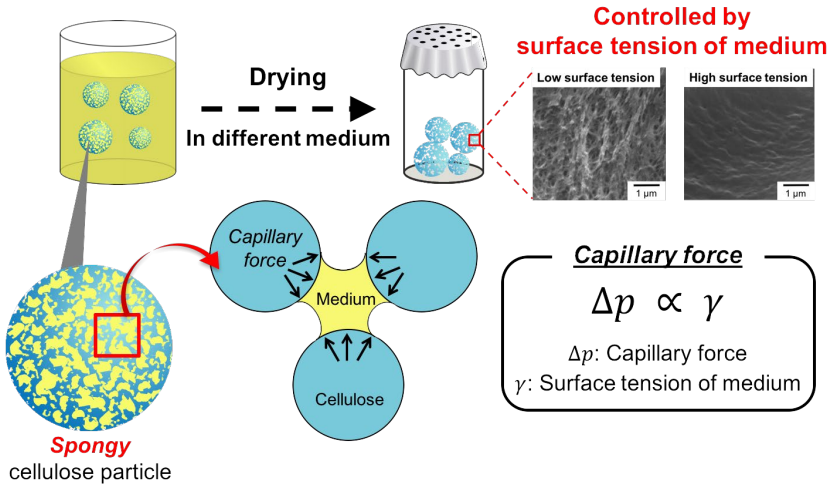


**Abstract:** Cellulose particles prepared by the solvent releasing method (SRM) had a porous structure filled with a surrounding medium. However, the structure was fragile and easily collapsed because of the capillary pressure as the medium evaporated, resulting in dense cellulose particles. To control the morphology of cellulose particles in a dry state, this chapter focused on the influence of surface tension of a surrounding medium on structure of cellulose particles because the capillary pressure is proportional to the surface tension. Different media such as toluene, acetone, and pentane were investigated. The morphologies of the resulting cellulose particles were estimated by volume changes, specific surface areas, and compressive strengths. From these results, as the surface tension of the media filling the particles was lowered, the particle's specific surface area increased, resulting in the formation of softer particles.

## Introduction

Cellulose is the most abundant natural polymer on earth. It is extensively used in various applications such as regenerated fibers and pulps because it is inexpensive, nontoxic, chemically stable, biodegradable, and modifiable.[1-3] In recent years, the utility of a particle state of cellulose has been recognized, such as in adsorbents and packing materials for biochromatography.[4-6] However, cellulose is insoluble in water and common organic solvents. Recently, the hypothesis in which this solubility property of cellulose is due to the its hydrophobic and amphiphilic characteristics (i.e., the Lindman hypothesis) has been supported.[7] Therefore, to dissolve cellulose in a solvent, it is necessary to use multistep processes or drastic conditions.[8-10]

Throughout the past decade, ionic liquids (ILs), which are salts but in a liquid state at ambient temperature, have been recognized as environmentally friendly media because of their nonvolatile property.[11-13] In 2002, Rogers et al. reported that ILs such as 1-butyl-3-methylimidazolium chloride ([Bmim]Cl) could dissolve cellulose under mild heat treatments.[14] Thereafter, there has been increasing interest in ILs as solvents for cellulose.[15-17]

Utilizing this knowledge, Minami et al. reported the successful preparation of cellulose particles by the solvent releasing method (SRM)[18-20] for droplets comprising cellulose, [Bmim]Cl, and *N*,*N*-dimethylformamide (DMF).[21] The obtained particles had a sponge-like fine porous structure which was filled with a surrounding medium in a wet state, that is, not independent pore but continuous pore.[22] Moreover, the filled medium in the porous structure was able to change by changing the surrounding medium regardless of its polarity without deforming the morphology of cellulose particles.[23] However, the structure collapsed and shrank because of the capillary pressure as the medium evaporated, resulting in dense cellulose particles. The spongy structure was observed only when the obtained particles were dried using

a freeze-drying technique or the supercritical carbon dioxide (scCO2) drying method.[24] However, these drying methods were accompanied by very complicated procedures. The morphology controls of cellulose material in the bulk state, such as films or membrane, were extensively investigated;[25-28] however, to the best of our knowledge, only a few papers have reported the post-treatment morphology control of dried "cellulose particles".[29]

***Chapter 1*** discusses a simple morphology control of porous cellulose particles in the dry state by focusing on the surface tension of the medium at drying. Porous cellulose particles were dried after the various media replacements with different surface tensions. The morphologies, specific surface areas, and mechanical properties of the obtained particles were investigated accordingly.

## Experimental Section

### Materials

Microcrystalline cellulose (powder, derived from cotton linter) and [Bmim]Cl were used as received from Aldrich Chemical Co., Ltd. DMF, *n*-hexane, 1-butanol, acetone, toluene, and *n*-pentane were used as received from Nacalai Tesque Inc. (Kyoto, Japan). Polydimethylsiloxane surfactant, VPS-1001 (Wako Pure Chemical Industries, Ltd.), was also used as received. All of the water used in these experiments was purified in an ErixUV (Millipore, Japan) purification system and had a resistivity of 18.2 MΩ cm.

### Preparation of cellulose particles by SRM

Cellulose particles were prepared by SRM following the procedures in our previous report.[21] Briefly, microcrystalline cellulose powder was dissolved in [Bmim]Cl at a weight ratio of 7:43 by heating to 100 °C for 7 h. To reduce the viscosity of this solution, DMF was added as a co-solvent. The homogeneous solution of cellulose–[Bmim]Cl–DMF (7/43/50, w/w/w, 0.2 g) was mixed with hexane (2.0 g) containing dissolved VPS-1001 (0.25 wt% of hexane) as a stabilizer and then stirred at 4000 rpm for 5 min by using a homogenizer (BM-1, Nihonseiki Kaisha Ltd., Tokyo, Japan), followed by a Shirasu porous glass (SPG) membrane (pore size = 30 μm; SPG12G30-30U, SPG TECHNOLOGY Co., Ltd., Miyazaki, Japan). The obtained dispersion was poured into a large amount of 1-butanol (20 g) and stirred to remove [Bmim]Cl and DMF from the cellulose–[Bmim]Cl–DMF droplet, wherein cellulose should precipitate to form cellulose particles. The precipitated particles were washed three times with 1-butanol to remove any remaining [Bmim]Cl, DMF, and hexane. Finally, the cellulose particles thus obtained were dispersed in 1-butanol.

**Preparation of millimeter-sized cellulose beads**

To prepare millimeter-sized cellulose beads, the SRM-like procedure was carried out.[23] The solution of cellulose–[Bmim]Cl–DMF (7/43/50, w/w/w, 0.2 g) was dropped by a syringe into a large amount of 1-butanol (20 g). To completely remove [Bmim]Cl and DMF, the precipitated cellulose beads (containing [Bmim]Cl and DMF) were left for over 6 h after being dropped into 1-butanol, followed by washing twice with 1-butanol. Cellulose beads remained standing for not less than 2 h at each washing step.

**Drying of cellulose particles and beads**

After the cellulose particles or beads were washed, the medium was replaced with toluene, acetone, pentane, or distilled water and then dried under reduced pressure. In the case of $scCO_2$ drying, the drying process of cellulose particles was as follows. First, the cellulose particles dispersed in acetone were putted into a 25 mL stainless-steel reactor, and the reactor was pressurized with liquid $CO_2$ to 15 MPa at room temperature using a high-pressure pump. Next, $CO_2$ and acetone were vented out from the reactor. Before all of the liquid $CO_2$ and acetone evaporated (2 MPa), liquid $CO_2$ was added until the pressure reached 15 MPa. This process was repeated at least eight times to ensure the complete removal of acetone from the reactor. The reactor was subsequently dipped into a temperature-controlled water bath at 40°C, in which CO2 should exist as $scCO_2$. Finally, $scCO_2$ was vented out slowly from the reactor to obtain $scCO_2$-dried cellulose particles.

**Characterizations**

Cellulose particles were observed by optical microscopy (ECLIPSE 80i, Nikon, Tokyo, Japan) and scanning electron microscopy (SEM, JSM-6510, JEOL Ltd., Tokyo, Japan).

Nitrogen adsorption measurements were performed with Quantachrome NOVA 3200e (USA). Before the analysis, the dried samples were further dried under reduced pressure using the NOVA 3200e instrument. The Brunauer–Emmett–Teller (BET) specific surface area was assessed from the adsorption branch of the isotherm for a relative pressure of 0.05–0.3 at 77 K. The Barrett–Joyner–Halenda (BJH) pore distribution was determined from the desorption branch of the isotherm with the instrument software.

The mechanical properties of cellulose particles in the dry state were measured using microcompressive testing machine (DUH-W201, SHIMADZU) with a 50-μm-diameter flat indenter at a rate of 1.4 mN/s at room temperature. The microcompression device was equipped with an optical microscope, thus enabling an approximate estimation of the diameter of a single particle being tested and allowing one to select particles of a suitable size within the distribution for testing.

## Results and Discussion

### *Control of Porosity of Dried Cellulose Particles*

Cellulose particles prepared by SRM have a porous structure, which was filled with a surrounding medium. Moreover, the medium could be replaced with another medium regardless of polarity without deforming the particle morphology. However, the porous structure collapsed because of the evaporation of the medium, in which a capillary pressure was generated and acted as an attraction force between the cellulose pillar of the porous structure in the direction of each other. The capillary pressure ($\Delta p$) is proportional to the surface tension of the medium ($\gamma$) according to the Young–Laplace equation

$$\Delta p = \frac{2\gamma}{R}$$

where $R$ is the radius of curvature of the surface of the medium, the value of which depends on the pore diameter of the porous structure. From the equation, when the medium with a lower surface tension was used, the degree of collapse of the porous structure was expected to be suppressed. $R$ should also change when the medium is replaced; however, in the case of the medium having a lower surface tension, $R$ increased (contact angle increased) owing to the high hydrophilicity of cellulose, resulting in the decrease in $\Delta p$. Therefore, to control the capillary pressure, series of media were chosen, such as toluene, acetone, and pentane, with different surface tensions: 27.7, 23.0,[30] and 16.0 mN/m,[31] respectively. In either case, a medium filling the porous structure of cellulose particles were able to be replaced with above media without deforming particle morphology. The morphologies of the cellulose particles after drying were evaluated by volume changes, specific surface areas, and compressive strengths. The moisture in the air would affect the morphology of cellulose particles after drying due to their hygroscopic property. However, the drying of the particles was performed under reduced pressure, in which the influence of moisture should be suppressed.

Figure 1 shows the cellulose particles dispersed in each medium and the dried particles after evaporation of the medium. The cellulose particles were prepared by SRM using 1-butanol as a precipitation solvent, and then the medium was replaced with different medium. In the case of toluene and acetone, the volumes of the dried particles decreased to around 10 vol% of wet particles (Figure 1a, a', b, b'). Because the volume fraction of cellulose in the initial droplet was around 9.3 vol% (from densities of amorphous cellulose, [Bmim]Cl, and DMF (g/cm3): 1.38, 1.05, and 0.95, respectively), their porosities were calculated to be approximately 6%, indicating that almost the all porous structures were likely to be collapsed. On the contrary, the volume ratio was about 30% before and after the drying in the case of pentane (Figure 1c, c'), indicating the porosity was 69%. This result suggests that the porous structure was expected to remain in the case of pentane as an evaporating medium.

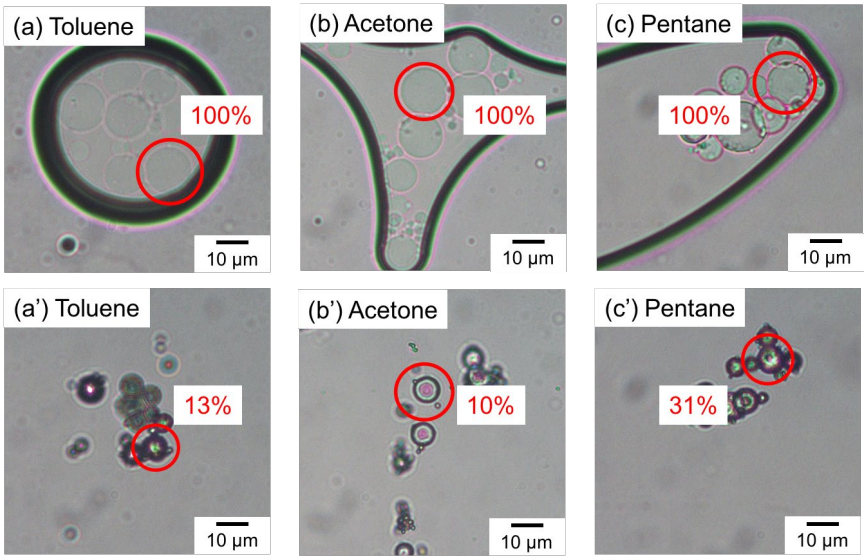


**Figure 1.** Optical micrographs of cellulose particles before (a, b, c) and after (a', b', c') drying from toluene (a, a'), acetone (b, b'), and pentane (c, c').

Figure 2 shows the SEM images of the particles and their inner morphologies, which were dried from different media. The obtained particles dried from toluene and acetone had a

smooth surface and a dense structure (Figure 2a, b, d, e, g, h). However, in the case of pentane, a bumpy surface and a porous structure were observed, as expected (Figure 2c, f, i).

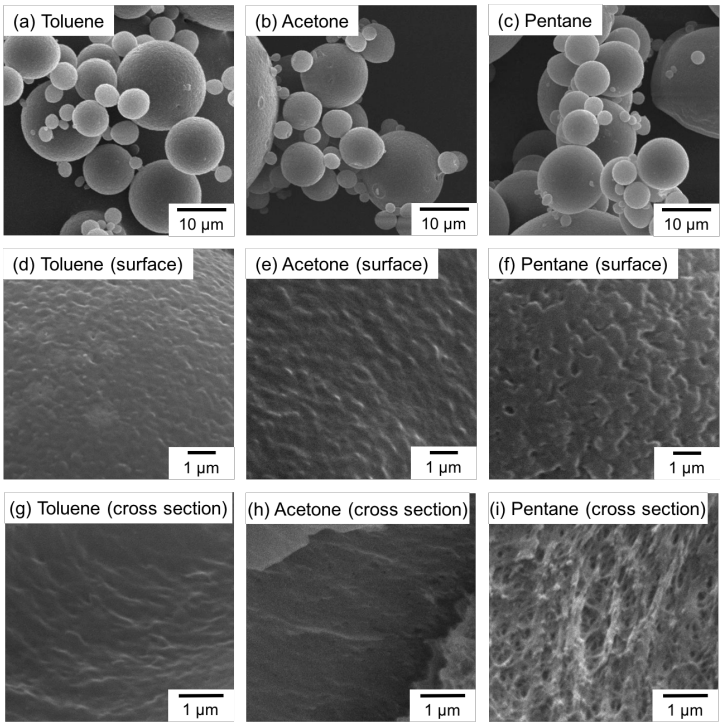


**Figure 2.** SEM images of cellulose particles (a, b, c), their surfaces (d, e, f), and their cross section (g, h, i) after drying from toluene (a, d, g), acetone (b, e, h), and pentane (c, f, i).

To investigate the structure of each particle in detail, nitrogen adsorption measurements were carried out. In the case of the toluene and acetone systems, adsorption/desorption hysteresis was not observed because of the dense structure. In addition, the specific areas for toluene and acetone were 0.31 and 0.91 $m^2/g$, respectively, as estimated with the BET method, indicating that these cellulose particles had a dense structure. On the contrary, when pentane was used as the evaporating medium, distinctive isotherms and adsorption/desorption hysteresis were observed. Figure 3 shows the nitrogen adsorption and desorption isotherms, and pore distribution from the desorption branch of cellulose particles

after drying from pentane. The obtained isotherm was of type IV according to the IUPAC classification, which indicates the presence of mesopore structure (2–50 nm). Moreover, using the BJH method for this isotherm, the fine porous structure existed besides the several hundred nanometer-sized macropores observed with SEM. The specific surface area was 23.3 $m^2/g$, and the volume was different from those in the case of the toluene and acetone systems. These results also indicate that the porous structure could be maintained using a medium with a lower surface tension in the dry state.

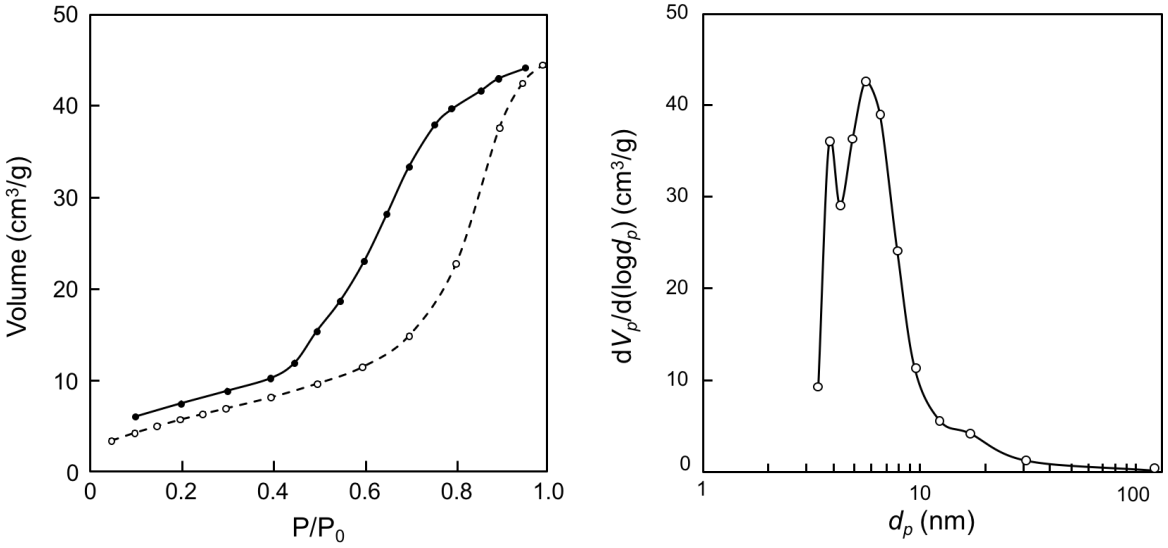


**Figure 3.** Nitrogen adsorption (open circles) and desorption (close circles) isotherms, and pore size distribution (from desorption branch; $d_p$ = pore diameter, $V_p$ = pore volume) of the cellulose particles dried from pentane.

To visually observe these structural variations, the same experiments were carried out using millimeter-sized cellulose beads with a porous structure similar to that of the micrometer-sized particles.[23] In the case of toluene and acetone, similar to the micrometer-sized particles, the volume of the dried beads reduced to about 10 vol% of the wet beads (Figure 4a, b, d, e); however, the volume of the beads dried from pentane was about 20 vol% (Figure 4c, f). In

addition, the dried beads of the pentane system appeared turbid and white (Figure 4d, e, f), due to the decrease in transmittance from light scattering by the porous structure. Subsequently, each dried bead was dipped in water (Figure 4g, h, i), and the morphological changes in the dried beads from the toluene and acetone systems were not observed (Figure 4g, h). On the contrary, in the case of the pentane system, as the bubbles came out from inside of the beads, the beads gradually appeared transparent (Figure 4i), indicating that the porous spaces were replaced from air to water. From these results, it is evident that cellulose particles (beads) dried from pentane retained the porous structure.

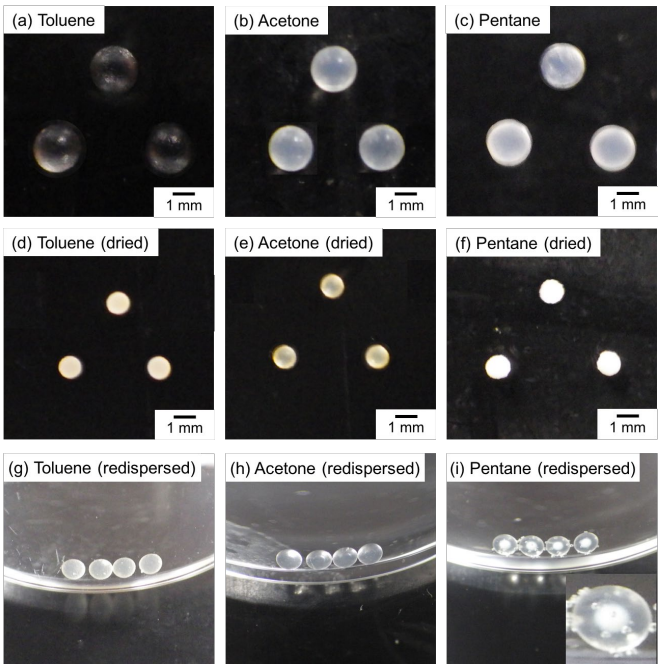


**Figure 4.** Visual appearances of cellulose beads before (a, b, c), and after drying (d, e, f), and then dipped in water (g, h, i, i'). The medium dispersing the cellulose beads was toluene (a, d, g), acetone (b, e, h), or pentane (c, f, i). Magnified image: the lower right corner of (i).

***Mechanical Property of Dried Cellulose Particles***

To estimate the influence of the internal structure of dried cellulose particles on their mechanical properties, microcompressive tests were conducted. The instrument enables the measurement of individual particles, and the results truly represent the mechanical properties of a single particle. Figure 5 shows the force–deformation curves of around 10-μm-sized cellulose particles after drying from each medium. For comparison, particles dried with $scCO_2$ were investigated as a reference. Particles after drying from water were also measured, and they exhibited a dense structure similar to particles in the toluene system because of the high surface tension ($\gamma$ = 72.7 mN/m). As shown in Figure 5, the breaking point was not observed in all samples. Hence, the present study focused on the slope of the curve in the initial stage of compression (at 10% deformation of the particles). When a steep slope is observed, the examined sample should be stiff; when the yielded slope is gentle, the sample should be soft. As shown in Figure 5, the slope became gentler with the decrease in the surface tension of the medium. The compressive curve of the pentane system was close to that of particles dried by $scCO_2$ (resulting in a spongy structure). These results suggest that with decreasing surface tension of the medium filling in the particles, the compressive strength of the particles decreased, and the particles became more porous.

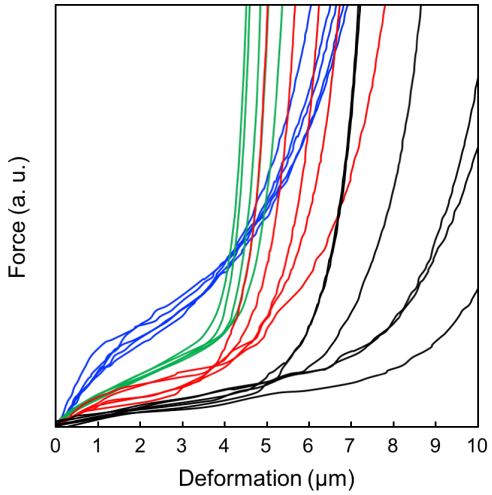


**Figure 5.** Force–deformation curves measured by a microcompressive testing machine at a rate of 1.4 mN/s for cellulose particles dried from water (blue), toluene (green), pentane (red), and $scCO_2$ (black).

## Conclusion

The morphology of porous cellulose particles have successfully been controlled from the porous to the dense structure in the dry state by changing the evaporating medium during the drying process. By using the drying medium with lower surface tensions, such as pentane, the collapse of the porous structure was suppressed. Moreover, the obtained particles had a higher specific surface area and a lower compressive strength owing to the remaining porous structure. This knowledge is expected to contribute to the simple control of structures and physical strengths of cellulose particles in multitudinous purpose.

## References

1. Eichhorn, S. J., *Soft Matter* **2011,** 7 (2), 303-315.

2. Moon, R. J.; Martini, A.; Nairn, J.; Simonsen, J.; Youngblood, J., *Chem. Soc. Rev.* **2011,** 40 (7), 3941-3994.

3. Nogi, M.; Iwamoto, S.; Nakagaito, A. N.; Yano, H., *Adv. Mater* **2009,** 21 (16), 1595-1598.

4. Du, K.-F.; Yan, M.; Wang, Q.-Y.; Song, H., *J. Chromatogr. A* **2010,** 1217 (8), 1298-1304.

5. Ettenauer, M.; Loth, F.; Thuemmler, K.; Fischer, S.; Weber, V.; Falkenhagen, D., *Cellulose* **2011,** 18 (5), 1257-1263.

6. Gericke, M.; Trygg, J.; Fardim, P., *Chem. Rev.* **2013,** 113 (7), 4812-4836.

7. Glasser, W. G.; Atalla, R. H.; Blackwell, J.; Malcolm Brown, R., Jr.; Burchard, W.; French, A. D.; Klemm, D. O.; Nishiyama, Y., *Cellulose* **2012,** 19 (3), 589-598.

8. Ma, M.; Tan, L.; Dai, Y.; Zhou, J., *Iran. Polym. J.* **2013,** 22 (9), 689-695.

9. Metaxa, A.-F.; Efthimiadou, E. K.; Boukos, N.; Kordas, G., *J. Colloid Interface Sci.* **2012,** 384 (1), 198-206.

10. Sescousse, R.; Gavillon, R.; Budtova, T., *J. Mater. Sci.* **2011,** 46 (3), 759-765.

11. Earle, M. J.; Esperanca, J. M. S. S.; Gilea, M. A.; Canongia Lopes, J. N.; Rebelo, L. P. N.; Magee, J. W.; Seddon, K. R.; Widegren, J. A., *Nature* **2006,** 439 (7078), 831-834.

12. Sheldon, R., *Chem. Commun.* **2001,** 2399-2407.

13. Welton, T., *Chem. Rev.* **1999,** 99 (8), 2071-2083.

14. Swatloski, R. P.; Spear, S. K.; Holbrey, J. D.; Rogers, R. D., *J. Am. Chem. Soc.* **2002,** 124 (18), 4974-4975.

15. Pinkert, A.; Marsh, K. N.; Pang, S. American Chemical Society: 2010; pp AGRO-48.

16. Remsing, R. C.; Swatloski, R. P.; Rogers, R. D.; Moyna, G., *Chem. Commun.* **2006,** 1271-1273.

17. Wang, H.; Gurau, G.; Rogers, R. D., *Chem. Soc. Rev.* **2012,** 41 (4), 1519-1537.

18. Okubo, M.; Konishi, Y.; Sebki, S.; Minami, H., *Colloid Polym. Sci.* **2002,** 280 (8), 765-769.

19. Okubo, M.; Konishi, Y.; Takebe, M.; Minami, H., *Colloid Polym. Sci.* **2000,** 278 (10), 919-926.

20. Tanaka, T.; Okayama, M.; Minami, H.; Okubo, M., *Langmuir* **2010,** 26 (14), 11732-11736.

21. Suzuki, T.; Kono, K.; Shimomura, K.; Minami, H., *J. Colloid Interface Sci.* **2014,** 418, 126-131.

22. Imagawa, K.; Omura, T.; Ihara, Y.; Kono, K.; Suzuki, T.; Minami, H., *Cellulose* **2017,** 24 (8), 3111-3118.

23. Omura, T.; Imagawa, K.; Kono, K.; Suzuki, T.; Minami, H., *ACS Appl. Mater. Interfaces* **2017,** 9 (1), 944-949.

24. Buchtova, N.; Budtova, T., *Cellulose* **2016,** 23 (4), 2585-2595.

25. Cai, J.; Kimura, S.; Wada, M.; Kuga, S.; Zhang, L., *ChemSusChem* **2008,** 1 (1-2), 149-154.

26. Isobe, N.; Kim, U.-J.; Kimura, S.; Wada, M.; Kuga, S., *J. Colloid Interface Sci.* **2011,** 359 (1), 194-201.

27. Jin, H.; Nishiyama, Y.; Wada, M.; Kuga, S., *Colloids Surf., A* **2004,** 240 (1-3), 63-67.

28. Mi, Q.-y.; Ma, S.-r.; Yu, J.; He, J.-s.; Zhang, J., *ACS Sustainable Chem. Eng.* **2016,** 4 (3), 656-660.

29. Lindh, J.; Ruan, C.; Stroemme, M.; Mihranyan, A., *Langmuir* **2016,** 32 (22), 5600-5607.

30. Enders, S.; Kahl, H.; Winkelmann, J., *J. Chem. Eng. Data* **2007,** 52 (3), 1072-1079.

31. Mohsen-Nia, M.; Rasa, H.; Naghibi, S. F., *J. Chem. Thermodyn.* **2009,** 42 (1), 110-113.

# *Chapter 2*

## Preparation of Disk-like Cellulose Particles

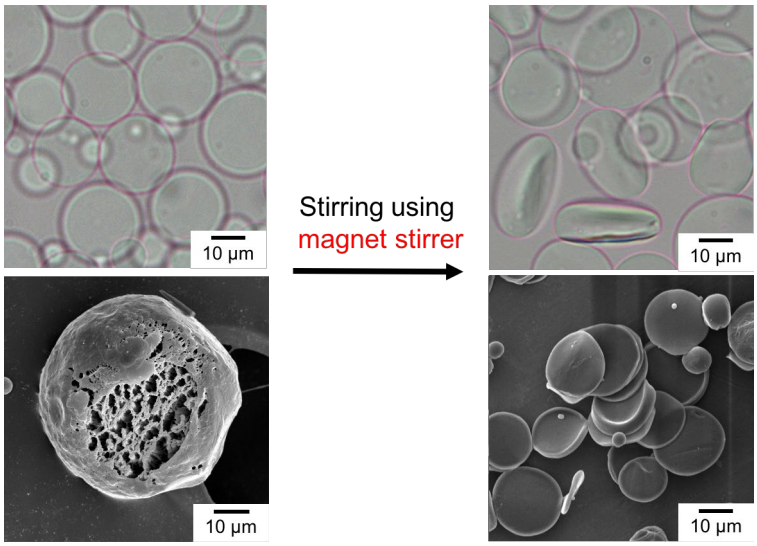


**Abstract:** Disk-like cellulose particles were facilely prepared by stirring a dispersion of porous cellulose particles, which were prepared by the solvent releasing method (SRM), with a magnetic stir bar. The obtained particles had thick and disk-like morphologies, and retained their porous structures in the wet state. The thick and disk-like particles became thinner in a specific direction upon drying because of capillary force as media evaporated. In contrast, when the same procedure was applied on cellulose particles having dense structures, the particle shapes did not change. Moreover, when stirring process was carried out using a shaking bath or a touch mixer, the shape transformation was not observed. These results suggest that the porous structures of cellulose particles would be a pseudo-plasticization state, which could cause the cellulose particles to deform. The disk-like particles formed as a result of the grinding of porous cellulose particles between the stir bar and the vial. In addition, the number of disk-like particles and the degree of deformation increased with increase in the stirring time, the speed, and the contact areas between stir bars and the vessels.

## Introduction

Cellulose is the most abundant natural polymer on Earth. It is extensively used in industrial materials such as regenerated fibers and pulp because it is chemically stable and biodegradable.[1-2] In recent years, cellulose particles have been recognized as promising carrier particles and as materials for immunochromatography because of their capacity for the nonspecific adsorption of proteins and surface functionalization.[3-6] However, cellulose is insoluble in water and in most organic solvents due to hydrogen bonding network at a molecular level. Recently, it is debating that the solubility or insolubility properties of cellulose are based on the its hydrophobic and amphiphilic molecular interactions (the Lindman hypothesis).[7] Therefore, for dissolving cellulose and controlling particle shape, multistep processes or harsh conditions is necessary.[8-9]

Ionic liquids (ILs), which consist entirely of organic ions but are in a liquid state at ambient temperature, have attractive attention because of their low vapor pressures, highly thermal stability, and non-flammability. Moreover, they can be good solvents for organic and inorganic materials which are insoluble in most conventional solvents.[10-12] In 2002, Rogers et al. reported that ILs such as 1-butyl-3-methylimidazolium chloride ([Bmim]Cl) can dissolve cellulose under mild heat treatment.[13] Thereafter, ionic liquids have attracted increasing interest as solvents for cellulose.[14-16]

Utilizing this knowledge, Minami *et al*. have reported the successful preparation of cellulose particles with porous structures using a [Bmim]Cl solution of cellulose by the solvent releasing method (SRM)[17].

Other than SRM, cellulose particles have been prepared via various methods, including the viscose process.[18-20] However, to the best of our knowledge, most of cellulose particles was

spherical in shape, and few papers have been reported flake-shape cellulose particles.[21] Therefore, controlling morphology of cellulose particles remains a challenge.

Interestingly, in the previous study, non-spherical cellulose particles were observed via optical microscopy when wet, porous cellulose particles were stirred with a magnetic stir bar for several hours and disk-like cellulose particles were obtained upon drying. Such disk-like particles are expected to contribute to various fields such as cosmetics and biomedicine.

***Chapter 2*** shows demonstrated the preparation of disk-like cellulose particles and attempted to clarify their formation mechanism by changing different treatment conditions.

## Experimental Section

### Materials

Microcrystalline cellulose (powder, derived from cotton linter) and [Bmim]Cl were used as received from Aldrich Chemical Co. Ltd. Acetone, *N*,*N*-dimethylformamide (DMF), *n*-hexane, and 1-butanol were used as received from Nacalai Tesque Inc. (Kyoto, Japan). Polydimethylsiloxane surfactant VPS-1001 (JNC Co.; Tokyo, Japan) was also used as received.

### Preparation of Cellulose Particles

Cellulose particles were prepared via SRM in accordance with the procedures in our previous report.[17, 22] Microcrystalline cellulose powder was dissolved in ionic liquid with a weight ratio of 7 to 43 by heating at 100°C for 7 h. To reduce the viscosity of the solution, DMF was added as a co-solvent. The solution of cellulose–[Bmim]Cl–DMF (7/43/50, w/w/w; 0.2 g) was mixed with hexane (2.0 g) as a continuous phase containing dissolved VPS-1001 (0.25 wt% hexane) as a colloidal stabilizer and stirred at 4000 rpm for 5 min using a homogenizer (BM-1; Nihonseiki Kaisha Ltd.; Tokyo, Japan) or a Shirasu Porous Glass (SPG) membrane (pore size = 30 μm; SPG12G30-30U, SPG TECHNOLOGY Co., Ltd.; Miyazaki, Japan) to prepare a dispersion. The obtained dispersion was poured into a large amount of 1-butanol (*ca.* 20 g) under stirring to remove [Bmim]Cl and DMF from the cellulose–[Bmim]Cl–DMF droplet wherein cellulose was precipitate to form cellulose particles. The precipitated particles were washed three times with 1-butanol to remove any remaining components.

### Preparation of Disk-like Cellulose Particles

The dispersion containing cellulose particles prepared by SRM (*ca.* 1.3 mL, dispersed in 1-butanol; particles concentration: 1.3 wt%) was stirred using different stirring methods for

different periods of time at room temperature.

**Characterizations**

Cellulose particles were observed by optical microscopy (ECLIPSE 80i, Nikon, Tokyo, Japan) and scanning electron microscopy (SEM, JSM-6510, JEOL Ltd., Tokyo, Japan). In the case of observing $scCO_2$-dried cellulose particles, the drying process of cellulose particles was as follows. First, cellulose particles dispersed in acetone were putted into a 25 mL stainless-steel reactor, and the reactor was pressurized with liquid $CO_2$ to 15 MPa at room temperature using a high-pressure pump. Next, $CO_2$ and acetone were vented out from the reactor. Before all of the liquid $CO_2$ and acetone evaporated (2 MPa), liquid $CO_2$ was added until the pressure reached 15 MPa. This process was repeated at least eight times to ensure the complete removal of acetone from the reactor. The reactor was subsequently dipped into a temperature-controlled water bath at 40˚C, in which $CO_2$ should exist as $scCO_2$. Finally, $scCO_2$ was vented out slowly from the reactor to obtain $scCO_2$-dried cellulose particles.

Qualitative analyses of the products were conducted on a Fourier transform infrared spectrometer (FT-IR; FT/IR-6200, JASCO Corporation, Tokyo, Japan) using a pressed KBr pellet technique and X-ray diffractometer (XRD, RINT-TTR, Rigaku Co. Ltd.) using $2\theta/\theta$ method with Cu Kα radiation (λ= 1.5418 Å) generated at 50 kV and 300 mA at a scanning rate of 4°/min.

## Results and Discussion

***Preparation of disk-like cellulose particles and characterization***

Cellulose particles were prepared by SRM, in which a dispersion consisting of [Bmim]Cl-DMF droplets containing dissolved cellulose and hexane medium was poured into a large amount of 1-butanol. The obtained particles were well dispersed in 1-butanol without coagulation. Figure 1 shows FT-IR spectra of the obtained particles at each washing step. Just after SRM, the characteristic peak of [Bmim]Cl still appeared at around 1600 $cm^{-1}$, showing that [Bmim]Cl remained in the particles as [Bmim]Cl, which is non-volatile and should not evaporate during the drying process. However, the peak disappeared after the 1st washing, and the spectrum of the washed particles was consistent with that of pure cellulose (Figure 1b-d). These results indicate that the obtained particles comprised almost pure cellulose after washing.

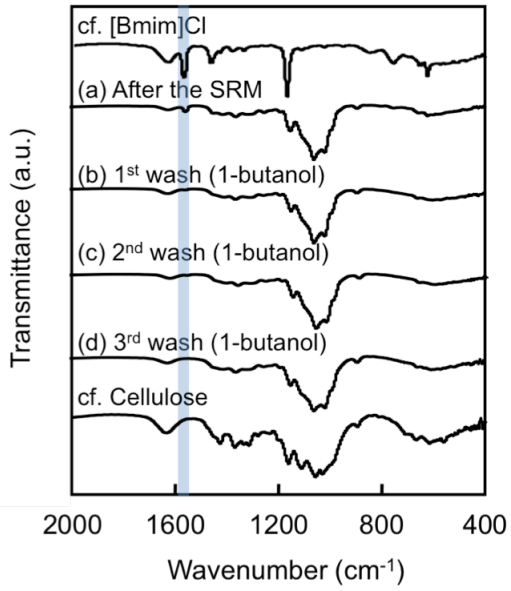


**Figure 1.** FT-IR spectra of cellulose particles prepared by SRM using 1-butanol for cellulose–[Bmim]Cl–DMF (7/43/50, w/w/w) droplets dispersed in hexane, followed by wash processes with 1-butanol. Wash process: (a) after the SRM; (b) 1st wash; (c) 2nd wash; (d) 3rd wash.

Figure 2 shows XRD spectra of microcrystalline cellulose powder and cellulose particles prepared by SRM after washing. The microcrystalline cellulose showed typical spectrum of cellulose I type crystal (Figure 2a). On the other hand, the particles showed a different broad spectrum, which was attributed to cellulose II type with very small crystal,[23] indicating that the cellulose was completely dissolved in [Bmim]Cl.

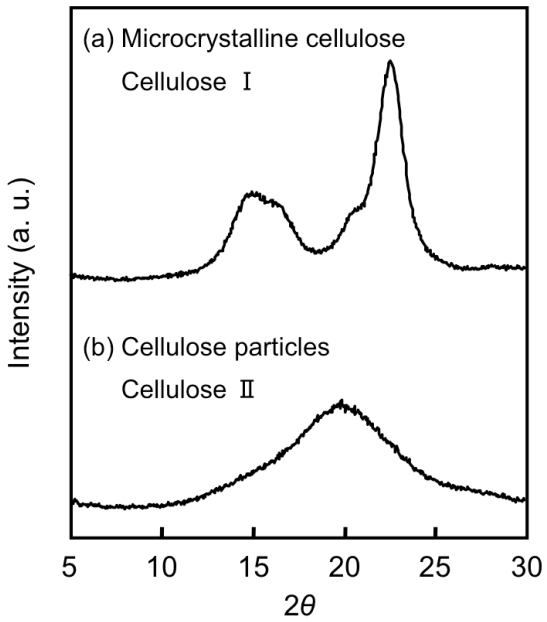


**Figure 2.** XRD spectra of microcrystalline cellulose powder (a) and cellulose particles prepared by SRM using 1-butanol for cellulose–[Bmim]Cl–DMF (7/43/50, w/w/w) droplets dispersed in hexane.

Figure 3a, b, c show optical micrographs and SEM image of a dispersion of cellulose particles before and after drying. When the dispersion of cellulose particles was allowed to stand without stirring, the particles retained their spherical shape; upon drying, the particles shrank as medium evaporated, and spherical shapes were maintained, indicating that the obtained cellulose particles possessed fragile porous structures before drying (Figure 3d). On the contrary, when a dispersion was stirred at 800 rpm for 4 h using a magnetic stir bar at room temperature, the cellulose particles deformed into thick, non-spherical (disk-like) shapes (Figure 3e). Moreover, after drying, thin and disk-like particles were observed (Figure 3f); these

particles resulted from the shrinking (primarily in the vertical direction) of the non-spherical cellulose particles due to a capillary force during the drying process. In addition, the fine porous structures were retained when the non-spherical particles were freeze-dried (Figure 3g). On the other hand, when alternative stirring methods (shaking in a shaker bath or touch mixer for 4 h) were employed on porous and spherical cellulose particles, the cellulose particles were not deformed (Figure 3h–k). These results strongly suggest that the deformation of the spherical cellulose particles to disk-like particles resulted from stirring.

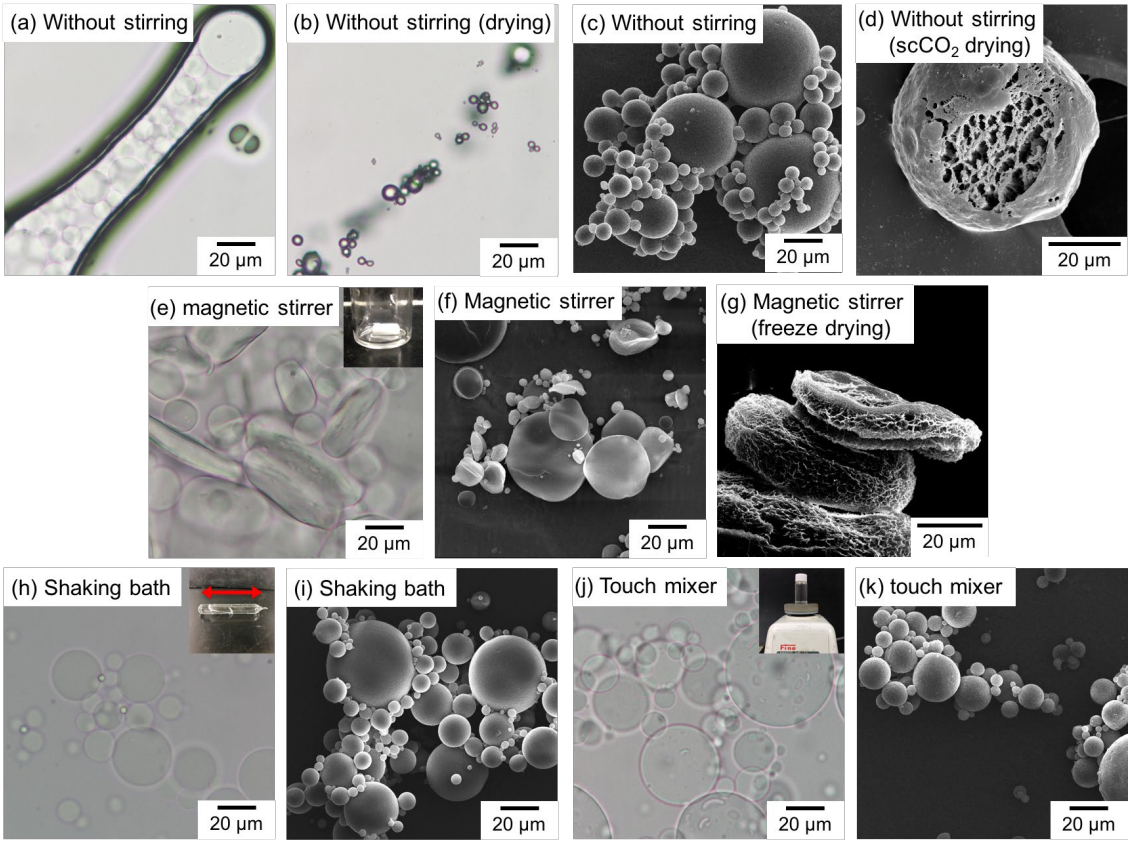


**Figure 3.** Optical micrographs (a, b, e, h, and j) and SEM images (c, d, f, g, i, and k) of cellulose particles, prepared by SRM using 1-butanol for cellulose–[Bmim]Cl–DMF (7/43/50, w/w/w) droplets, without stirring (a–d), with stirring using a magnetic stir bar (800 rpm) (e–g), shaking bath (h and i), or touch mixer (j and k) for 4 h at room temperature. Drying method: (d) $scCO_2$ drying; (g) freeze drying.

It should be noted that the obtained particles were very polydisperse (around sub-micronmeter–several tens of micrometers) because the primary droplets were prepared by mechanical agitation using a homogenizer. On the other hand, in the case of using SPG membrane emulsification, the obtained cellulose particles were relatively monodisperse (Figure 4) and the size of droplets can be controlled by changing SPG pore sizes, which indicates size-controlled monodisperse disk-like particles can be prepared. However, to investigate the effect of particle size to deformation simultaneously, polydisperse cellulose particles were used hereafter.

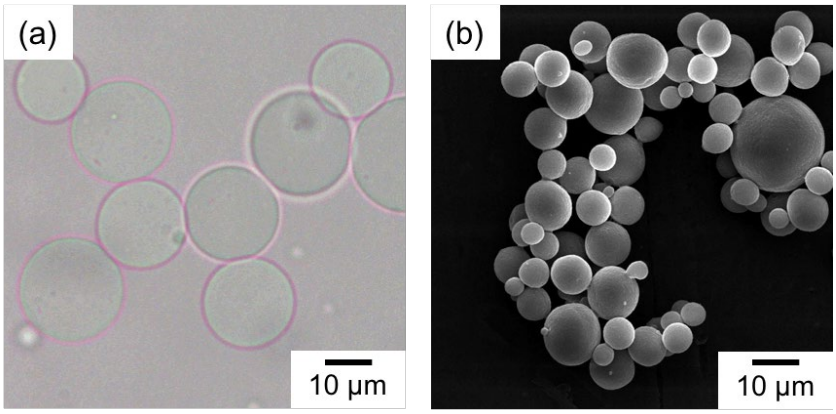


**Figure 4.** Optical micrograph (a) and SEM image (b) of cellulose particles prepared by SRM using 1-butanol for cellulose–[Bmim]Cl–DMF (7/43/50, w/w/w) droplets dispersed in hexane by SPG membrane emulsification.

***Morphology Control of disk-like cellulose particles***

In order to investigate effect of stirring on deformation of cellulose particles, dispersions of cellulose particles were stirred using a stir bar for various times and stirring speeds. With increase in stirring time with fixed stirring speed (500 rpm), the number of disk-like particles increased and almost all particles were deformed after 12 h (Figure 5). Moreover, large particles were preferentially deformed. In the case of other stirring speed, same tendency was observed.

Upon varying the stirring speed, it was found that the number of disk-like particles and the degree of deformation increased with increase in stirring speed (Figure 6).

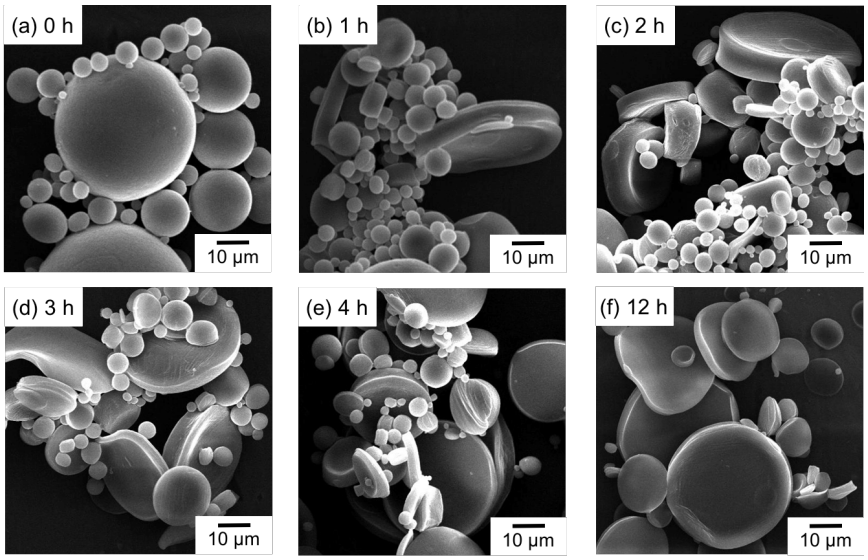


**Figure 5.** SEM images of cellulose particles, prepared by SRM using 1-butanol for cellulose–[Bmim]Cl–DMF (7/43/50, w/w/w) droplets, under stirring at room temperature and 500 rpm for various times (hours): (a) 0; (b) 1; (c) 2; (d) 3; (e) 4; (f) 12.

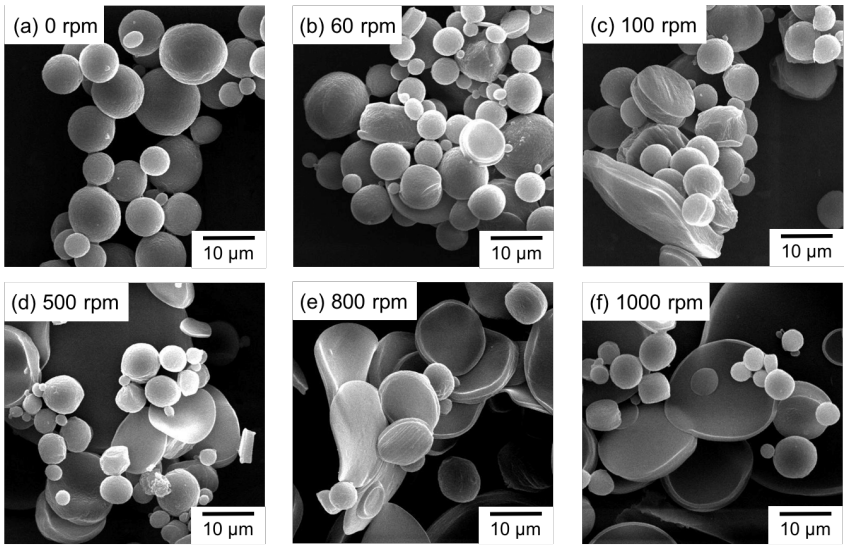


**Figure 6.** SEM images of cellulose particles, prepared by SRM using 1-butanol for cellulose–[Bmim]Cl–DMF (7/43/50, w/w/w) droplets dispersed in hexane, under stirring at room temperature for 4 h at different stirring speeds (rpm): (a) 0; (b) 60; (c) 100; (d) 500; (e) 800; (f) 1000.

To investigate effect of stir bar shape on cellulose particle deformation, stir bars with various shapes were used. Figure 7 shows the obtained cellulose particles after stirring with pentagon-shaped, stick-shaped, and cross-shaped stir bars; the contact areas between the bottom of the vial and these stir bars were approximately 0.50, 8.0, and 11.1 $mm^2$, respectively. The degree of particle deformation increased as the contact area was increased, suggesting that the main deformation mechanism of the disk-like cellulose particles is the compression of porous cellulose particles between the stir bar and the vessel during stirring. Moreover, cellulose particles had rigid-skin surface layers and porous structures, which were maintained after $scCO_2$-drying (Figure 3d). The rigid-skin layers would be cracked by the compression during stirring. Thus, in addition to compression, the deformation mechanism should include particle shrinkage in the vertical direction to the crack, which was easy to deform by the drying.

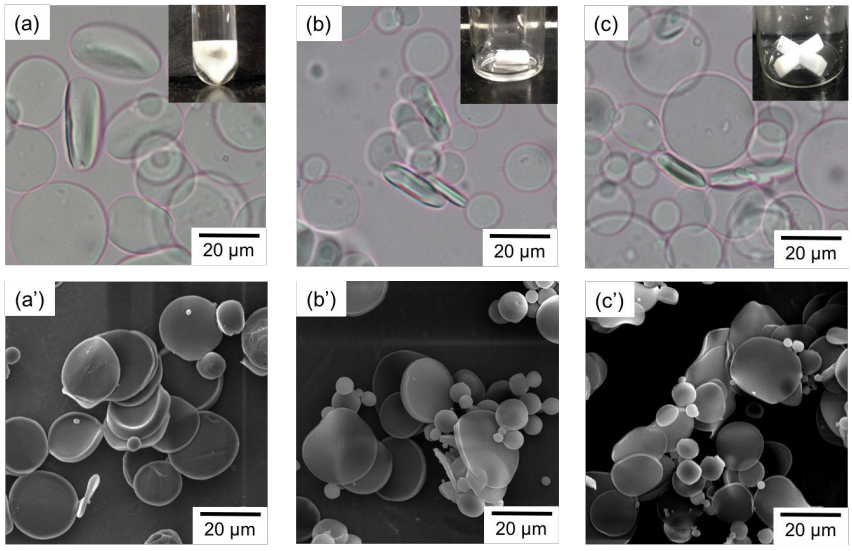


**Figure 7.** Optical micrographs (a–c) and SEM images (a'–c') of cellulose particles, prepared by SRM using 1-butanol for cellulose–[Bmim]Cl–DMF (7/43/50, w/w/w) droplets, under stirring at room temperature and 500 rpm for 4 h with different stir bars: (a, a′) pentagon-shaped; (b, b′) stick-shaped; (c, c′) cross-shape.

To further investigate the mechanism of deformation of cellulose particles, a dispersion of cellulose particle with dense structures which were redispersed in 1-butanol after drying (Figure 8a) was stirred with a stick-shaped stir bar at 800 rpm for 4 h. The morphology of cellulose particles did not deform after stirring (Figure 8b) even if the stirring time and speed increased. This results suggests that the porous structures are necessary for the formation of the disk-like morphology because the porous structure of cellulose particles would be sort of plasticization state by containing a lot of media in the particles.[24]

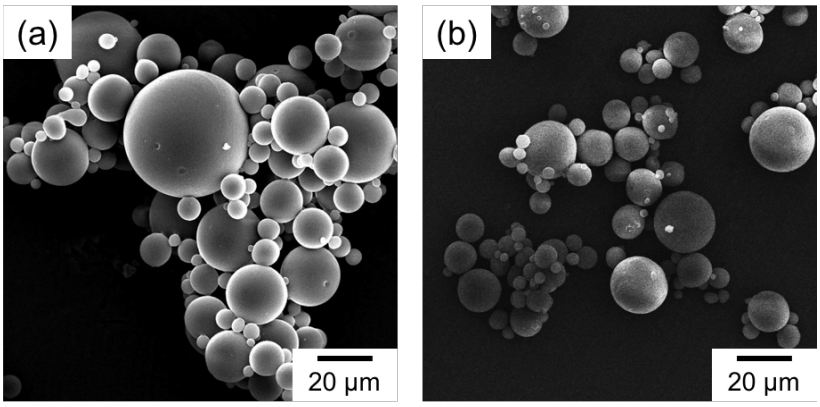


**Figure 8.** SEM images of dense cellulose particles redispersed in 1-butanol after drying (a), followed by stirring process with a stick-shaped stir bar at 800 rpm for 4 h.

## Conclusion

Disk-like Cellulose particle have successfully been prepared and their formation mechanism was clarified: the porous structures of precursor cellulose particles and the direction of shrinkage of the particles at drying were found to be important factors in the formation of disk-like cellulose particles. Moreover, it has been found that the number of disk-like particles and the degree of deformation increased with increase in stirring time, speed, and contact areas between stir bars and the vessels. The obtained disk-like cellulose particles are expected to be applied in various fields, such as cosmetics and medicals.

## References

1. Sannino, A.; Demitri, C.; Madaghiele, M., *Materials* **2009,** 2 (2), 353-373.

2. Zhang, L.; Liu, H.; Zheng, L.; Zhang, J.; Du, Y.; Feng, H., *Industrial & Engineering Chemistry Research* **1996,** 35 (12), 4682-4685.

3. Breier, A.; Gemeiner, P.; Hagarova, D., *Chem. Pap.* **1994,** 48 (3), 141-5.

4. Butun, S.; Ince, F. G.; Erdugan, H.; Sahiner, N., *Carbohydr. Polym.* **2011,** 86 (2), 636-643.

5. Nagaoka, S.; Ihara, H.; Honbo, J.; Hirayama, C.; Kurisaki, H.; Ikegami, S., *Anal. Sci.* **1994,** 10 (4), 543-551.

6. Nagaoka, S.; Nagata, M.; Arinaga, K.; Shigemori, K.; Takafuji, M.; Ihara, H., *Coloration Technology* **2007,** 123 (6), 344-350.

7. Glasser, W. G.; Atalla, R. H.; Blackwell, J.; Malcolm Brown, R., Jr.; Burchard, W.; French, A. D.; Klemm, D. O.; Nishiyama, Y., *Cellulose* **2012,** 19 (3), 589-598.

8. Cai, J.; Zhang, L. *Macromolecular Bioscience* **2005,** 5 (6), 539-548.

9. Kim, C.-W.; Kim, D.-S.; Kang, S.-Y.; Marquez, M.; Joo, Y. L., *Polymer* **2006,** 47 (14), 5097-5107.

10. Chiappe, C.; Pieraccini, D., *J. Phys. Org. Chem.* **2005,** 18 (4), 275-297.

11. Fredlake, C. P.; Crosthwaite, J. M.; Hert, D. G.; Aki, S. N. V. K.; Brennecke, J. F., *Journal of Chemical & Engineering Data* **2004,** 49 (4), 954-964.

12. Ngo, H. L.; LeCompte, K.; Hargens, L.; McEwen, A. B., *Thermochim. Acta* **2000,** 357-358, 97-102.

13. Swatloski, R. P.; Spear, S. K.; Holbrey, J. D.; Rogers, R. D., *J. Am. Chem. Soc.* **2002,** 124 (18), 4974-4975.

14. Pinkert, A.; Marsh, K. N.; Pang, S.; Staiger, M. P., *Chem. Rev.* **2009,** 109 (12), 6712-6728.

15. Remsing, R. C.; Swatloski, R. P.; Rogers, R. D.; Moyna, G., *Chem. Commun.* **2006,** (12), 1271-1273.

16. Wang, H.; Gurau, G.; Rogers, R. D., *Chem. Soc. Rev.* **2012,** 41 (4), 1519-1537.

17. Suzuki, T.; Kono, K.; Shimomura, K.; Minami, H., *J. Colloid Interface Sci.* **2014,** 418, 126-131.

18. Du, K.-F.; Yan, M.; Wang, Q.-Y.; Song, H., *J. Chromatogr. A* **2010,** 1217 (8), 1298-1304.

19. Nagaoka, S.; Arinaga, K.; Kubo, H.; Hamaoka, S.; Sakurai, T.; Takafuji, M.; Ihara, H., *Polym. J.* **2005,** 37 (3), 186-191.

20. Zhang, J.; Elder, T. J.; Pu, Y.; Ragauskas, A. J., *Carbohydr. Polym.* **2007,** 69 (3), 607-611.

21. Araki, K.; Kaneko, S.; Matsumoto, K.; Nagatani, A.; Tanaka, T.; Arao, Y., *Advanced Materials Research* **2014,** 844, 318-321.

22. Omura, T.; Imagawa, K.; Kono, K.; Suzuki, T.; Minami, H., *ACS Appl. Mater. Interfaces* **2017,** 9 (1), 944-949.

23. Nam, S.; French, A. D.; Condon, B. D.; Concha, M., *Carbohydr. Polym.* **2016,** 135, 1-9.

24. Liu, B.; Wang, D., *Langmuir* **2012,** 28 (15), 6436-64

# *Chapter 3*

## Preparation of Cellulose Particles Having Hollow Structure

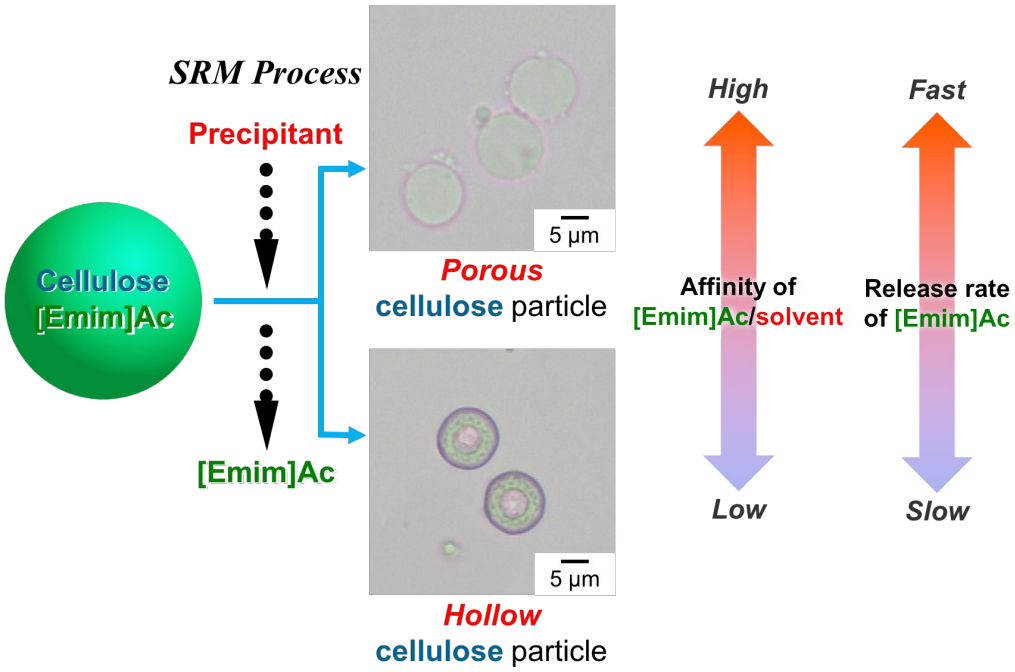


**Abstract:** Cellulose particles with different morphologies were prepared by the solvent-releasing method (SRM); a dispersion consisting of 1-ethyl-3-methylimidazolium acetate ([Emim]Ac) droplets containing cellulose in hexane medium was added to large amounts of different solvents that acted as cellulose precipitants. Porous structures were obtained using precipitants with high affinity for [Emim]Ac, namely ethanol and t-butanol. On the contrary, the use of acetone and n-octanol, which have low affinity for [Emim]Ac, resulted in hollow structures. Moreover, the release rate of [Emim]Ac from the cellulose–[Emim]Ac solution into the solvent decreased with the precipitant's affinity for [Emim]Ac, contributing to the formation of such hollow structures.

## Introduction

Hollow polymer particles have been attracting much attention due to their characteristics,[1, 2] especially their low density[3] and the possibility of encapsulating different materials in their hollow structure.[4] They are used in many fields and applications, such as coatings, cosmetics,[2, 5, 6] drug delivery,[3] medical diagnostics,[7] and catalysis.[8] Various preparation methods have been developed,[9] including suspension polymerization,[10, 11] interfacial polymerization,[12] layer-by-layer process,[13] emulsion evaporation,[14] self-assembly of amphiphilic block copolymers,[15] and self-templating shell-selective crosslinking.[16]

Cellulose is the most abundant renewable biopolymer on Earth and has many attractive properties, such as thermal and chemically stability, nontoxicity, biocompatibility, and biodegradability;[17] thus, it is used extensively in various applications, including such as pulp, regenerated fibers, and membranes.[18] Cellulose particle have been recognized recently as functional materials[19] to be used in removers for organic substances or metals,[20, 21] biochromatography;[22] protein immobilization,[19] and drug carriers[23] due to their low nonspecific adsorption of proteins[24] and surface modification capability.[25, 26] Those with a hollow structure have also attracted considerable attention in various fields; however, there are a few reports about the preparation of hollow cellulose particles and their fabrication is complicated, Carrick et al. synthesized the fabrications of hollow cellulose capsules via the microfluidic method[27] and the solution precipitation method by using a suitable gas.[28] Moreover, the dissolution of cellulose needs multistep processes or drastic conditions as cellulose is insoluble in water and most organic solvents because of its hydrogen bonding and hydrophobic interaction.

In 2002, Rogers et al.[29] were able to dissolve cellulose in ionic liquids (ILs) such as 1-butyl-3-methylimidazolium chloride ([Bmim]Cl) under mild heating conditions; thereafter,

many researchers have been using ILs as solvents to control the morphology of cellulose materials.[30-32] Using this knowledge, Minami et al. successfully prepared porous cellulose particles[33-35] via the solvent-releasing method (SRM),[36] in which a dispersion of [Bmim]Cl–*N*,*N*-dimethylformamide (DMF) droplets containing dissolved cellulose in hexane medium was poured into a large amount of 1-butanol. As 1-butanol is miscible with [Bmim]Cl and DMF but cannot dissolve cellulose, [Bmim]Cl and DMF were released from the droplets, while cellulose precipitated, forming porous particles. However, the morphology control of cellulose particles is still challenging and crucial for their applications as functional materials.

In ***Chapter 3***, the precipitant of cellulose particles with a hollow structure via the SRM by using the IL, 1-ethyl-3-methylimidazolium acetate ([Emim]Ac) without a co-solvent. Their formation mechanism was also discussed according to the preparation conditions.

# Experimental Section

## Materials

Cellulose materials with different number-average molecular weights ($M_n$) were used: microcrystalline cellulose powder (derived from cotton linter, $M_n = 3.0 \times 10^4$ from the literature;[37] Aldrich Chemical Co., Ltd.), cellulose powder ($M_n = 1.0 \times 10^5$; Nacalai Tesque Inc., Kyoto, Japan), and Whatman No. 1 filter paper ($M_n = 3.2 \times 10^5$ from the literature[38]). [Emim]Ac was ued as received from Aldrich Chemical Co., Ltd. Ethanol, *t*-butanol, *n*-octanol, *n*-hexane, and acetone (Nacalai Tesque Inc.) were used. Polydimethylsiloxane surfactant (VPS-1001, Wako Pure Chemical Industries, Ltd.) and polyoxyethylene sorbitan monooleate (Tween 81, HLB 10.0; Kao-Atlas Co., Ltd.) were also used. All these materials were used as received. The water for the experiments, purified using an ErixUV purification system (Millipore), had a resistivity of 18.2 MΩ cm.

## Preparation of Cellulose Particles by the SRM

Cellulose particles were prepared via the SRM by following the procedure described in ***Chapter 1***. Cellulose was dissolved in [Emim]Ac on heating at 100°C for 5 h and its homogeneous solution (cellulose concentration of 5, 10, or 15 wt% based on the solution, 0.2 g) was mixed with n-hexane (2.0 g) containing dissolved VPS-1001 (0.25 wt% of hexane) as a colloidal stabilizer. This mixture was homogenized by a homogenizer (BM-1, Nihonseiki Kaisha Ltd.) at 8000 rpm for 5 min and a Shirasu porous glass (SPG) membrane (pore size = 20 μm; SPG12G20-20U, SPG TECHNOLOGY Co., Ltd.) which was used to control size of droplets. The resulting dispersion was added to acetone, ethanol, t-butanol, or n-octanol ([Emim]Ac:precipitant = 1:200 (w/w)); the obtained particles were washed three times with acetone, ethanol, and water to remove any remaining impurities.

**Release Rate of Ionic Liquid into the Precipitant**

The release rate of [Emim]Ac from the cellulose–[Emim]Ac droplets was estimated as follows. A mixture of hexane (4.0 g) and a precipitant (36 g; [Emim]Ac:precipitant = 1:100 (w/w)) was poured into a cellulose–[Emim]Ac solution (0.4 g) in a 50 mL glass beaker and, then, magnetically stirred at 100 rpm; a part of the supernatant was sampled at decided time intervals, in which released [Emim]Ac should be contained. The extracted supernatants were dried in a vacuum oven at 80°C to evaporate the hexane and precipitant. The [Emim]Ac concentration in the supernatant was evaluated by measuring the weight of the supernatant before and after drying.

**Characterization**

The as-prepared cellulose particles were observed with an optical microscope (ECLIPSE 80i, Nikon Corp.), a scanning electron microscope (SEM, JSM-6510, JEOL Ltd.), and a transmission electron microscope (TEM, JEM-1230, JEOL Ltd.) operated at 100 kV. To analyze the inner morphology of the particles, dried samples were embedded in epoxy matrixes, cured at 40°C for 24 h, and subsequently sliced by using cryomicrotome (Leica EM UC6 equipped with EM FC7) at –140°C. Before the SEM and TEM analysis, cellulose particles prepared by using ethanol or *t*-butanol as precipitants were immersed in liquid nitrogen, freeze-dried in a freeze-dryer (FDU-1200, Tokyo Rikakikai Co., Ltd.; Tokyo, Japan); the other cellulose particles were dried in a vacuum condition at room temperature. The interfacial tensions were measured via the pendant drop method at room temperature (ca. 20°C) by using a Drop Master 500 (Kyowa Interface Science Co., Ltd.).

## Results and Discussion

### *Preparation of Hollow Cellulose Particles*

Cellulose particles were prepared via the SRM; a dispersion consisting of cellulose–[Bmim]Cl–DMF droplets in hexane medium was poured into a large amount of 1-butanol. [Bmim]Cl and DMF were immediately released from the droplets into 1-butanol, while the cellulose precipitated, forming a porous structure. DMF was added as the co-solvent to reduce the viscosity of the cellulose–[Bmim]Cl solution. However, the formation mechanism of this hollow structure was difficult to discuss in terms of [Bmim]Cl affinity with a precipitant. Thus, to investigate the effect of the precipitant on the final morphology, cellulose particles were prepared using [Emim]Ac. As [Emim]Ac also dissolves cellulose and its viscosity is much lower than [Emim]Ac, there is no need for a co-solvent. The precipitants, ethanol, *t*-butanol, *n*-octanol, and acetone were used with different values of the Hildebrand solubility parameter (SP): 26.0, 21.7, 20.9, and 20.1 $MPa^{1/2}$,[39] respectively. A precipitant with lower SP should have lower affinity for [Emim]Ac (32.1 $MPa^{1/2}$).[40]

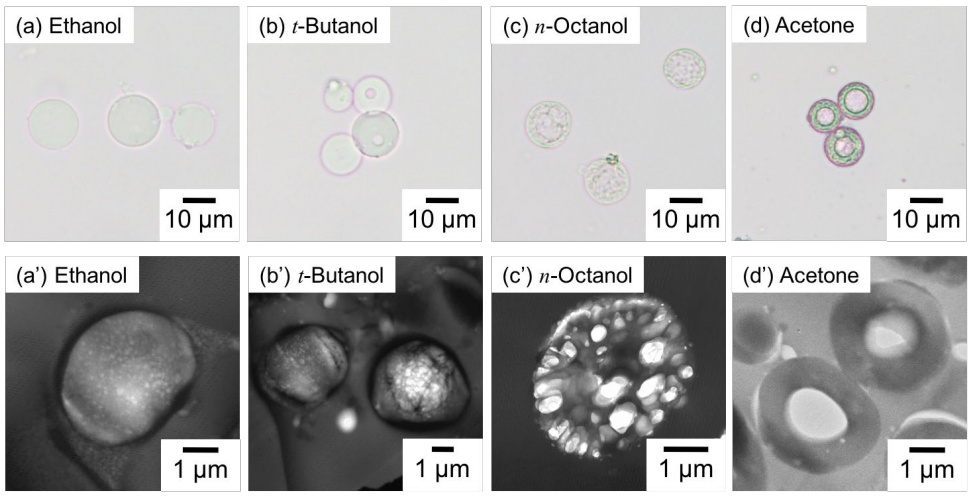


**Figure 1.** Optical micrographs (top row) and TEM images of ultrathin cross-sections (bottom row) of cellulose particles prepared via the SRM using ethanol (a, a'), *t*-butanol (b, b'), *n*-octanol (c, c'), and acetone (d, d') as precipitants ([Emim]Ac:precipitant = 1:200 (w/w)) for cellulose–[Emim]Ac (10/90, w/w) droplets.

Figure 1 shows the optical micrographs and TEM images of ultrathin cross-sections of the cellulose particles prepared by using the different precipitants; the use of ethanol and *t*-butanol resulted in porous structures, as is the case of 1-butanol; the particles prepared using *n*-octanol showed not a porous structure, but a multi-hollow structure; in the case of acetone, the particles exhibited a hollow structure. These results indicate that a hollow structure probably forms when using a precipitant with low affinity for [Emim]Ac.

However, in the case of acetone, the hollow structure was not observed at the beginning of the SRM process (after 1 min) and the phase separation of cellulose proceeded gradually; it became clearly visible after 10 min (Figure 2). On the other hand, ethanol led to the formation of a porous structure formed within ca. 30 s.[33] This suggests that [Emim]Ac was released slowly into acetone, while cellulose precipitated gradually in the droplets. Therefore, the [Emim]Ac release rate into a precipitant should be a crucial factor for the morphology control of cellulose particles.

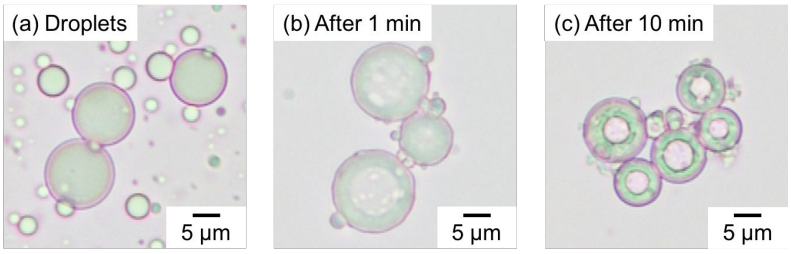


**Figure 2.** Optical micrographs of cellulose–[Emim]Ac (10:90, w/w) droplets dispersed in hexane containing dissolved VPS-1001 as a stabilizer before (a), 1 min after (b), and ca. 10 min after (c) the addition of acetone.

To investigate the release rate of [Emim]Ac from the primary droplets, its amount released into the precipitant was monitored. However, as it was difficult to measure this directly in the dispersion system, the measurements were conducted in a bulk system: a mixture of

hexane and a precipitant was added to the cellulose–[Emim]Ac solution. Therefore, small amounts of precipitant containing [Emim]Ac were taken for this analysis. Figure 3 shows the derived relationship between the contact time and the [Emim]Ac concentration released from cellulose–[Emim]Ac solutions (10 wt%) into the various precipitants. [Emim]Ac was released completely into each solvent after 24 h; however, as expected, the lower the precipitant affinity for [Emim]Ac, the slower the [Emim]Ac release rate, and consequently, the slower the cellulose precipitation. This suggests that the [Emim]Ac release rate significantly determines the morphology of cellulose particles prepared via the SRM.

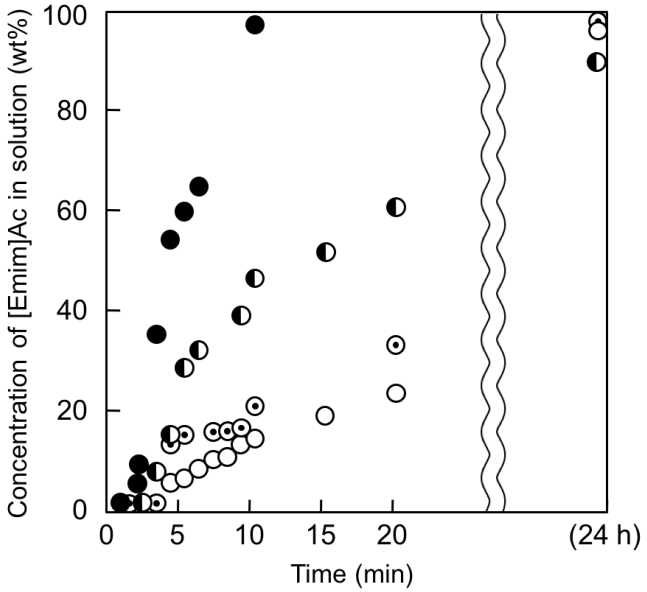


**Figure 3.** Concentration of [Emim]Ac released from cellulose–[Emim]Ac solution into ethanol (closed circles), *t*-butanol (left-closed circles), *n*-octanol (center-closed circles), and acetone (open circles) over time.

According to these results, the following formation mechanism is proposed. When using a precipitant with a high affinity for [Emim]Ac, solvent exchange of [Emim]Ac and precipitant proceeds rapidly, and then, phase separation of cellulose and [Emim]Ac is arrested in a short time. Consequently, the cellulose precipitates immediately in droplets after starting

the phase separation, forming a porous cellulose network. On the other hand, when using a precipitant with a low affinity for [Emim]Ac, [Emim]Ac and the precipitant slowly diffuse into each other. This slow diffusion process delays the time when a phase separated structure is pinned and a motion of cellulose is arrested. As a result, cellulose molecules, which can be thought of as an amphiphilic molecule,[41] can diffuse and should adsorb at the inner interface between the [Emim]Ac droplet and the precipitant to reduce the interfacial tension. In the case of fast precipitation, the particle morphology is determined by the cellulose precipitation rate; thus, it is controlled mainly by kinetics. In the case of slow precipitation, instead, there is time for cellulose molecules to diffuse to the inner interface of the droplet before motion of cellulose molecules are arrested and precipitates. To test whether cellulose molecules would diffuse to the inner interface, the interfacial tension ($\gamma$) between the precipitant and [Emim]Ac containing dissolved cellulose was measured as a function of the cellulose concentration.

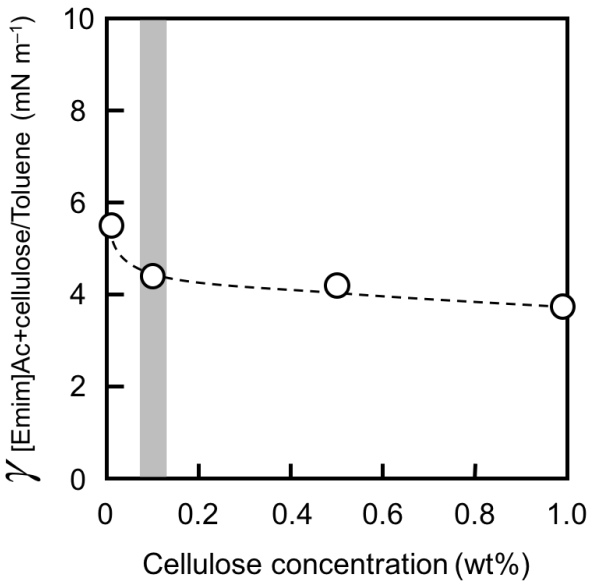


**Figure 4.** Interfacial tensions between toluene and [Emim]Ac containing dissolved cellulose as a function of the cellulose concentration, measured by the pendant drop method at room temperature; the dashed line is shown to guide the eye.

However, this measurement was difficult in the case of acetone ($\gamma_{cellulose\text{-}IL/acetone}$) because cellulose precipitated gradually at the interface while performing the pendant drop method. Therefore, acetone was replaced by toluene, which is immiscible with [Emim]Ac and has an SP value (18.2 $MPa^{1/2}$)[39] similar to that of acetone. Figure 4 shows the interfacial tension results when using toluene ($\gamma_{cellulose\text{-}IL/toluene}$); $\gamma_{cellulose\text{-}IL/toluene}$ decreased in a small amount of cellulose, suggesting that cellulose should adsorb at the inner interface to reduce the interfacial tension.

To further test this mechanism, the surfactant Tween 81 (HLB ≈ 10) was added to acetone to reduce the interfacial tension between [Emim]Ac and acetone ($\gamma_{IL/acetone}$). According to the mechanism described above, the lower $\gamma_{IL/acetone}$ of the cellulose–[Emim]Ac droplets should suppress the cellulose molecules adsorption at their interface, resulting in a non-hollow structure. In practice, the presence of 0.5 wt% Tween 81 decreased the interfacial tension from 2.2 ($\gamma_{IL/acetone}$) to 0.7 mN $m^{-1}$ ($\gamma_{IL/T81\text{-}acetone}$). In addition, in the case of 5 wt% Tween 81, $\gamma_{IL/T81\text{-}acetone}$ was too low (< 0.1 mN $m^{-1}$) to be measured accurately. Figure 5 shows the optical micrographs of the cellulose particles prepared using acetone containing dissolved Tween 81 at different concentrations (0, 0.5, and 5 wt%); with the decrease in interfacial tension, the particles exhibited not a single-hollow structure, but a multi-hollow and non-hollow structures. These results indicate that the surfactant in acetone suppresses the cellulose adsorption on the interface and that the proposed mechanism of hollow structure formation is correct.

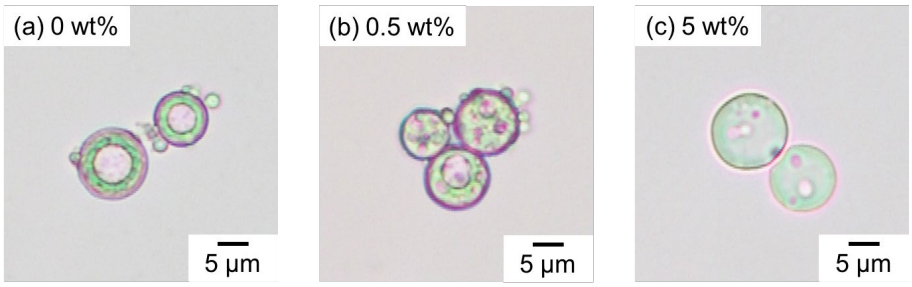


**Figure 5.** Optical micrographs of cellulose particles prepared via the SRM for cellulose–[Emim]Ac (10:90, w/w) droplets using acetone solution containing Tween 81 at different concentrations as the precipitant: (a) 0, (b) 0.5, and (c) 5 wt% (based on acetone).

To discuss the [Emim]Ac-core/cellulose-shell structure in the SRM process using acetone in terms of thermodynamics, the spreading coefficient ($S$, mN m$^{-1}$) is considered, which is useful in predicting the particle morphology:[42]

$$S_i = \gamma_{jk} - (\gamma_{ij} + \gamma_{ik}) \quad (1)$$

where $\gamma$ is the interfacial tension (mN/m) among three components ($ij$, $jk$, $ik$) and the suffixes $i$, $j$, and $k$ indicate cellulose, [Emim]Ac, and acetone, respectively. If a particle had the [Emim]Ac-core/cellulose-shell morphology in acetone, each $S$ value should satisfy the following relationship.

$$S_{cellulose} > 0, S_{[Emim]Ac} < 0, S_{acetone} < 0 \quad (2)$$

$\gamma_{IL/acetone}$ (2.2 mN m$^{-1}$) was determined by the pendant drop method. Moreover, the interfacial tensions of cellulose/[Emim]Ac (or acetone) were calculated by the Fowkes equation (Eq. (3)) based on the surface tension of cellulose (37.7 mN m$^{-1}$),[43] [Emim]Ac (45.7 mN m$^{-1}$),[44] and acetone (23.0 mN m$^{-1}$):[45]

$$\gamma_{SL} = \gamma_S + \gamma_L - 2\sqrt{\gamma_S \gamma_L} \quad (3)$$

where the suffixes $S$ and $L$ mean solid (cellulose) and liquid ([Emim]Ac or acetone), respectively. In this system, the calculated spreading coefficients were as follows: $S_{cellulose}$=

+0.02 > 0, $S_{[Emim]Ac}$ = –0.78 < 0, and $S_{acetone}$ = –3.6 < 0, satisfying Eq. (2). This result suggests that the [Emim]Ac-core/cellulose-shell structure in acetone has a thermodynamically stable morphology, namely, thermodynamics determines the hollow structure.

***Morphology Control of Hollow Cellulose Particles***

The above findings indicate that the formation of hollow cellulose particles prepared via the SRM is influenced by the phase separation rates of cellulose and [Emim]Ac in the droplets. The phase separation, in turn, should be affected by the viscosity inside the primary droplets. To investigate the viscosity effect on the final morphology, different amounts of cellulose were dissolved in the [Emim]Ac droplets (5, 10, and 15 wt%); the optical micrographs, and the SEM and TEM images of the ultrathin cross-sections of the resulting particles are shown in Figure 6.

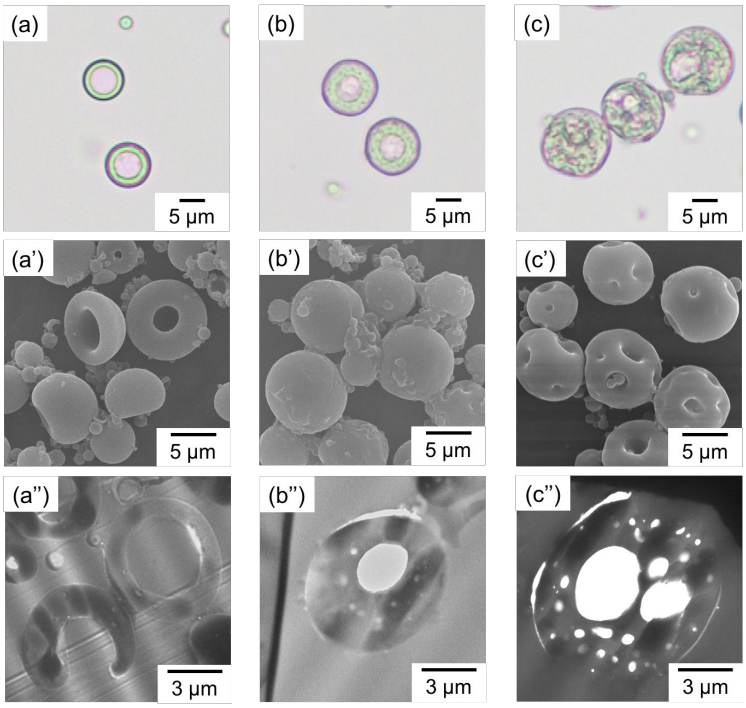


**Figure 6.** Optical micrographs (top row), and SEM (middle row) and TEM images of ultrathin cross-sections (bottom row) of the cellulose particles prepared via the SRM by using acetone for cellulose–[Emim]Ac droplets with different cellulose concentrations: (a, a', a") 5; (b, b', b") 10; (c, c', c") 15 wt% based on the cellulose.

In the 5 and 10 wt% cases, the cellulose particles exhibited a single-hollow structure. The hollow size of the particles increased with the cellulose concentration, although the particles at 5 wt% concentration had a dent after drying due to the buckling of the thin shell. In contrast, when the cellulose concentration was 15 wt%, the particles showed a multi-hollow structure because of the higher viscosity in the primary droplets because the higher cellulose concentration suppressed the cellulose diffusion leading to insufficient phase separation.

Then, to further confirm the viscosity effect in the primary droplets, the molecular weight of the dissolved cellulose was varied. Figure 7 shows the optical micrographs of the cellulose particles prepared using different $M_n$ ($3.0 \times 10^4$, $1.0 \times 10^5$, and $3.2 \times 10^5$). As expected, the use of using $M_n$ did not produce single-hollow structures. This indicates that the viscosity of the primary droplets, influenced by the cellulose concentration and the molecular weight, is also crucial to control the inner morphology of the cellulose particles. These results also support the proposed formation mechanism of the hollow cellulose particles.

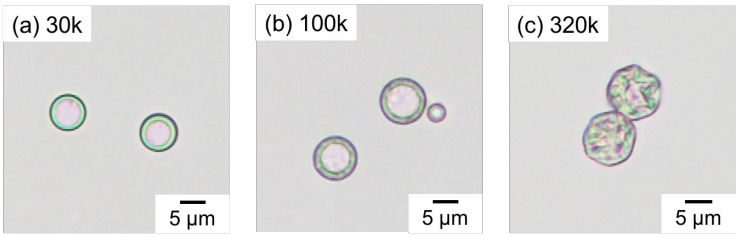


**Figure 7.** Optical micrographs of the cellulose particles prepared via the SRM by using acetone for cellulose–[Emim]Ac (5:95, w/w) droplets with different cellulose molecular weights: (a) $3.0 \times 10^4$, (b) $1.0 \times 10^5$, (c) $3.2 \times 10^5$.

## Conclusion

A facile method to control the morphology of cellulose particles was demonstrated by changing the precipitant used in the SRM. A lower precipitant affinity for [Emim]Ac decreased the release rate of [Emim]Ac from the cellulose–[Emim]Ac solution, changing the morphology of the precipitated particles from porous to hollow, thermodynamically stable structure. Moreover, the inner morphology of these hollow particles was able to controlled by varying the cellulose concentration and molecular weight.

## References


1. J. C. Auger and D. McLoughlin, *J. Coat. Technol. Res.*, 2015, **12**, 693-709.
2. S. Nuasaen and P. Tangboriboonrat, *Prog. Org. Coat.*, 2015, **79**, 83-89.
3. S. Freiberg and X. X. Zhu, *Int. J. Pharm.*, 2004, **282**, 1-18.
4. Y. Zhao and L. Jiang, *Adv. Mater. (Weinheim, Ger.)*, 2009, **21**, 3621-3638.
5. D. L. Wilcox and M. Berg, *MRS Proceedings*, 1994, **372**, 3.
6. R. F. G. Brown, C. Carr and M. E. Taylor, *Prog. Org. Coat.*, 1997, **30**, 185-194.
7. X. Wang, J. Feng, Y. Bai, Q. Zhang and Y. Yin, *Chem. Rev. (Washington, DC, U. S.)*, 2016, **116**, 10983-11060.
8. S. Miao, C. Zhang, Z. Liu, B. Han, Y. Xie, S. Ding and Z. Yang, *J. Phys. Chem. C*, 2008, **112**, 774-780.
9. R. A. Ramli, *RSC Advances*, 2017, **7**, 52632-52650.
10. M. Okubo, Y. Konishi and H. Minami, *Prog. Colloid Polym. Sci.*, 2004, **124**, 54-59.
11. R. Nakamura, M. Tokuda, T. Suzuki and H. Minami, *Langmuir*, 2016, **32**, 2331-2337.
12. C. Scott, D. Wu, C.-C. Ho and C. C. Co, *J. Am. Chem. Soc.*, 2005, **127**, 4160-4161.
13. F. Caruso, R. A. Caruso and H. Moehwald, *Science (Washington, D. C.)*, 1998, **282**, 1111-1114.
14. S. Hyuk Im, U. Jeong and Y. Xia, *Nat. Mater.*, 2005, **4**, 671-675.
15. B. M. Discher, Y.-Y. Won, D. S. Ege, J. C. M. Lee, F. S. Bates, D. E. Discher and D. A. Hammer, *Science (Washington, D. C.)*, 1999, **284**, 1143-1146.
16. Y. Kitayama, *Polymer Journal*, 2019, DOI: 10.1038/s41428-019-0219-y.
17. D. Klemm, B. Heublein, H.-P. Fink and A. Bohn, *Angew. Chem., Int. Ed.*, 2005, **44**, 3358-3393.
18. S. Wang, A. Lu and L. Zhang, *Prog. Polym. Sci.*, 2016, **53**, 169-206.
19. M. Gericke, J. Trygg and P. Fardim, *Chem. Rev. (Washington, DC, U. S.)*, 2013, **113**, 4812-4836.
20. X. Guo and F. Chen, *Environ. Sci. Technol.*, 2005, **39**, 6808-6818.
21. N. Li and R. Bai, *Sep. Purif. Technol.*, 2005, **42**, 237-247.
22. K.-F. Du, M. Yan, Q.-Y. Wang and H. Song, *J. Chromatogr. A*, 2010, **1217**, 1298-1304.
23. A.-F. Metaxa, E. K. Efthimiadou, N. Boukos and G. Kordas, *J. Colloid Interface Sci.*, 2012, **384**, 198-206.

24. D. J. Gardner, G. S. Oporto, R. Mills and M. A. S. A. Samir, *J. Adhes. Sci. Technol.*, 2008, **22**, 545-567.
25. D. Roy, M. Semsarilar, J. T. Guthrie and S. Perrier, *Chem. Soc. Rev.*, 2009, **38**, 2046-2064.
26. S. Eyley and W. Thielemans, *Nanoscale*, 2014, **6**, 7764-7779.
27. C. Carrick, P. A. Larsson, H. Brismar, C. Aidun and L. Wagberg, *RSC Adv.*, 2014, **4**, 19061-19067.
28. C. Carrick, M. Ruda, B. Pettersson, P. T. Larsson and L. Wagberg, *RSC Adv.*, 2013, **3**, 2462-2469.
29. R. P. Swatloski, S. K. Spear, J. D. Holbrey and R. D. Rogers, *J. Am. Chem. Soc.*, 2002, **124**, 4974-4975.
30. M. B. Turner, S. K. Spear, J. D. Holbrey and R. D. Rogers, *Biomacromolecules*, 2004, **5**, 1379-1384.
31. J.-i. Kadokawa, M.-a. Murakami and Y. Kaneko, *Carbohydr. Res.*, 2008, **343**, 769-772.
32. Q.-y. Mi, S.-r. Ma, J. Yu, J.-s. He and J. Zhang, *ACS Sustainable Chem. Eng.*, 2016, **4**, 656-660.
33. T. Suzuki, K. Kono, K. Shimomura and H. Minami, *J. Colloid Interface Sci.*, 2014, **418**, 126-131.
34. K. Imagawa, T. Omura, Y. Ihara, K. Kono, T. Suzuki and H. Minami, *Cellulose (Dordrecht, Neth.)*, 2017, **24**, 3111-3118.
35. T. Omura, K. Imagawa, K. Kono, T. Suzuki and H. Minami, *ACS Appl. Mater. Interfaces*, 2017, **9**, 944-949.
36. M. Okubo, Y. Konishi, M. Takebe and H. Minami, *Colloid Polym. Sci.*, 2000, **278**, 919-926.
37. K. A. Le, C. Rudaz and T. Budtova, *Carbohydr. Polym.*, 2014, **105**, 237-243.
38. Y. H. P. Zhang and L. R. Lynd, *Biomacromolecules*, 2005, **6**, 1510-1515.
39. C. M. Hansen and Editor, *Hansen Solubility Parameters: A User's Handbook*, CRC Press LLC, 2007.
40. D. Kim, N. L. Le and S. P. Nunes, *J. Membr. Sci.*, 2016, **520**, 540-549.
41. W. G. Glasser, R. H. Atalla, J. Blackwell, R. Malcolm Brown, Jr., W. Burchard, A. D. French, D. O. Klemm and Y. Nishiyama, *Cellulose (Dordrecht, Neth.)*, 2012, **19**, 589-598.

42. S. Torza and S. G. Mason, *Journal of Colloid and Interface Science*, 1970, **33**, 67-83.
43. D. F. Steele, R. C. Moreton, J. N. Staniforth, P. M. Young, M. J. Tobyn and S. Edge, *The AAPS journal*, 2008, **10**, 494-503.
44. J. Schuermann, T. Huber, D. LeCorre, G. Mortha, M. Sellier, B. Duchemin and M. P. Staiger, *Cellulose*, 2016, **23**, 1043-1050.
45. S. Enders, H. Kahl and J. Winkelmann, *Journal of Chemical & Engineering Data*, 2007, **52**, 1072-1079.

# *Chapter 4*

## Encapsulation of Either Hydrophilic or Hydrophobic Substances in Spongy Cellulose Particles

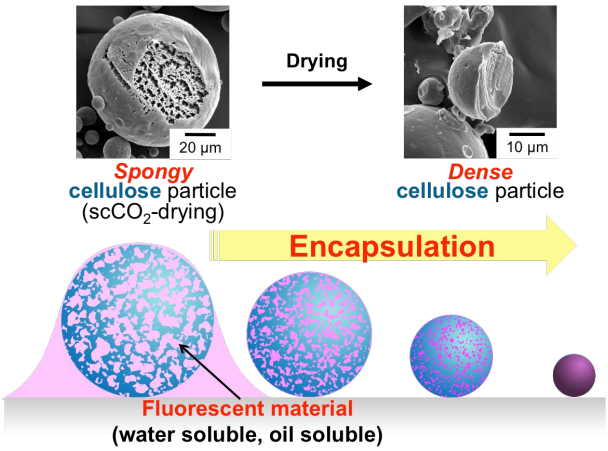


**Abstract:** Cellulose particles with a spongy structure were prepared by the solvent releasing method (SRM) from cellulose droplets comprising cellulose, 1-butyl-3-methylimidazoliumchrolide ([Bmim]Cl), and *N*,*N*-dimethylformamide (DMF). The spongy structure collapsed as the medium evaporated, resulting in dense cellulose particles. In this chapter, Encapsulations of the hydrophilic and hydrophobic fluorescent substances in these particles were demonstrated to investigate the use of such particles in potential applications that require encapsulating of substances (e.g., drug delivery). Wet cellulose particles retained their spongy structure in both hydrophobic and hydrophilic media. When the spongy cellulose particles were dispersed in a solution containing nonvolatile solutes, these solutes were driven into the cellulose particles as media evaporated. Subsequently, the cellulose particles collapsed and encapsulated the nonvolatile solutes. Regardless of whether the solute was hydrophilic or hydrophobic, the encapsulation efficiency exceeds 80%. The maximum loading reflected the saturated solubility of solute in solution that filled the cellulose beads. Moreover, the encapsulated solute was released by dispersing the cellulose beads in the solvent, and the rate of release of the encapsulated solute could be controlled by coating the cellulose beads with a conventional polymer.

## Introduction

Microcapsules have been used in many applications such as functional paper coating,[1] enzymatic microreactors[2] and nanomedicine.[3] Various methods to prepare such microcapsules have been reported, including the layer-by-layer deposition onto the colloid that serves as a template,[4] the microfluidic method,[5] the solvent evaporation from emulsion,[6] interfacial polymerization on the emulsion droplets,[7] and suspension polymerization.[8-9] However, with these techniques, the polarity of the encapsulated substances remains limited to being hydrophilic or hydrophobic. When the polarity of the encapsulated substances changes, the method and type of encapsulant must also change.

Cellulose is the most abundant biorenewable polymer and has many attractive properties such as thermal and chemically stability, nontoxicity, biocompatibility, and biodegradability.[10] Thus cellulose is extensively used in materials such as pulp, regenerated fibers, and membranes.[11-13] Recently, particulate cellulose has found use in various applications, mainly for biochromatography, immobilization, and as a drug carrier.[14-17] Cellulose particles as encapsulants have also attracted attention. However, because cellulose is insoluble in water and in most organic solvents, the fabrication of cellulose capsules is a multistep process.[18-21]

In 2002, Rogers et al.[22] reported that cellulose can be dissolved in ionic liquids (ILs), such as 1-butyl-3-methylimidazolium chloride ([Bmim]Cl), under only mild heat treatment to dissolve cellulose. Thereafter, interest increased in the use of ILs as solvents to control cellulose morphology.[23-28]

In the previous study, Minami et al. successfully prepared the cellulose particles using [Bmim]Cl as the solvent[29] and applying the solvent releasing method (SRM),[30-32] in which cellulose–[Bmim]Cl–*N*,*N*-dimethylformamide (DMF) droplets were dispersed in hexadecane containing a dissolved surfactant. Interestingly, the cellulose particles thus obtained have a

spongy structure and may be filled with solvent without deforming their morphology simply by changing the surrounding medium regardless of polarity. Moreover, the spongy structure collapsed when the medium evaporated, resulting in a dense structure. This behavior indicates that the spongy cellulose particles may be used as the encapsulants for both hydrophilic and hydrophobic materials. This may be considered as the "Egg of Columbus" for encapsulation strategy.

In ***Chapter 4***, it is demonstrated that a simple method to encapsulate nonvolatile, hydrophilic and hydrophobic fluorescent substances within spongy cellulose particles dispersed in a medium. The encapsulation mechanism and the release of the encapsulated substance from the cellulose particles were also discussed.

# Experimental Section

## Materials

Microcrystalline cellulose (powder, derived from cotton linter) and the IL, [Bmim]Cl, were used as received from Aldrich Chemical Co., Ltd. *N*,*N*-Dimethylformamide (DMF), *n*-hexane, 1-butanol, methanol, toluene, Rhodamine B (RB), and sodium chloride (NaCl) were used as received from Nacalai Tesque Inc. (Kyoto, Japan). Polydimethylsiloxane surfactant, VPS-1001 (Wako Pure Chemical Industries, Ltd.), and Nile red (NR; Tokyo Chemical Industry Co., Ltd.) were also used as received. All water used in these experiments was purified an ErixUV (Millipore) purification system and had a resistivity of 18.2 MΩ cm.

## Preparation of Cellulose Particles by SRM

Cellulose particles were prepared by the SRM as follows: microcrystalline cellulose powder was dissolved in [Bmim]Cl at a weight ratio of 7:43 by heating to 100°C for 7 h. To reduce the viscosity of this solution, DMF was added as a co-solvent. A solution of cellulose–[Bmim]Cl–DMF (7:43:50, w/w/w) (0.2 g) was mixed with hexane (2.0 g) containing dissolved VPS-1001 (0.25 wt % of hexane) as a colloidal stabilizer and stirred at 4000 rpm for 5 min using a homogenizer (BM-1, Nihonseiki Kaisha Ltd.; Tokyo, Japan). The obtained dispersion was poured into a large amount of 1-butanol (ca. 20 mL) and stirred to remove [Bmim]Cl and DMF from the cellulose–[Bmim]Cl–DMF droplet, thereby allowing the cellulose to precipitate and form cellulose particles. The precipitate was washed three times to with 1-butanol to remove any remaining [Bmim]Cl, DMF, and hexane. Then, the washed cellulose/1-butanol dispersions were replaced with water, acetone, or toluene.

**Observation of the Spongy Cellulose Particles by SEM**

The cellulose particles were dried by using supercritical carbon dioxide ($scCO_2$) drying. First, the cellulose particles dispersed in acetone were poured into a 25 mL stainless-steel reactor, and the reactor was pressurized with liquid $CO_2$ to 15 MPa at room temperature by using a high-pressure pump. Next, $CO_2$ and acetone were vented from the reactor. Before all liquid $CO_2$ and acetone evaporated (2 MPa), liquid $CO_2$ was added until the pressure was 15 MPa. This process was repeated at least eight times to ensure complete removal of acetone from the reactor. The reactor was subsequently dipped in a temperature-controlled water bath at 40°C, in which $CO_2$ should exist as $scCO_2$. Finally, the $scCO_2$ was vented slowly from the reactor to obtain the $scCO_2$-dried cellulose particles.

**Preparation of millimeter-sized Cellulose Beads**

The SRM-like procedure to prepare 1 mm cellulose beads was used: a solution of cellulose–[Bmim]Cl–DMF (7:43:50, w/w/w) was dropped by a syringe into a large amount of 1-butanol (ca. 20 mL). To completely remove [Bmim]Cl and DMF, the cellulose beads (containing [Bmim]Cl and DMF) were left over 6 h after dropping into 1-butanol, after which they were washed twice with 1-butanol. Between each washing, the cellulose beads remained standing over 2 h.

**Encapsulation of Substances Using Cellulose Particles and Cellulose Beads**

RB aqueous solution ($1.21 \times 10^{-4}$ mol/L, 25 mg) was added to a dispersion of cellulose particles (3.0 g) in water, following which the dispersion was dried in vacuum. For the hydrophobic fluorescent substance, the dispersion (3.0 g) was done in a toluene solution containing dissolved NR ($1.79 \times 10^{-4}$ mol/L, 25 mg) and the solution was then dried in a

vacuum. Similarly, wet spongy cellulose beads (4 mg) were dispersed in 0.1 g of RB aqueous solution, NR toluene solution, and various amounts of NaCl methanol solution (0.045 wt %). The solutions were then dried in a vacuum. Moreover, dense cellulose beads were also used to encapsulate the fluorescent substances.

The presence of fluorescent substances in cellulose particles was observed using a confocal laser scanning microscope (CLSM, C2si, Nikon Corp., Tokyo, Japan) with extinction by a He–Ne laser at 543 nm and a 552–617 nm emission bandpass filter. The inner morphologies of the cellulose beads encapsulating the fluorescent substances were detected by using a stereomicroscope (M3584, Carton Optical Industries, Ltd., Tokyo, Japan).

**Amount of Substance Encapsulated in Cellulose Beads**

After encapsulation, the beads were removed from the glass test tubes, and water or toluene (2.4 g) was added to the tubes to dissolve any fluorescent remaining in the test tube was determined by analyzing the test tube with an UV–vis analysis (UV-2500 UV–vis spectrophotometer, Shimazu Corporation; Kyoto, Japan). The calibration curves were linear for the RB concentration over the range 0.01–0.15 × $10^{-4}$ mol/L at 553 nm and for the NR concentration over the range 0.01–0.18 × $10^{-4}$ mol/L at 525 nm.

The amount of NaCl encapsulated in cellulose beads was calculated based on the weight loss of the composite beads, which was measured by thermogravimetry (TGA, EXSTAR TG/DTA6200, S Π Nano-Technology Inc., Japan) at a heating rate of 10 °C/min from 30 to 1000°C under a nitrogen atmosphere.

**Release of Fluorescent Substance in Solution**

The complete release of fluorescent substances was determined basis of the optical

absorption of RB and NR in the cellulose beads. The cellulose bead encapsulating RB was dispersed in water (2.4 g). At predefined time intervals, the solution was analyzed for the RB fluorescent signal using the UV–vis spectrophotometer. To control the rate at which the encapsulated substance is released, the cellulose beads encapsulating the RB were first dipped in chloroform containing dissolved poly(methyl methacrylate) (PMMA, weight-average molecular weight ($M_w$) = $1.0 \times 10^5$, 5 wt %) and then dried in vacuum. Next, the cellulose beads were dispersed in water (2.4 g). Cellulose beads encapsulating NR were similarly dispersed and analyzed in toluene (2.2 g).

**Characterization**

Cellulose particles were observed by using scanning electron microscopy (SEM, JSM-6510, JEOL Ltd.; Tokyo, Japan). The specific surface area of the $scCO_2$-dried and vacuum-dried cellulose particles was determined by using a surface area analyzer (NOVA 3200e, Quantachrome Instruments) with nitrogen as sorption gas.

## Results and Discussion

### *Encapsulation of Fluorescent Materials by Cellulose Particles*

As mentioned in the Introduction section, the cellulose particles having spongy structures prepared using SRM, in which cellulose−[Bmim]Cl−DMF droplets dispersed in *n*-hexane containing a dissolved surfactant were poured into a large amount of 1-butanol, can be filled with solvent without deforming their morphology by simply changing the surrounding medium regardless of polarity. However, the spongy structure collapsed upon evaporation of the medium, resulting in a dense structure. The spongy structure took form in the dry state (after $scCO_2$ drying). Figure 1 shows SEM images of the cellulose particles after $scCO_2$ drying and vacuum drying process. No spongy structure appeared in Figure 1a, although numerous nanosized pores appeared on the surface of the particles (Figure 1d). However, the images of fractured particles (Figure 1b, e) clearly show the spongy structure inside the particles. The specific surface area of the particles was 371.3 $m^2/g$, which was much greater than that calculated for a dense structure (0.38 $m^2/g$).[29] Before drying, all the cellulose particles prepared using the SRM were expected to have such a spongy structure. Upon drying (e.g., vacuum drying), the particles developed a smooth surface and formed a dense structure (Figure 1c, f) with a specific surface area less than 1 $m^2/g$.

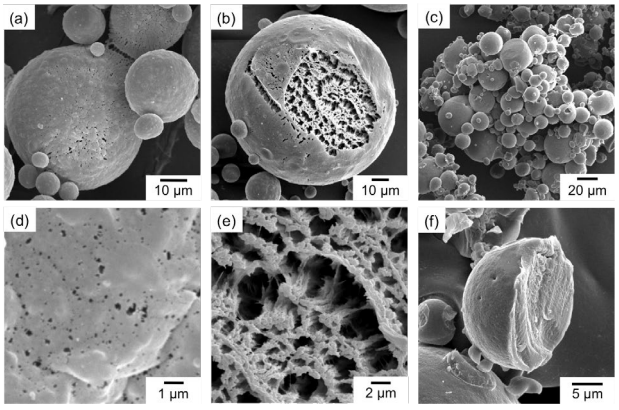


**Figure 1.** SEM images of $scCO_2$-dried (a, b, d, e) and vacuum-dried (c, f) cellulose particles prepared by SRM using 1-butanol for cellulose–[Bmim]Cl–DMF (7/43/50, w/w/w) droplets dispersed in hexane. Before fractioning (a, c, d) and after (b, e) fractioning the particles. Low (a, b) and high (d, e) magnification are shown.

Figure 2a, a′, b, and b′ show optical and CLSM micrographs of the cellulose particles dispersed in RB aqueous solution (RB is a water-soluble fluorescent substance) before and after drying. (After drying, it was difficult to clearly observe the cellulose particles using the optical microscope because the medium surrounding the particles evaporated.) Before drying the aqueous dispersion, all particles were bright red, as was the surrounding solvent. This indicates that the RB aqueous solution penetrates into the cellulose particles. The fluorescence of the particles is brighter than that of the solvent because the RB adsorbs onto the cellulose by a hydrophobic interaction. Although RB is water-soluble, it has greater affinity to the hydrophobic medium than to water because it contains a polycyclic aromatic moiety. However, after drying, only the cellulose particles fluoresce brightly, indicating that RB is present only within the cellulose particles, although a small quantity of the fluoresce may also exist on the surface of the shrunk cellulose particles (it should be negligible). A similar situation occurred for the cellulose particles dispersed in the toluene solution containing dissolved NR (an oil-soluble fluorescent: see Figure 2c, d′). These results suggest that these spongy cellulose particles can encapsulate both water-soluble and oil-soluble substances.

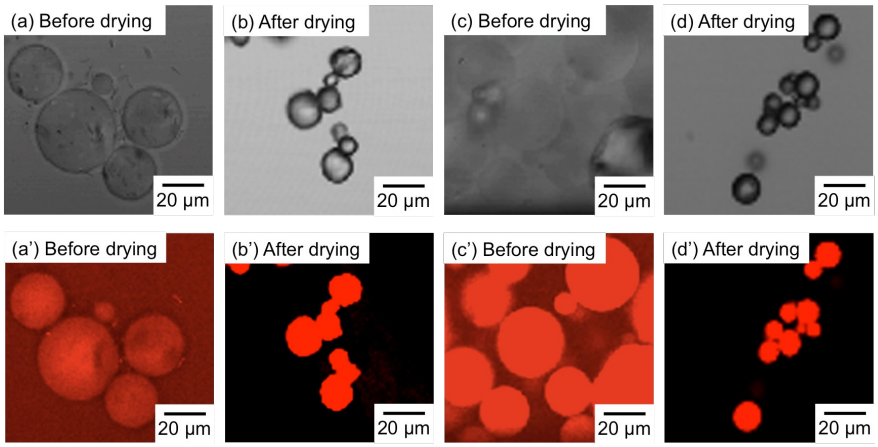


**Figure 2.** Optical micrographs (a–d) and confocal laser scanning microscope (CLSM) images (a'–d') of cellulose particles before (a, a', c, c') and after (b, b', d, d') drying from an aqueous solution containing dissolved Rhodamine B (a, a', b, b') and toluene solution containing dissolved Nile Red (c, c', d, d').

***Encapsulation of Fluorescent Materials by Cellulose Beads***

Millimeter-sized cellulose beads were used to estimate the amount of fluorescent substance encapsulated per cellulose bead.[29] The cellulose beads may be handled by tweezers without deforming them, and media in the beads may be replaced by soaking them in hydrophobic or hydrophilic media. As the medium evaporated from the bead, the bead shrank, as shown in Figure 3. This indicates that the millimeter-sized cellulose beads have a spongy structure similar to that of the micrometer-sized cellulose particles.

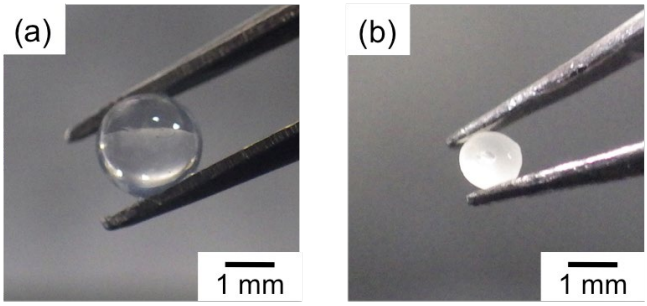


**Figure 3.** Visual appearances of cellulose bead prepared by dropping a cellulose–[Bmim]Cl–DMF (7/43/50, w/w/w) solution into a large amount of 1-butanol and then washing with 1-butanol (a), followed by drying (b).

When the spongy cellulose beads were dipped in the RB aqueous solution (Figure 4a) and then dried, the cellulose beads became red, and only a small amount of RB remained in the vial (Figure 4b). Although the dense cellulose beads, i.e., the dried spongy beads prior to dipping, were colored red in the same way as the spongy beads, much more RB was likely to remain in the vial than that remaining for the spongy beads (Figure 4e, f).

The RB absorbance ratio was estimated by subtracting the amount of RB remaining in the bottle; this ratio was 90 wt% in many cases, and at least 80 wt% in all cases. However, for dense cellulose beads, the RB absorbance ratio was calculated to be less than 30 wt%. The encapsulation ratio of hydrophobic fluorescent substance was similarly obtained for a toluene

solution containing dissolved NR. The results were similar to those for the RB system: the absorbance ratio of NR exceeded 80 wt% for the spongy cellulose beads but was less than 30 wt% for the dense beads. These results suggest that almost all nonvolatile substances, regardless of their polarity, dissolved in the solution are encapsulated within the spongy cellulose beads, which highlights the usefulness of spongy structures for encapsulation.

Moreover, after drying, the beads were cut and their cross-sections were examined. The cross-sections of spongy beads in both the RB and NR systems were colored throughout their bulk by RB and NR, respectively (Figure 4c, d). However, for dense cellulose beads, only the outer edges of the cross-sections of the bead were colored (Figure 4g, h). These results also indicate that the spongy structure is important for encapsulation.

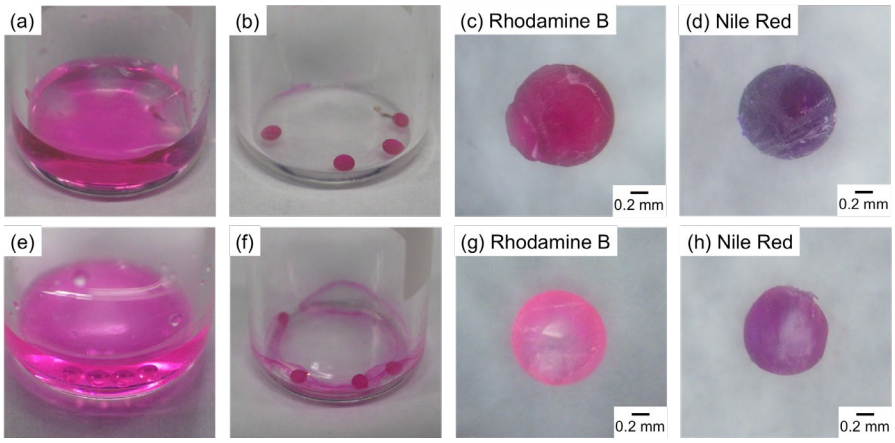


**Figure 4.** Visual appearances of spongy (a–d) and dense (e–h) cellulose beads. Intact beads (a, b, e, f) and their cross-sections (c, d, g, h). Beads were dispersed in an aqueous solution containing dissolved Rhodamine B (c, g) or toluene solution containing dissolved Nile Red (d, h). Before (a, e) and after (b, f) drying the aqueous solution containing dissolved Rhodamine B.

The process of encapsulation is explained as follows: Upon dispersing spongy cellulose particles (beads) in a solution containing nonvolatile solutes, these solutes penetrate into the cellulose particles (beads) via the solution and become concentrated inside the cellulose particles (beads) as solvent evaporates. Subsequently, the particles (beads) collapse because the solvent inside them evaporates, leaving the nonvolatile solutes encapsulated inside the particles (beads). If encapsulation occurs through this mechanism, the maximum loading should be consistent with the saturated solubility of the solute in the solution that fills the spongy cellulose particles (beads). To confirm this mechanism, NaCl was dissolved in methanol (NaCl has low solubility in methanol) and then proceeded to encapsulate the NaCl in the cellulose beads. The amount of encapsulated NaCl was then measured using TGA. At high temperatures, it was assumed that most cellulose burned off and that only NaCl remained. However, cellulose has a high char yield (nonvolatile carbonaceous material) on pyrolysis (Figure 5, line 1), and NaCl melts above 800°C and evaporates as a volatile material.[33] In fact, all of the weight loss of NaCl was measured by using TGA (Figure 5, line 2) at 1000°C. Therefore, the amount of NaCl encapsulated in the cellulose bead was determined by the weight loss of NaCl from 800 to 1000°C, after the decomposition of cellulose (Figure 5, line 3). By the use of this procedure, the amount of the encapsulated NaCl was measured for various amount of NaCl methanol solution (0.045 wt %). Figure 6 shows the NaCl encapsulated in cellulose beads as a function of the total mass of NaCl dissolved in methanol. Below 0.2 mg NaCl in methanol, the NaCl encapsulated in the beads increased in proportion to the amount of dissolved NaCl, which indicates that almost all dissolved NaCl is encapsulated in the cellulose beads. However, the encapsulated NaCl reached a limit when the NaCl dissolved in methanol exceeded 0.2 mg in Figure 6, which nearly equaled the solubility limit of NaCl in the volume of methanol filling the cellulose beads (vertical dashed line). When the amount of dissolved NaCl exceeds the

solubility limit in the volume of methanol filling the cellulose beads, an excess amount of NaCl should be precipitated before encapsulation as methanol evaporated. These results are consistent with the abovementioned mechanism for encapsulation. Therefore, for nonvolatile solutes dissolved in solutions at concentrations below the solubility limit of solute in the volume of solvent filling the cellulose beads, most of the nonvolatile solute is driven into the cellulose particles (beads) as the solvent evaporates, thereby effectively encapsulating in the cellulose particles (beads).

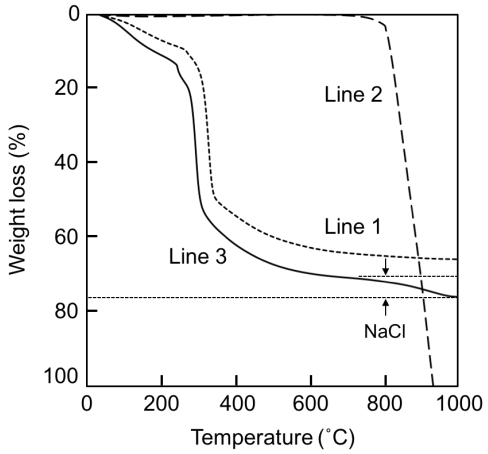


**Figure 5.** Thermal decomposition profiles of dried cellulose beads (line1), NaCl (line 2), and dried cellulose beads encapsulating NaCl (line 3), which were heated under a nitrogen atmosphere at 10˚C/min.

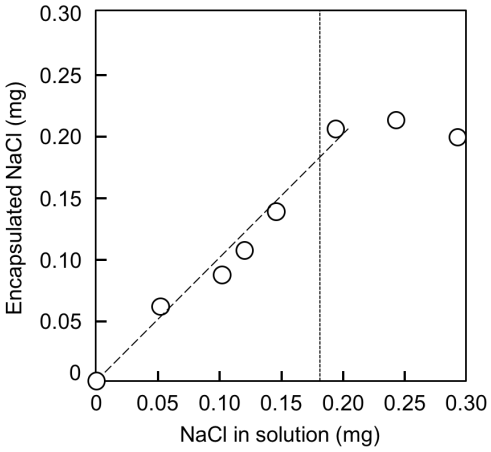


**Figure 6.** Relationship of between amounts of NaCl in solution amonunts of NaCl encapsulated in cellulose bead measured using TG-DTA. The dashed vertical line shows the solubility limit of NaCl in the volume of methanol filling the cellulose beads.

***Release of Fluorescent Substance from Cellulose Beads***

It is now discussed the release of fluorescent substance from the cellulose beads to clarify their potential application in drug delivery. Here, RB as a model hydrophilic compound and NR as a hydrophobic compound were used. The amounts of RB and NR released from the cellulose beads were determined using UV−vis spectroscopy. Figure 7 shows the percent of encapsulated RB (NR) released from the cellulose beads into water (toluene). Over a period of about 5 h, over 80% of the RB encapsulated in the bead was released into water. However, after 10 h, less than 10% of the encapsulated NR was released into toluene. This difference is attributed to the compatibility of cellulose with water and toluene. In water, cellulose does not dissolve but slightly swells. Conversely, in toluene, cellulose does not swell. This swelling in water facilitates the liberation of RB, which leads to the difference in release rates. Furthermore, to control the rate of release of RB into water, the surface of the cellulose beads was coated with PMMA. To do this, the cellulose beads encapsulating RB were dipped into chloroform containing dissolved PMMA (5 wt%) and then dried in a vacuum. As shown in Figure 7, the release rate of RB encapsulated in PMMA-coated cellulose beads was less than that for RB encapsulated in uncoated cellulose beads. These results suggest the rate of release of substances encapsulated in the cellulose beads may be controlled by coating the beads with conventional polymer.

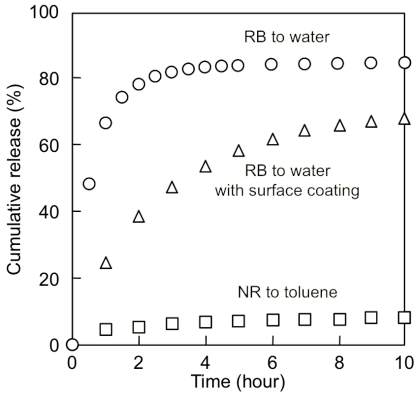


**Figure 6.** Cumulative amounts of RB (open circles and triangles) and NR (squares) released into water and toluene, respectively, from cellulose beads. Open circles and triangles correspond to RB released from cellulose beads without and with PMMA coating.

## Conclusion

Upon dispersing spongy cellulose particles (beads) into solutions, the particles (beads) absorb nonvolatile solutes from the solution. Subsequently, the particles (beads) are dried to remove any remaining solvent, leaving the solute encapsulated within the particles (beads). The solutes are encapsulated in the particles (beads) regardless of whether they are hydrophilic or hydrophobic, as the media in the particles (beads) can be replaced from hydrophobic to hydrophilic media. Efficient encapsulation requires that the concentration of the solute in the solution is less than the saturated solubility of the solute in of the solution that fills the cellulose beads. In addition, upon dispersion in the solvent, the cellulose beads released the encapsulated substance, and the rate of release of the encapsulated substance was controlled by coating the beads with a conventional polymer. This encapsulation strategy offers significant promise for various applications. Cellulose−commodity polymer composite particles were successfully prepared using spongy cellulose particles and will be reported in the future.

## References

1. Xu, L.; He, J., *Langmuir* **2012,** 28 (19), 7512-7518.

2. Kreft, O.; Prevot, M.; Moehwald, H.; Sukhorukov, G. B., *Angew. Chem., Int. Ed.* **2007,** 46 (29), 5605-5608.

3. Zhao, Y.; Lin, L.-N.; Lu, Y.; Chen, S.-F.; Dong, L.; Yu, S.-H., *Adv. Mater.* **2010,** 22 (46), 5255-5259.

4. Caruso, F.; Caruso, R. A.; Moehwald, H., *Science* **1998,** 282 (5391), 1111-1114.

5. Kim, S.-H.; Shum, H. C.; Kim, J. W.; Cho, J.-C.; Weitz, D. A., *J. Am. Chem. Soc.* **2011,** 133 (38), 15165-15171.

6. Hyuk Im, S.; Jeong, U.; Xia, Y., *Nat. Mater.* **2005,** 4 (9), 671-675.

7. Li, W.; Yoon, J. A.; Matyjaszewski, K., *J. Am. Chem. Soc.* **2010,** 132 (23), 7823-7825.

8. Minami, H.; Okubo, M.; Oshima, Y., *Polymer* **2005,** 46 (4), 1051-1056.

9. Chaiyasat, P.; Ogino, Y.; Suzuki, T.; Okubo, M., *Colloid Polym. Sci.* **2008,** 286 (6-7), 753-759.

10. Klemm, D.; Heublein, B.; Fink, H.-P.; Bohn, A., *Angew. Chem., Int. Ed.* **2005,** 44 (22), 3358-3393.

11. Nogi, M.; Iwamoto, S.; Nakagaito, A. N.; Yano, H., *Adv. Mater.* **2009,** 21 (16), 1595-1598.

12. Eichhorn, S. J., *Soft Matter* **2011,** 7 (2), 303-315.

13. Moon, R. J.; Martini, A.; Nairn, J.; Simonsen, J.; Youngblood, J., *Chem. Soc. Rev.* **2011,** 40 (7), 3941-3994.

14. Du, K.-F.; Yan, M.; Wang, Q.-Y.; Song, H., *J. Chromatogr. A* **2010,** 1217 (8), 1298-1304.

15. Ettenauer, M.; Loth, F.; Thuemmler, K.; Fischer, S.; Weber, V.; Falkenhagen, D., *Cellulose* **2011,** 18 (5), 1257-1263.

16. Carrick, C.; Ruda, M.; Pettersson, B.; Larsson, P. T.; Wagberg, L., *RSC Adv.* **2013,** 3 (7), 2462-2469.

17. Gericke, M.; Trygg, J.; Fardim, P., *Chem. Rev.* **2013,** 113 (7), 4812-4836.

18. Sescousse, R.; Gavillon, R.; Budtova, T., *J. Mater. Sci.* **2011,** 46 (3), 759-765.

19. Metaxa, A.-F.; Efthimiadou, E. K.; Boukos, N.; Kordas, G., *J. Colloid Interface Sci.* **2012,** 384 (1), 198-206.

20. Ma, M.; Tan, L.; Dai, Y.; Zhou, J., *Iran. Polym. J.* **2013,** 22 (9), 689-695.

21. Barkhordari, S.; Yadollahi, M., *Appl. Clay Sci.* **2016,** 121-122, 77-85.

22. Swatloski, R. P.; Spear, S. K.; Holbrey, J. D.; Rogers, R. D., *J. Am. Chem. Soc.* **2002,** 124 (18), 4974-4975.

23. Turner, M. B.; Spear, S. K.; Holbrey, J. D.; Rogers, R. D., *Biomacromolecules* **2004,** 5 (4), 1379-1384.

24. Kadokawa, J.-i.; Murakami, M.-a.; Kaneko, Y., *Carbohydr. Res.* **2008,** 343 (4), 769-772.

25. Prasad, K.; Mine, S.; Kaneko, Y.; Kadokawa, J.-i., *Polym. Bull.* **2010,** 64 (4), 341-349.

26. Freire, M. G.; Teles, A. R. R.; Ferreira, R. A. S.; Carlos, L. D.; Lopes-da-Silva, J. A.; Coutinho, J. A. P., *Green Chem.* **2011,** 13 (11), 3173-3180.

27. Shi, F.; Lin, D.-Q.; Phottraithip, W.; Yao, S.-J., *J. Appl. Polym. Sci.* **2011,** 119 (6), 3453-3461.

28. Haerdelin, L.; Thunberg, J.; Perzon, E.; Westman, G.; Walkenstroem, P.; Gatenholm, P., *J. Appl. Polym. Sci.* **2012,** 125 (3), 1901-1909.

29. Suzuki, T.; Kono, K.; Shimomura, K.; Minami, H., *J. Colloid Interface Sci.* **2014,** 418, 126-131.

30. Okubo, M.; Konishi, Y.; Takebe, M.; Minami, H., *Colloid Polym. Sci.* **2000,** 278 (10), 919-926.

31. Okubo, M.; Konishi, Y.; Sebki, S.; Minami, H., *Colloid Polym. Sci.* **2002,** 280 (8), 765-769.

32. Tanaka, T.; Okayama, M.; Minami, H.; Okubo, M., *Langmuir* **2010,** 26 (14), 11732-11736.

33. Ye, L.; Tang, C.; Chen, Y.; Yang, S.; Tang, M., *Thermochim. Acta* **2014,** 596, 14-20.

# *Chapter 5*

## Preparation of Cellulose/Silver Composite Particles Having Recyclable Catalytic Property

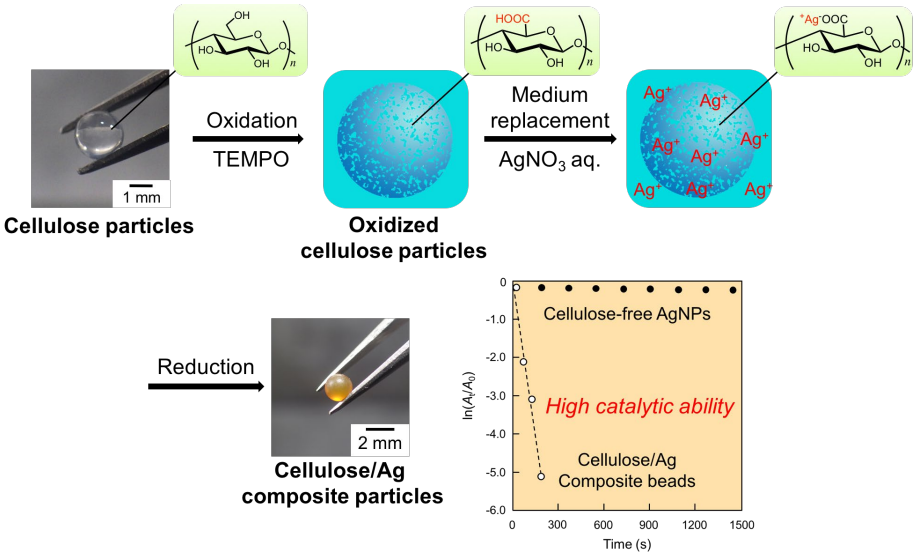


**Abstract:** In previous chapter, the porous cellulose particles were prepared by the solvent-releasing method (SRM), in which a solution of cellulose, dissolved in 1-butyl-3-methylimidazolium chloride ([Bmim]Cl) and *N*,*N*'-dimethylformamide (DMF), was dropped into a large amount of 1-butanol using a syringe. The obtained particles had a high specific area due to their porous structures. Herein, to functionalize the cellulose particles, carboxylate groups are introduced into their porous structure by 2,2,6,6-tetramethylpiperidine-1-oxyl (TEMPO)-mediated oxidation, and ion exchange of carboxylate groups to silver (Ag) cations is conducted out. Composite cellulose/Ag particles are synthesized by a reduction reaction. The obtained composite particles exhibited a high catalytic ability, which was evaluated by studying the reduction of 4-nitrophenol. Moreover, we found that the catalytic efficiency was maintained for at least three cycles by immobilizing Ag on the cellulose particles.

## Introduction

Metal nanoparticles have attracted considerable attention owing to their broad range of applications in areas such as electronics, optics,[1, 2] catalysis,[3] biomedicine,[3] and sensors.[3-5] Additionally, silver nanoparticles (AgNPs) have been utilized in antibacterial,[6, 7] catalyitc,[8, 9] and electronic[10] applications. However, metal nanoparticles—including AgNPs—are generally unstable owing to their large surface area; thus, they tend to aggregate in a medium, which significantly decreases their catalytic activity. Therefore, the addition of a surfactant (stabilizer)[11-13] or surface modification[14] of metal nanoparticles is usually required to prevent the self-aggregation. The immobilization and encapsulation of metal nanoparticles with polymer matrices, including polymer particles,[15-20] micelles,[21] and hydrogel,[22] have also been reported as possible methods to prevent aggregations using high polymer's tunability. However, these polymer/AgNPs composite materials having catalytic property were complplicated to be isolated form the reduction reaction system owing to their nano-, micron size in diameter.[16-19, 21] Moreover, the catalytic performance test was carried out only once in most of the research, which is considered as less practical materials.

Cellulose is the most abundant natural polymer on Earth and it exhibits many attractive properties, including thermal and chemical stability, nontoxicity, and biocompatibility.[23] Thus, cellulose is extensively used to produce industrial materials such as pulps, regenerated fibers, and membranes.[24] Recently, cellulose particles have been recognized as functional materials[25] that can be used in many applications, including removers for organic substances or metals,[26, 27] column-packing materials for biochromatography,[28] or supports for protein immobilization,[25] owing to their interesting characteristics, which include a low nonspecific adsorption of proteins[29] and the availability for surface modification,[30, 31] in addition to the abovementioned properties. Therefore, cellulose particles have a great potential for use as matrices of metal

nanoparticles. However, most reports on cellulose/metal NPs composites show that AgNPs were synthesized in the presence of cellulose matrices, in which large amounts of free AgNPs should be generated in the medium and laborious washing should be required; Zhao and Xu et al. successfully synthesized AgNPs on porous cellulose microspheres by hydrothermal reduction, in which the cellulose microspheres played a role of a reducing agent for Ag ions, limiting the reduction site only on the cellulose microspheres.[20] However, in this report, dissolution of cellulose was still needed drastic conditions due to the slightly solubility of cellulose. In addition, the composite with AgNPs were used as a catalyst only once.

In 2002, Rogers and coworkers reported that ionic liquids (ILs), such as 1-butyl-3-methylimidazolium chloride ([Bmim]Cl), could dissolve cellulose under mild heating condition.[32] Since then, ILs have attracted increasing interest as solvents for cellulose.[10, 33, 34]

Minami et al. reported the preparation of porous cellulose particles by the solvent-releasing method (SRM)[35, 36] using a [Bmim]Cl solution of cellulose.[37] The obtained particles exhibited a high specific surface area,[38-40] which makes them promising for functional materials applications upon modifying their surface. In addition, millimeter-sized cellulose particles having a high specific surface area were also obtained using a similar method. Owing to their size, the millimeter-sized cellulose particles are easy to handle, and have a great potential for recyclable scaffolds for catalysis.

In ***Chapter 5***, carboxylate groups were introduced into the porous cellulose particles by 2,2,6,6-tetramethylpiperidine-1-oxyl (TEMPO)-mediated oxidation,[41] which enabled us to selectively convert the hydroxyl groups at the C6 position of the surface of the cellulose microfibrils into carboxylate groups.[42-45] AgNPs were efficiently synthesized on the porous structures using the carboxylate groups as a scaffold, followed by the immobilization of AgNPs on cellulose particles. Moreover, we evaluated the catalytic performance and catalyst-recycling

ability of the composite cellulose/Ag particles by studying the reduction of 4-nitrophenol to 4-aminophenol.

# Experimental Section

## Materials

Microcrystalline cellulose (powder, derived from cotton linter, $M_n$; $3.0 \times 10^4$, particles size; 51 μm), 1-butyl-3-methylimidazolium chloride ([Bmim]Cl), 2,2,6,6-tetramethylpiperidine-1-oxyl (TEMPO), and cysteamine were used as received from Aldrich Chemical Co., Ltd. *N*,*N*-Dimethylformamide (DMF), 1-butanol, ethanol, a phosphate pH standard equimolal solution (pH 6.86 at 25°C), a sodium hypochlorite (NaClO) solution, sodium chlorite ($NaClO_2$), hydrochloric acid, sodium hydrate (NaOH), silver nitrate ($AgNO_3$), sodium borohydride, 4-nitrophenol (4-NP), and *N*,*N'*-dicyclohexylcarbodiimide (DCC) were used as received from Nacalai Tesque Inc. (Kyoto, Japan). *N*-Hydroxysuccinimide (NHS) was also used as received from Tokyo Chemical Industry Co., Ltd. The water used in the experiments was purified using an ErixUV (Millipore, Japan) purification system and had a resistivity of 18.2 MΩ cm.

## Preparation of Cellulose Particles by the SRM

Millimeter-sized cellulose particles were prepared by the SRM, according to our previous reports.[37, 40] Microcrystalline cellulose powder was dissolved in [Bmim]Cl at a weight ratio of 7:43 upon heating at 100°C for 7 h. DMF was added as a co-solvent to reduce the viscosity of the solution. This cellulose–[Bmim]Cl–DMF (7/43/50, w/w/w) (8.57 g) mixture was then dropped into a large amount of 1-butanol (ca. 100 mL) under stirring (using a syringe) to remove the [Bmim]Cl and DMF from the drops. The cellulose present in the solution immediately precipitated in the form of cellulose particles, which were washed three times with 1-butanol and twice with water to remove any remaining impurities. The cellulose particles were stirred for 2 h between each washing step. The original microcrystalline cellulose had

cellulose I type crystal. On the other hand, the particles prepared by SRM changed crystal structure to cellulose II type with very small crystal.[39]

**TEMPO-Mediated Oxidation of Porous Cellulose Particles**

TEMPO-mediated oxidation was conducted according to the following procedure: TEMPO (3 mg) and $NaClO_2$ (22 mg) were dissolved in a phosphate pH standard equimolar solution (10 mL, pH 6.86 at 25°C). Then, a NaClO solution (7.5 wt%, 10 mL; diluted in a standard buffer solution) was added into the mixture, and the cellulose particles (80 mg) were immersed in this solution for 1 h upon stirring. Oxidation was performed by stirring the mixture at 60˚C in a 50 mL flask, and the obtained carboxylated cellulose particles were thoroughly washed with water.

**Preparation of Composite Cellulose/Ag Particles**

The carboxylated cellulose particles (80 mg) were immersed in an aqueous $AgNO_3$ solution (40 mL, 6.4 mM) for 5 h at room temperature upon stirring. The obtained particles were washed with water twice over 2 h to remove the free Ag cations. Reduction of the Ag cations was performed for 2 h using either an aqueous $NaBH_4$ solution at room temperature in a glass bottle or ethanol at 160°C in an autoclave. The obtained cellulose/Ag particles were thoroughly washed with water to remove the free Ag cations and AgNPs.

In the case of immobilizing the as-prepared AgNPs on the cellulose particles for improving the recyclable catalytic performance, the immobilization through covalent bonds was achieved as follows: the obtained cellulose/Ag particles (35 mg) were first dispersed in a DMF (10.0 g) medium containing dissolved DCC (26.9 mg), NHS (14.9 mg), and cysteamine

(1.2 mg) and then stirred at room temperature for 2 h. The obtained cellulose–Ag particles were thoroughly washed with DMF and preserved in water.

**Estimation of the Catalytic Performance of AgNPs in the Composite Cellulose Particles**

The catalytic efficiencies of the composite cellulose particles were evaluated using the reduction of 4-nitrophenol (4-NP) to 4-aminophenol (4-AP) in the presence of $NaBH_4$ as a model reaction. The AgNPs were used as catalysts. In the experiments, $NaBH_4$ (90.8 mg) was first added to an aqueous 4-NP solution (40 mL, 0.06 mM); further, a part of the obtained mixture (4 g) was poured into a quartz cuvette, and the composite particles (3.5 mg) were dispersed in it. The reduction reaction occurred in the quartz cuvette and was monitored at fixed time intervals by UV–visible spectroscopy (UV-2500 UV–vis spectrophotometer, Shimadzu Corp., Kyoto, Japan).

**Characterization**

The cellulose particles were immersed in liquid nitrogen, freeze-dried in a freeze-dryer (FDU-1200, Tokyo Rikakikai Co., Ltd.; Tokyo, Japan), and observed using a scanning electron microscope (SEM, JSM-6510, JEOL, Tokyo, Japan) on an accelerating voltage 20 kV after platinum coating. To analyze their inner morphology, ultrathin (100 nm-thick) cross sections of the particles were prepared using a cryomicrotome (Leica EM UC6 equipped with EM FC7). The sliced samples were then observed using a transmission electron microscope (TEM, JEM-1230, JEOL, Tokyo, Japan). The number-average diameter ($D_n$) and the coefficient of variation ($C_V$) was estimated from 200 AgNPs on the TEM images using image-analysis (WinRoof, Mitani Co., ltd., Japan). Nitrogen adsorption measurements were performed using a Quantachrome NOVA 3200e instrument (USA). The Brunauer–Emmett–Teller (BET) specific

surface area of the cellulose particles was assessed from the adsorption branch of the isotherm for a relative pressure of 0.05–0.3 at 77 K.

The products were qualitatively analyzed using a Fourier-transform infrared spectrometer (FT-IR, FT/IR-6200, JASCO, Tokyo, Japan) and the pressed KBr pellet technique. The electric conductivity titration method was applied to quantify the amount of carboxylate in the cellulose particles.[50] Briefly, dried cellulose particles (80 mg) were immersed in hydrochloric acid (15 mL, 0.01 M) and disintegrated into a well-dispersed slurry by ultrasonication. Further, an aqueous NaOH solution (0.01 M) was added to the mixture at a rate of 0.4 mL $min^{-1}$ while monitoring the electric conductivity of the system using a conductance meter (F-74, HORIBA Corp., Kyoto, Japan).

The amount of AgNPs supported on the cellulose particles was measured using a thermogravimetric analyzer (TGA, EXSTAR TG/DTA6200, SII Nano Technology Inc., Japan) at a heating rate of 10 °C $min^{-1}$ from 30 to 900°C under a nitrogen atmosphere.

## Results and Discussion

### *TEMPO-Mediated Oxidation of Porous Cellulose Particles*

The cellulose particles were oxidized by a TEMPO-mediated reaction in which the hydroxyl groups at the C6 position of cellulose can be selectively converted to carboxyl groups. Figure 1 shows photos of the wet cellulose particles and SEM images of the cross sections of the freeze-dried samples before and after TEMPO oxidation. Both cellulose particles had a spherical shape and a porous structure. In order to investigate microscopic structures, nitrogen adsorption/desorption measurements were carried out. Figure 2 shows isotherms and BJH pore size distributions for the particles before and after particles. Both isotherms are categorized to type IV according to IUPAC classification with a hysteresis loop, suggesting the presence of micropore structures beside mesopore structures. The BJH pore sizes and volumes of the particles before and after oxidation was approximately 1.5 nm; 0.18 $cm^3\ g^{-1}$, and 1.9 nm; 0.14 $cm^3\ g^{-1}$, respectively. In addition, the specific surface areas of the particles were 112 $m^2\ g^{-1}$ and 107 $m^2\ g^{-1}$, respectively, measured by the BET method. These results indicate that the shape and porous structure were maintained after the TEMPO oxidation.

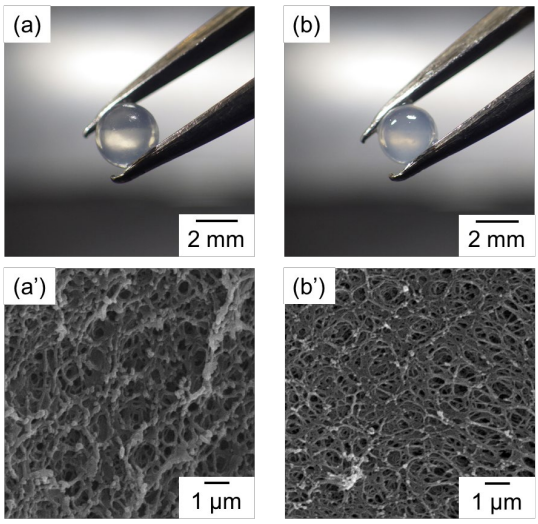


**Figure 1.** Photos of cellulose particles (a, b) and SEM images of the cross sections of freeze-dried cellulose particles (a', b') before (a, a') and after (b', b') TEMPO-mediated oxidation.

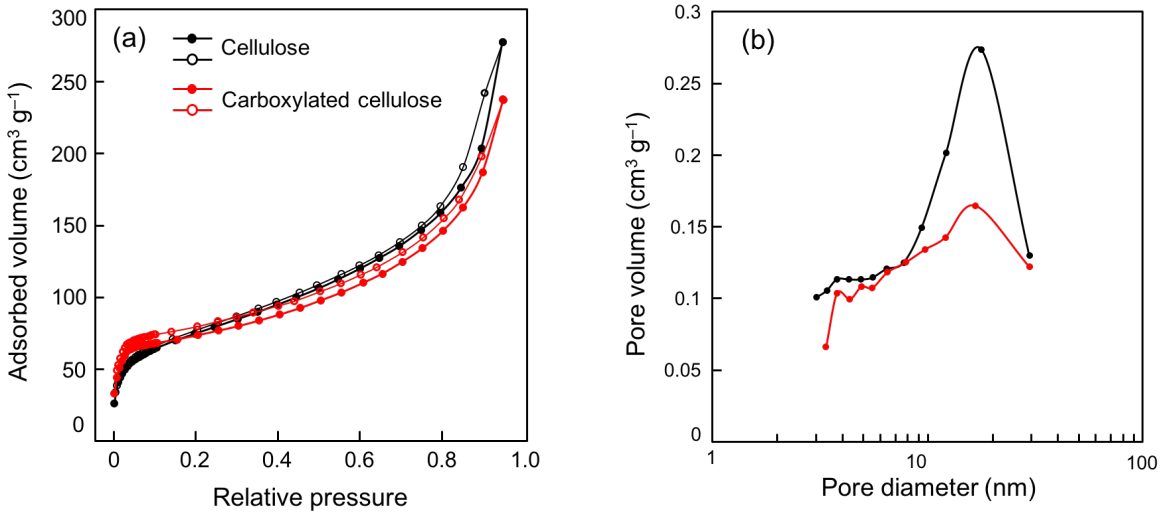


**Figure 2.** Nitrogen adsorption (closed circles) and desorption (open circles) isotherms (a) and BJH pore size distributions (b) of freeze-dried cellulose particles before (black) and after (red) the oxidation.

FT-IR measurements were performed to confirm the presence of carboxyl groups in the oxidized cellulose particles. Figure 3 shows the FT-IR spectra of the samples before and after oxidation. The oxidized cellulose particles exhibited an absorption band at 1620 $cm^{-1}$, which can be attributed to the carboxylate ion, and was not present in the spectrum of the untreated particles. This indicates that the oxidized cellulose particles contained carboxyl groups, which were quantified by electric conductivity titration. Figure 4 shows the relation between the oxidation time and carboxylate content of the oxidized cellulose particles. The carboxylate content increased from 0.1 to 0.4 mmol $g^{-1}$-cellulose with the oxidation time during first 15 min and then reached a plateau level, indicating that the oxidation reaction occurred within 15 min. In contrast, in the case of cellulose particles having dense structures (5.7 $m^2$ $g^{-1}$), which were obtained by drying porous cellulose particles after the preparation, the carboxylate content was 0.2 mmol $g^{-1}$-cellulose for 3 h. These results indicate that almost all the hydroxyl groups on the surface and inside the porous structures were converted into carboxyl groups.

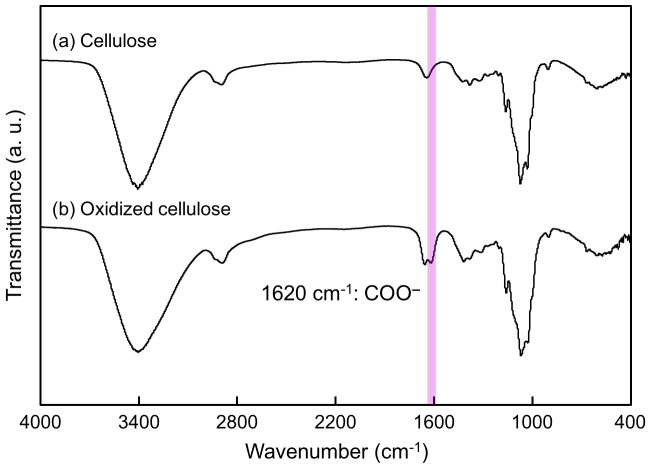


**Figure 3.** FT-IR spectra of cellulose particles before (a) and after (b) TEMPO-mediated oxidation.

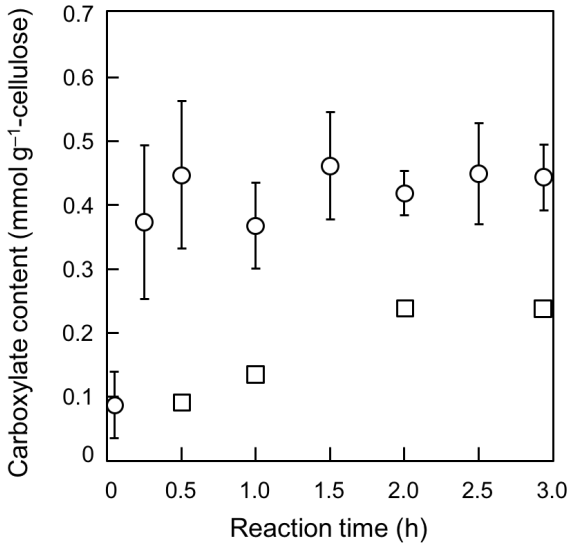


**Figure 4.** Carboxylate contents of porous (circles) and dense (squares) cellulose particles oxidized by TEMPO-mediated oxidation at various oxidation time.

***Preparation of Composite Cellulose/Ag Particles***

To prepare the composite cellulose/Ag particles, the carboxylated cellulose particles were dipped in an aqueous $AgNO_3$ solution for 5 h, where the Ag cations were coordinated to the carboxyl groups on the cellulose particles. Reduction of the Ag cations was then conducted using an aqueous $NaBH_4$ solution. The color of the cellulose particles changed from whitish to yellow-brown, and from the TEM image of the ultrathin cross section AgNPs ($D_n$, 8.6 nm; $C_v$, 33.2%) were successfully synthesized in them (Figure 5a, d). Moreover, the AgNPs content on the cellulose particles was measured by TGA analysis. Figure 6 shows TGA curves of the cellulose particles and cellulose composite particles. The analysis was carried out a nitrogen atmosphere considering the possibility of the oxidation of AgNPs to $Ag_2O$ under an oxygen atmosphere. The amount of AgNPs was determined from the remaining weight considering the weight loss of cellulose at 900°C. The TGA results indicate that 58.5 mg of AgNPs were supported on 1 g of cellulose particles. However, it can be seen in the cross section of the obtained cellulose/Ag particles that the inside of the material was remained colorless, suggesting that the AgNPs were produced only at the particle surface (Figure 5b). The TEM images of the ultrathin cross section show clearly that most of the AgNPs aggregated near the surface of the composite cellulose particles (Figure 5b, c). These results can be attributed to the reduction procedure: when the carboxylated cellulose particles dipped in an aqueous $AgNO_3$ were immersed in the $NaBH_4$ solution, most of the $NaBH_4$ molecules were consumed to reduce the Ag cations on the surface of the particles before they could diffuse into the particles.

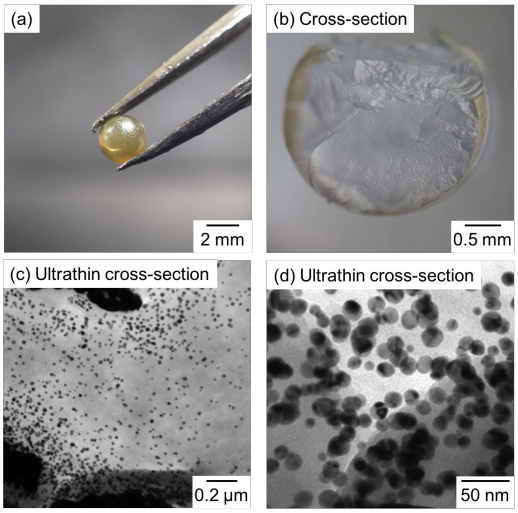


**Figure 5.** Photos of a composite cellulose/Ag particle (a), cross section of the particle (b), and TEM images of ultrathin cross section of the particle (c, d) after the reduction of Ag cations using an aqueous $NaBH_4$ solution. Low (c) and high (d) magnifications.

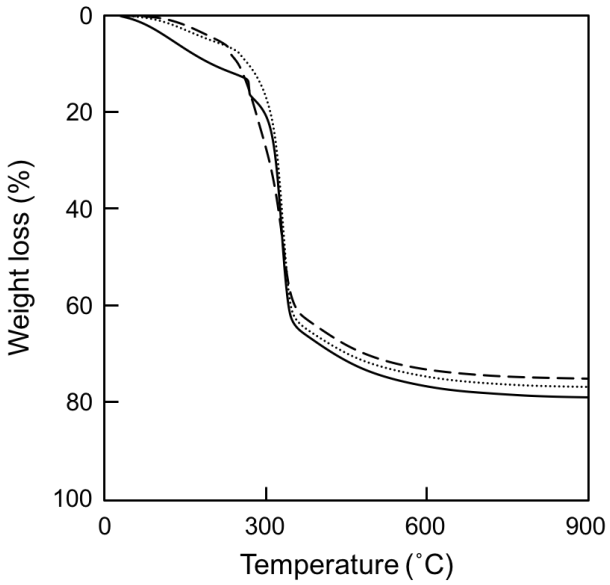


**Figure 6.** Thermal decomposition profiles (under $N_2$ atmosphere) of cellulose particles (solid line) and composite cellulose/Ag particles prepared by the reduction of Ag cations in carboxylated cellulose particles using $NaBH_4$ (dashed line) and ethanol (dotted line).

The alcohol reduction method was applied at 160°C to synthesize AgNPs inside the porous structures of cellulose particles. The medium filling in the porous structure of the particles can be changed from water to alcohol at room temperature before reduction reaction,[40] which made it possible for the Ag cations to be reduced uniformly inside the porous structures. After the reduction of Ag cations at 160°C for 2 h, using ethanol as both the reduction agent and the surrounding medium, the color of the surface and the cross section of the obtained particles became yellow-brown, whereas there was no color change in the reaction medium, which indicated that AgNPs were efficiently synthesized without free AgNPs (Figure 7a, b, c).

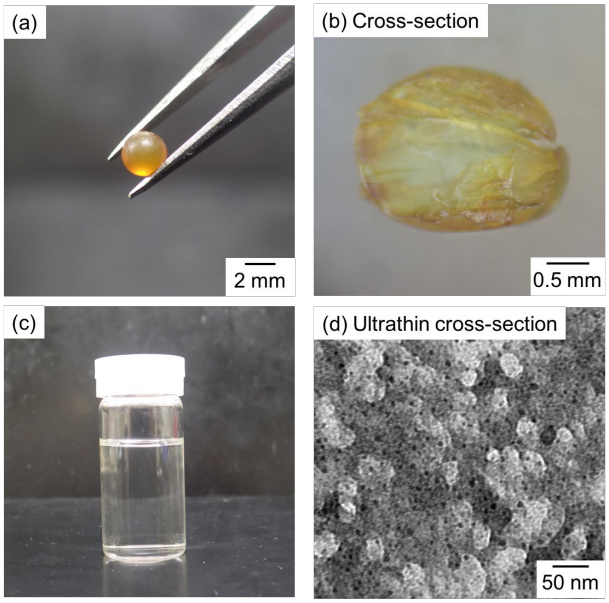


**Figure 7.** Photos of a composite cellulose/Ag particle (a), cross section of the particle (b), photo of the reaction medium (c), and TEM image of ultrathin cross section of the particle after the reduction of Ag cations in ethanol at 160°C for 2 h.

In addition, the cellulose particles maintained their spherical shape and size, indicating that the cellulose did not degrade during the reduction. The TEM image of the ultrathin cross section of the particles shows that AgNPs with much higher contrast were supported on the porous structures of the obtained particles with lower contrast (Figure 7d). The $D_n$ and $C_v$ of the AgNPs

were 9.8 nm and 25.3%, respectively, which is approximately consistent with the color of the obtained particles owing to the surface plasmon resonance effect.[7, 46, 47] These results indicate that AgNPs were successfully prepared not only on the surface but also inside the porous structure of the cellulose particles. In addition, from the TGA measurement (Figure 6), 30.8 mg of AgNPs were supported on 1 g of cellulose particles, which agrees well with the theoretical value (i.e., 39.7 mg per g of cellulose particles) calculated from the amount of carboxyl in the samples.

***Catalytic Properties of the Composite Cellulose/Ag Particles***

The catalytic performance of the cellulose/Ag particles was estimated by monitoring the reduction of 4-NP to 4-AP in the presence of $NaBH_4$ by UV–visible spectroscopy. In this reaction, 4-NP is firstly converted into 4-NP ion after addition of $NaBH_4$, and then the 4-NP ion is reduced into 4-AP ion by $NaBH_4$ in the presence of a catalyst.[48] When the reduction reaction occurred after addition of the obtained cellulose/Ag particles as a catalyst, the intensity of the characteristic peak for the 4-NP ion (at 400 nm) decreased, whereas that of the peak for the 4-AP ion (at 300 nm) increased (Figure 8). If the concentration of $NaBH_4$ is adjusted to be in largely excess of that of 4-NP, the reaction should be first order with regard to the 4-NP concentration; thus, the catalytic rate can be evaluated. In addition, the apparent kinetic rate constant $k_{app}$ is known to be proportional to the total surface area of AgNPs because the catalytic reduction proceeds on the surface of AgNPs.[20, 48] We calculated the rate constant $k_1$ normalized to $S$, which is the total surface area of AgNPs normalized to the unit volume of the reaction system, defined by the following equation:

$$-\frac{dC_t}{dt} = k_{app}C_t = k_1 S C_t$$

where $C_t$ is concentration of 4-NP at time $t$. To calculate $S$, the bulk density of silver ($\rho = 10.5\times 10^3$ kg m$^{-3}$) was used. The amount of AgNPs was estimated from TGA analysis and the amount was

not changed after the immobilization reaction and the reduction of 4-NP. Moreover, the diameter of AgNPs was determined by TEM results.

Figure 9 shows the relation between $\ln(A_t/A_0)$ and the reaction time for the cellulose/Ag particles and cellulose-free AgNPs, where $A_t$ is the absorbance at determined given time and $A_0$ is the initial absorbance at $t = 0$. In both cases, a linear correlation was found between $\ln(A_t/A_0)$ and the reaction time, indicating that the catalytic reduction proceeded with first-order kinetics for 4-NP reduction. When composite cellulose/Ag particles were used as the catalyst in the reaction, $k_{app}$ and the reaction conversion for 25 min, calculated from the slope, were $2.83 \times 10^{-2}$ $s^{-1}$ and almost 100%, respectively, whereas the value for the cellulose-free AgNPs were $3.66 \times 10^{-5}$ $s^{-1}$ and 6%, respectively, owing to their low specific surface area and coagulation. These results indicate that the porous cellulose particles made a great contribution to the improvement of the catalytic efficiency.

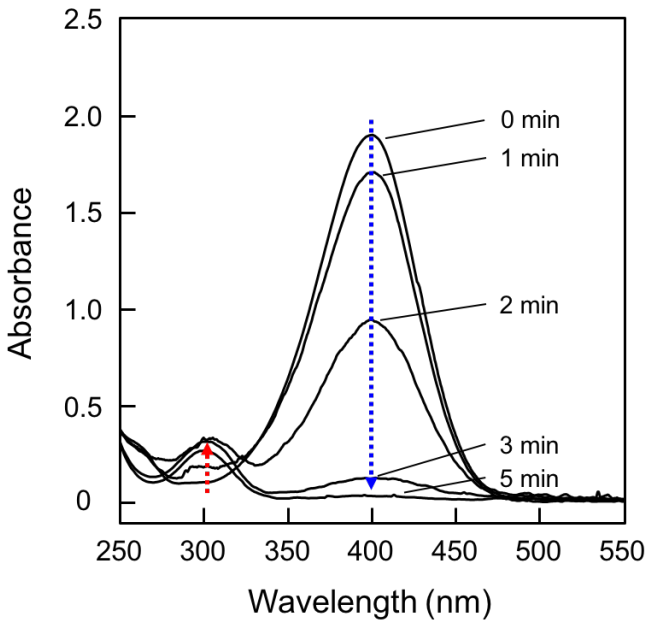


**Figure 8.** UV-vis spectra of solution of 4-nitrophenol during reduction of 4-nitrophenol using composite cellulose/Ag particles at different time.

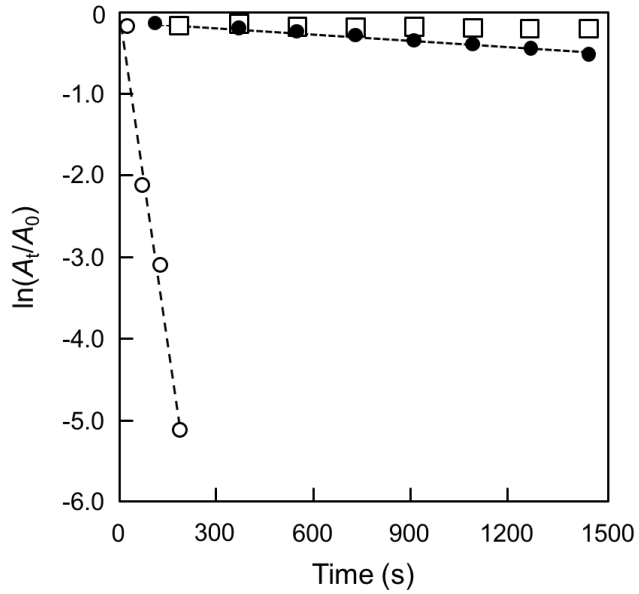


**Figure 9.** Relation between $\ln(A_t/A_0)$ and time for the catalytic reduction of 4-nitrophenol using composite cellulose/Ag particles (circles) and cellulose-free AgNPs (squares); the first (open circles and squares) and second (closed circles) runs are shown.

Moreover, we compared to the catalytic activities reported in the other systems, summarized in Table 1. The catalytic activity of AgNPs in the cellulose particles in this work ($1.86 \times 10^{-2}$ $s^{-1}$ $m^{-2}$ L) is comparable with those immobilized in cellulose microspheres ($4.42 \times 10^{-2}$ $s^{-1}$ $m^{-2}$ L),[20] PS-PNIPAm core-shell microgels ($5.02 \times 10^{-2}$ $s^{-1}$ $m^{-2}$ L)[18] and PS-PAA spherical polyelectrolyte brush particles ($7.81 \times 10^{-2}$ $s^{-1}$ $m^{-2}$ L),[19] and exhibits higher activity than those encapsulated in the bulk polymer hydrogel (7.80 or $7.31 \times 10^{-2}$ $s^{-1}$ $m^{-2}$ L).[22]

Table 1. Catalytic activity of the silver nanoparticles for the reduction reaction of 4-nitrophenol.

| Samples | Carrier system | $D_n$ [nm][a)] | $k_1$ [$s^{-1}$ $m^{-2}$ L][b)] |
|---|---|---|---|
| Cellulose/Ag 1st run | Cellulose particles; this work | 9.8±2.4 | $1.86\times10^{-2}$ |
| Cellulose-S-Ag 1st run | Cellulose particles; this work | 8.6±2.8 | $2.75\times10^{-5}$ |
| Cellulose-S-Ag 3rd run | Cellulose particles; this work | 8.6±2.8 | $3.37\times10^{-5}$ |
| Ref 20 | Cellulose microsphere | 8.3±3.4 | $4.42\times10^{-2}$ |
| Ref 16 | PS-PNIPAm core-shell microgel | 8.5±1.5 | $5.02\times10^{-2}$ |
| Ref 18 | PS-PAA-Ag anionic polyelectrolyte | 3±1.2 | $7.81\times10^{-2}$ |
| Ref 22 | PVA/PS-PEGMA hydrogel | 35±5 | $7.80\times10^{-5}$ |
| Ref 22 | PVA hydrogel | 45±5 | $7.31\times10^{-5}$ |

[a)] $D_n$, diameter of silver nanoparticles measured by TEM images
[b)] $k_1$, rate constant normalized to the total surface of the nanoparticles in the reduction system

Metal nanoparticle catalysts are generally supported on soluble, nano- or microsized materials, such as dendrimers,[2] or polymeric microspheres,[15, 16] for recycling. In this study, millimeter-sized composite cellulose particles could be easily isolated from the reaction system. However, when the reduction was conducted using recycled cellulose/Ag composite particles recovered after the first reduction, the catalyst activity decreased remarkably (Figure 8) because the AgNPs were detached from the cellulose particles during the reaction and the washing step.

To solve this problem, the AgNPs were immobilized on the cellulose particles through Ag–sulfur (Ag–S) bonds, which were formed by bridging thiol groups to the AgNPs.[49] A condensation reaction between the carboxyl groups of the cellulose/Ag particles and the amine groups of cysteamine was used to introduce the thiol groups on the cellulose particles and form the required Ag–S bonds. The obtained immobilized AgNPs–cellulose particles retained the yellow-brown color, and AgNPs ($D_n$, 8.6 nm; $C_v$, 33.2%) supported on the porous structure were observed in the TEM image of the ultrathin cross section, although some of the AgNPs coagulated (Figure 10). The recycling ability of the obtained particles was also investigated. Figure 11 shows the relation between $\ln(A_t/A_0)$ and the reaction time for immobilized AgNPs–cellulose particles during three runs. The reaction rate constant ($2.75 \times 10^{-5}$ $s^{-1}$ $m^{-2}$ L) of the immobilized AgNP–cellulose catalyst was lower than that observed with the composite cellulose/Ag particles during the first run ($1.86 \times 10^{-2}$ $s^{-1}$ $m^{-2}$ L). This was caused by the adsorption of cysteamine molecules on the surface of the AgNPs during the coupling reaction, leading to a drop in the catalytic efficiency. However, comparison with first run, the catalytic ability of the AgNPs-immobilized particles in third run was almost same, and the conversion of 4-NP was almost the same (approx. 100%) in each step, indicating that the coupling of Ag–S bonds could prevent the AgNPs from detaching from the cellulose particles and that the immobilized AgNPs–cellulose particles exhibit good recycling ability when used as a catalyst.

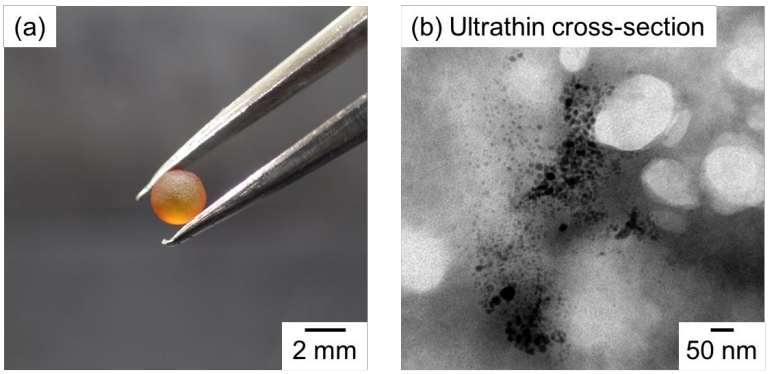


**Figure 10.** Photo (a) and TEM image of the ultrathin cross section (b) of an immobilized AgNPs–cellulose particle prepared by a condensation reaction between the carboxyl groups of composite cellulose/Ag particles and cysteamine.

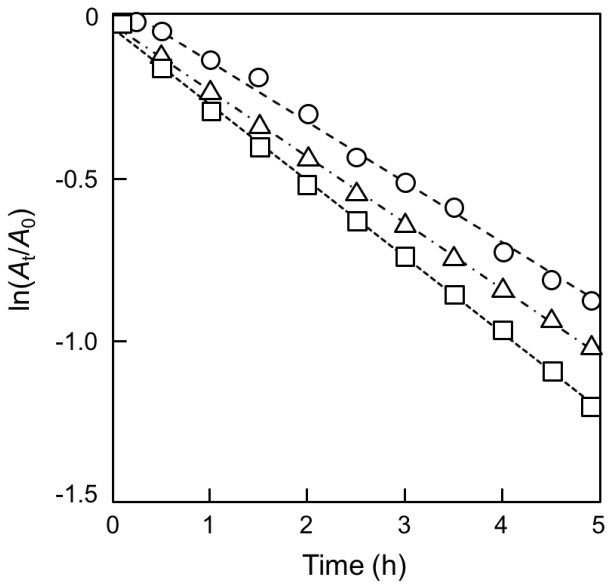


**Figure 11.** Relation between $\ln(A_t/A_0)$ and time for the catalytic reduction of 4-nitrophenol using immobilized AgNPs–cellulose particles; the first (circles), second (squares), and third runs (triangles) are shown.

## Conclusion

The composite cellulose/Ag particles have successfully prepared by introducing carboxylate groups into the porous structures of cellulose particles, which are used as a scaffold for the synthesis of AgNPs. The catalytic ability of the cellulose/Ag particles for the reduction of 4-NP to 4-AP was much higher than that of cellulose-free AgNPs. Furthermore, when AgNPs were immobilized on the cellulose/Ag particles via Ag–S bonds, the obtained immobilized particles maintained their catalytic performance during three cycles. The knowledge obtained in this study is readily available for the preparation of other metal nanoparticles on the cellulose particles and they can be to handled and recycled without complicated process. Therefore, resulting materials have a great potential for catalyst applications. Moreover, for making the preparation method easy, we have been trying to prepare cellulose composite particles immobilized metal nanoparticles via one step and will report it in the future.

## References


1. P. M. Tessier, O. D. Velev, A. T. Kalambur, J. F. Rabolt, A. M. Lenhoff and E. W. Kaler, *Journal of the American Chemical Society*, 2000, **122**, 9554-9555.
2. I. Hussain, M. Brust, A. J. Papworth and A. I. Cooper, *Langmuir*, 2003, **19**, 4831-4835.
3. P. Dauthal and M. Mukhopadhyay, *Industrial & Engineering Chemistry Research*, 2016, **55**, 9557-9577.
4. Y. C. Cao, R. Jin and C. A. Mirkin, *Science*, 2002, **297**, 1536.
5. N. L. Rosi and C. A. Mirkin, *Chemical Reviews*, 2005, **105**, 1547-1562.
6. V. K. Sharma, R. A. Yngard and Y. Lin, *Advances in Colloid and Interface Science*, 2009, **145**, 83-96.
7. S. Agnihotri, S. Mukherji and S. Mukherji, *RSC Advances*, 2014, **4**, 3974-3983.
8. J.-W. Kwon, S. H. Yoon, S. S. Lee, K. W. Seo and I.-W. Shim, *Bull. Korean Chem. Soc.*, 2005, **26**, 837-840.
9. M. Kaushik and A. Moores, *Green Chemistry*, 2016, **18**, 622-637.
10. I. Sultana, M. Idrees, M. Yasir Rafique, S. Ilyas, S. Q. Hussain, A. A. Kahn and A. Razaq, *J. Mater. Sci.: Mater. Electron.*, 2018, DOI: 10.1007/s10854-018-0194-7, Ahead of Print.
11. J. Fink, C. J. Kiely, D. Bethell and D. J. Schiffrin, *Chemistry of Materials*, 1998, **10**, 922-926.
12. K. Hayakawa, T. Yoshimura and K. Esumi, *Langmuir*, 2003, **19**, 5517-5521.
13. T. Huang, F. Meng and L. Qi, *The Journal of Physical Chemistry C*, 2009, **113**, 13636-13642.
14. G. Harada, H. Sakurai, M. M. Matsushita, A. Izuoka and T. Sugawara, *Chem. Lett.*, 2002, DOI: 10.1246/cl.2002.1030, 1030-1031.
15. W. Liu, X. Yang and W. Huang, *Journal of Colloid and Interface Science*, 2006, **304**, 160-165.
16. Y. Lu, Y. Mei, M. Drechsler and M. Ballauff, *Angewandte Chemie International Edition*, 2006, **45**, 813-816.
17. Y. Lu, Y. Mei, R. Walker, M. Ballauff and M. Drechsler, *Polymer*, 2006, **47**, 4985-4995.
18. Y. Lu, Y. Mei, M. Schrinner, M. Ballauff, M. W. Möller and J. Breu, *The Journal of Physical Chemistry C*, 2007, **111**, 7676-7681.
19. M. Zhang, L. Liu, C. Wu, G. Fu, H. Zhao and B. He, *Polymer*, 2007, **48**, 1989-1997.
20. J. Wu, N. Zhao, X. Zhang and J. Xu, *Cellulose*, 2012, **19**, 1239-1249.
21. H. Xu, J. Xu, Z. Zhu, H. Liu and S. Liu, *Macromolecules*, 2006, **39**, 8451-8455.
22. Y. Lu, P. Spyra, Y. Mei, M. Ballauff and A. Pich, *Macromolecular Chemistry and Physics*, 2007, **208**, 254-261.
23. D. Klemm, B. Heublein, H.-P. Fink and A. Bohn, *Angew. Chem., Int. Ed.*, 2005, **44**, 3358-3393.
24. S. Wang, A. Lu and L. Zhang, *Progress in Polymer Science*, 2016, **53**, 169-206.
25. M. Gericke, J. Trygg and P. Fardim, *Chemical Reviews*, 2013, **113**, 4812-4836.
26. X. Guo and F. Chen, *Environmental Science & Technology*, 2005, **39**, 6808-6818.
27. N. Li and R. Bai, *Separation and Purification Technology*, 2005, **42**, 237-247.
28. K.-F. Du, M. Yan, Q.-Y. Wang and H. Song, *Journal of Chromatography A*, 2010, **1217**, 1298-1304.
29. D. J. Gardner, G. S. Oporto, R. Mills and M. A. S. A. Samir, *Journal of Adhesion Science and Technology*, 2008, **22**, 545-567.

30. D. Roy, M. Semsarilar, J. T. Guthrie and S. Perrier, *Chemical Society Reviews*, 2009, **38**, 2046-2064.
31. S. Eyley and W. Thielemans, *Nanoscale*, 2014, **6**, 7764-7779.
32. R. P. Swatloski, S. K. Spear, J. D. Holbrey and R. D. Rogers, *Journal of the American Chemical Society*, 2002, **124**, 4974-4975.
33. A. Pinkert, K. N. Marsh, S. Pang and M. P. Staiger, *Chem. Rev. (Washington, DC, U. S.)*, 2009, **109**, 6712-6728.
34. H. Wang, G. Gurau and R. D. Rogers, *Chem. Soc. Rev.*, 2012, **41**, 1519-1537.
35. M. Okubo, Y. Konishi, M. Takebe and H. Minami, *Colloid Polym. Sci.*, 2000, **278**, 919-926.
36. M. Okubo, Y. Konishi, S. Sebki and H. Minami, *Colloid Polym. Sci.*, 2002, **280**, 765-769.
37. T. Suzuki, K. Kono, K. Shimomura and H. Minami, *J. Colloid Interface Sci.*, 2014, **418**, 126-131.
38. K. Imagawa, T. Omura, Y. Ihara, K. Kono, T. Suzuki and H. Minami, *Cellulose (Dordrecht, Neth.)*, 2017, **24**, 3111-3118.
39. T. Omura, K. Imagawa, K. Kono, T. Suzuki and H. Minami, *ACS Applied Materials & Interfaces*, 2017, **9**, 944-949.
40. T. Omura, K. Imagawa, T. Suzuki and H. Minami, *Langmuir*, 2018, **34**, 15490-15494.
41. A. E. J. de Nooy, A. C. Besemer and H. van Bekkum, *Tetrahedron*, 1995, **51**, 8023-8032.
42. T. Saito, Y. Nishiyama, J.-L. Putaux, M. Vignon and A. Isogai, *Biomacromolecules*, 2006, **7**, 1687-1691.
43. T. Saito, S. Kimura, Y. Nishiyama and A. Isogai, *Biomacromolecules*, 2007, **8**, 2485-2491.
44. M. Hirota, N. Tamura, T. Saito and A. Isogai, *Cellulose (Dordrecht, Neth.)*, 2009, **16**, 841-851.
45. A. Isogai, T. Saito and H. Fukuzumi, *Nanoscale*, 2011, **3**, 71-85.
46. Y. Habibi, H. Chanzy and M. R. Vignon, *Cellulose (Dordrecht, Neth.)*, 2006, **13**, 679-687.
47. E. Rodríguez-León, R. Iñiguez-Palomares, R. E. Navarro, R. Herrera-Urbina, J. Tánori, C. Iñiguez-Palomares and A. Maldonado, *Nanoscale Research Letters*, 2013, **8**, 318.
48. Y. Lee and S.-G. Oh, *Colloids and Surfaces A: Physicochemical and Engineering Aspects*, 2014, **459**, 172-176.
49. N. Pradhan, A. Pal and T. Pal, *Colloids and Surfaces A: Physicochemical and Engineering Aspects*, 2002, **196**, 247-257.
50. C. Battocchio, C. Meneghini, I. Fratoddi, I. Venditti, M. V. Russo, G. Aquilanti, C. Maurizio, F. Bondino, R. Matassa, M. Rossi, S. Mobilio and G. Polzonetti, *The Journal of Physical Chemistry C*, 2012, **116**, 19571-19578.

# *Chapter 6*

# Preparation of Aminated Cellulose Particles with Recyclable Catalytic Property

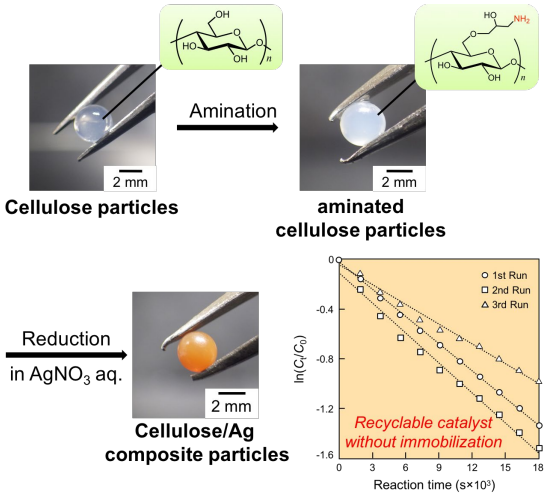


**Abstract:** Amine groups were introduced into porous cellulose particles, which were prepared by the solvent releasing method (SRM), and the medium containing the amineated cellulose particles was replaced to aqueous $AgNO_3$ solution. Amineated cellulose/Ag composite particles were synthesized by a reduction of Ag cation utilizing the amine groups as a reducing agent. The content of Ag nanoparticles (AgNPs) in the composite particles could be controlled by changing the molar ratio of $AgNO_3$ and amine groups. Catalytic efficiency of the composite particles was evaluated by a reduction reaction of 4-nitrophenol. When the amount of AgNPs was much larger than that of the amine groups due to a large ratio of $AgNO_3$/amine groups (10/1), the resulting AgNPs were detached from the cellulose particles, causing a remarkable decrease of the catalytic activity. On the other hand, in use of the composite particles prepared by the reduction at the equal ratio to each other, the catalytic efficiency was maintained for at least three cycles without immobilization of AgNPs on the cellulose particles because of the amine groups as a linkage of cellulose particles and AgNPs.

## Introduction

Metal nanoparticles have been widely investigated due to their unique optical, electrical, and catalytic properties. These unique properties make them great potential materials for applications in areas such as optics,[1, 2] electronics,[3] catalysis,[3, 4] and sensors.[5, 6] Silver nanoparticles (AgNPs) exhibit the unique characteristics including excellent electrical[7, 8] and thermal conductivity, catalytic activity,[7, 9, 10] and antibacterial action;[11, 12] however, colloidal particles are easy to aggregate in solutions due to their thermodynamically instability, causing deactivation of their unique properties. Thus, various strategies to prevent aggregation of AgNPs were developed such as addition of a surfactant (stabilizer),[13] surface modification of nanoparticles,[14] encapsulation and immobilization using polymer matrices (particles,[15, 16] micelles,[17] dendrimers[10], and nanofibers[18]). However, these polymer/AgNPs composite materials having catalytic properties were difficult to be separated from the reduction reaction systems owing to their nano-, micron size in diameter. Moreover, the catalytic performance tests were carried out only once in most of the research, which is considered as less practical materials.

Cellulose is one of the prime component of lignocellulosic biomass and the most abundant biopolymer on Earth, of which global production are estimated $1.5 \times 10^{12}$ tons per year.[19] In addition, it has many attractive properties such as thermal and chemical stability, nontoxicity, and biodegradability;[19, 20] thus, there are a lot of cellulose-based products, including pulp,[21] paper,[22] fiber, and membrane.[23] Recently, cellulose particles have been focused on as functional materials[24] such as removers of organic substances[25] or metal,[26] column packing materials for bio-chromatography,[27] and supports for protein immobilization[24] due to characteristics of cellulose, including the availability for surface modification[28] and a low nonspecific adsorption of proteins,[29] besides above-mentioned properties. Therefore,

cellulose particles are an attractive candidate for metal nanoparticles synthesis and support medium; however, the dissolution of cellulose needs multistep processes or drastic conditions as cellulose is insoluble in most common solvents owing to its strong hydrogen network.[30]

In 2002, Rogers et al.[31] discovered that some ionic liquids (ILs), such as 1-butyl-3-methylimidazolium chloride and bromide ([Bmim]Cl and [Bmim]Br), could dissolve cellulose under a mild condition. After this reports, ILs have been attracting interest as solvents for cellulose.[32-35] Utilizing this knowledge, Minami et al.[36] reported the successful preparation of porous cellulose particles using a [Bmim]Cl and by the solvent releasing method (SRM).[37, 38] The cellulose particles had a high specific surface area and the porous structure was filled with a surrounding medium.[39-41] In ***Chapter 5***, the carboxylate groups were introduced into porous cellulose particles by use of TEMPO-mediated oxidation, and AgNPs were successfully synthesized in the cellulose particles using their porous structures as a template. The composite cellulose/Ag particles were easy to handle owing to their millimeter-size and had a recyclable catalytic ability; however, without immobilization of AgNPs on the cellulose particles via Ag-sulfur covalent bonds the catalytic efficiency dropped remarkably during reuse of them. Therefore, the two-step – the synthesis and the immobilization of AgNPs on the cellulose particles – needed to obtain the composite particles having a high catalytic ability.

In ***Chapter 6***, composite cellulose/Ag particles with a recyclable catalytic ability were prepared without an immobilization of AgNPs by introduction of primary amine groups on the porous structures of cellulose particles, in which the amine groups would play key roles as a reducing agent for Ag cations and as a linkage of cellulose with the resulting AgNPs. Catalytic performances of the obtained cellulose/Ag particles were evaluated by use of a model reaction of 4-nitrophenol to 4-aminophenol, and the catalyst recycling ability was also studies.

# Experimental Section

## Materials

Microcrystalline cellulose (powder, derived from cotton linter) and [Bmim]Cl were used as received from Aldrich Chemical Co., Ltd. Acetone, 1-butanol, *N*,*N*-dimethylformamide (DMF), dimethyl sulfoxide (DMSO), ethanol, ammonium hydroxide (28% $NH_3$ in water), sodium hydrate (NaOH), silver nitrate ($AgNO_3$), 2-chloromethyloxirane, 4-nitrophenol (4-NP), and sodium borohydride ($NaBH_4$) were used as received from Nacalai Tesque Inc. (Kyoto, Japan). Hydrochloric acid (HCl; Wako Pure Chemical Industries, Ltd.), and tributylamine (TBA; Tokyo Chemical Industry Co., Ltd.) were also used as received. All the water used in the experiments was purified in an ErixUV (Millipore, Japan) purification system and had a resistivity of 18.2 MΩ cm.

## Preparation of Cellulose Particles by the SRM

Cellulose particles were prepared by the SRM as mentioned in ***Chapter 6***. The obtained cellulose particles were reserved in DMSO.

## Preparation of Amino-Functionalized Porous Cellulose Particles

Amino functionalization of cellulose particles was carried out following the literature:[42, 43] 2-Chloromethyloxirane (0.44 g) was added to ammonium hydroxide (0.87 g) and heated at 65°C for 2 h. The obtained solution was added to DMSO solution (20.4 g) containing dissolved TBA (0.24 g), and then cellulose particles (70 mg) were immersed in this solution for 1 h upon stirring in a round-bottom Schlenk flask sealed off with a silicon rubber septum. Reaction was performed by stirring the mixture at 50°C for 3 h, and the obtained aminated

cellulose particles were thoroughly washed with ethanol. The obtained cellulose particles were reserved in water.

**Preparation of Cellulose/Ag Composite Particles**

The aminated cellulose particles (35 mg) were immersed in an $AgNO_3$ aqueous solution (20 mL, 0.64 or 6.4 mM) for 1 h at room temperature upon stirring. Reduction of Ag cations was performed for 2 h at 80°C in a sealed grass tube placed in an oil bath with agitation at the rate of 100 cycles $min^{-1}$ (3 cm strokes). The obtained cellulose/Ag particles were thoroughly washed with water with water to remove the free Ag cations and free AgNPs.

**Estimation for Catalytic Performance of AgNPs in Composite Cellulose Particles**

The catalytic efficiencies of the composite cellulose particles were evaluated using the reduction of 4-nitrophenol (4-NP) to 4-aminophenol (4-AP) in the presence of $NaBH_4$ as a model reaction. The AgNPs were used as catalysts. In the experiments, $NaBH_4$ (90.8 mg) was first added to an aqueous 4-NP solution (40 mL, 0.06 mM); further, a part of the obtained mixture (4 g) was poured into a quartz cuvette, and the composite particles (2.1 mg) were dispersed in it. The reduction reaction occurred in the quartz cuvette and was monitored at fixed time intervals by UV–visible spectroscopy (UV-2500 UV–vis spectrophotometer, Shimadzu Corp., Kyoto, Japan).

**Characterization**

The cellulose particles were immersed in liquid nitrogen, freeze-dried in a freeze-dryer (FDU-1200, Tokyo Rikakikai Co., Ltd.; Tokyo, Japan), and observed using a scanning electron microscope (SEM, JSM-6510, JEOL, Tokyo, Japan) on an accelerating voltage 20 kV after

platinum coating. To analyze their inner morphology, ultrathin (100 nm-thick) cross sections of the particles were prepared using a cryomicrotome (Leica EM UC6 equipped with EM FC7). The sliced samples were then observed using a transmission electron microscope (TEM, JEM-1230, JEOL, Tokyo, Japan). The number-average diameter ($D_n$) and the coefficient of variation ($C_v$) was estimated from 200 AgNPs on the TEM images using image-analysis (WinRoof, Mitani Co., ltd., Japan). Nitrogen adsorption measurements were performed using a Quantachrome NOVA 3200e instrument (USA). The Brunauer–Emmett–Teller (BET) specific surface area of the cellulose particles was assessed from the adsorption branch of the isotherm for a relative pressure of 0.05–0.3 at 77 K. The products were qualitatively analyzed using a Fourier-transform infrared spectrometer (FT-IR, FT/IR-6200, JASCO, Tokyo, Japan) and the pressed KBr pellet technique. The electric conductivity titration method was applied to quantify the amine content in the cellulose particles. Briefly, dried cellulose particles (80 mg) were immersed in hydrochloric acid (15 mL, 0.01 M) and disintegrated into a well-dispersed slurry by ultrasonication. Further, an aqueous NaOH solution (0.01 M) was added to the mixture at a rate of 0.4 mL $min^{-1}$ while monitoring the electric conductivity of the system using a conductance meter (F-74, HORIBA Corp., Kyoto, Japan). The amount of AgNPs supported on the cellulose particles was measured using a thermogravimetric analyzer (TGA, EXSTAR TG/DTA6200, SII Nano Technology Inc., Japan) at a heating rate of 10 °C $min^{-1}$ from 30 to 900°C under a nitrogen atmosphere.

## Results and Discussion

### *Amine-functionalization of Porous Cellulose Particles*

Cellulose particles were functionalized with primary amine groups according to the method reported by Akhlaghi et al.[42] Figure 1 shows photos of the wet cellulose particles and SEM images of the cross sections of the freeze-dried cellulose particles before and after the amine-functionalization. The cellulose particles had a spherical shape and a porous structure (Figure 1a, a'), which were maintained even after the reaction. The specific surface area was 105 $m^2$ $g^{-1}$ measured by BET method.

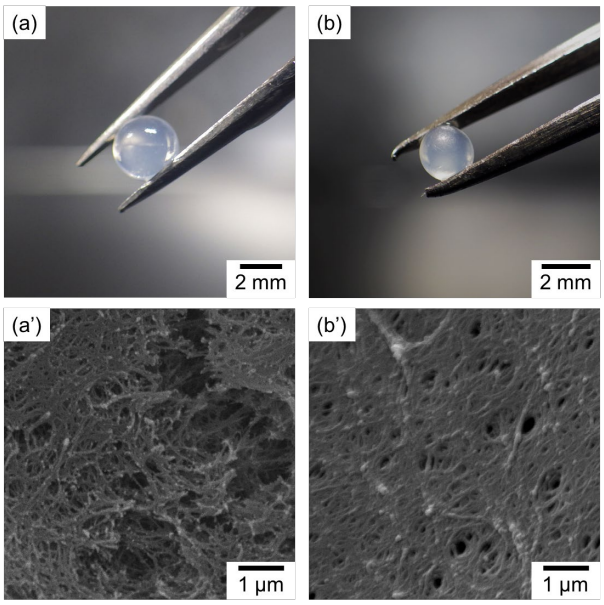


**Figure 1.** Photos of cellulose particles (a, b) and SEM images of the cross sections of freeze-dried cellulose particles (a', b') before (a, a') and after (b, b') functionalization with amine groups.

The FT-IR measurements were performed to confirm the presence of amine groups in the cellulose particles after the reaction. Figure 2 shows the FT-IR spectra of the samples before and after the reaction. The modified cellulose particles exhibited a new adsorption band at 1550-

1590 $cm^{-1}$ corresponded to N-H bending vibration of primary amine[42, 44], and was not present in the untreated particles (Figure2b). This result indicates that the modified cellulose particles contained primary amine groups, which were designed as aminated cellulose particles. Moreover, the amine content in the aminated cellulose particles was 0.37 mmol $g^{-1}$-cellulose measured by an electric conductivity titration.

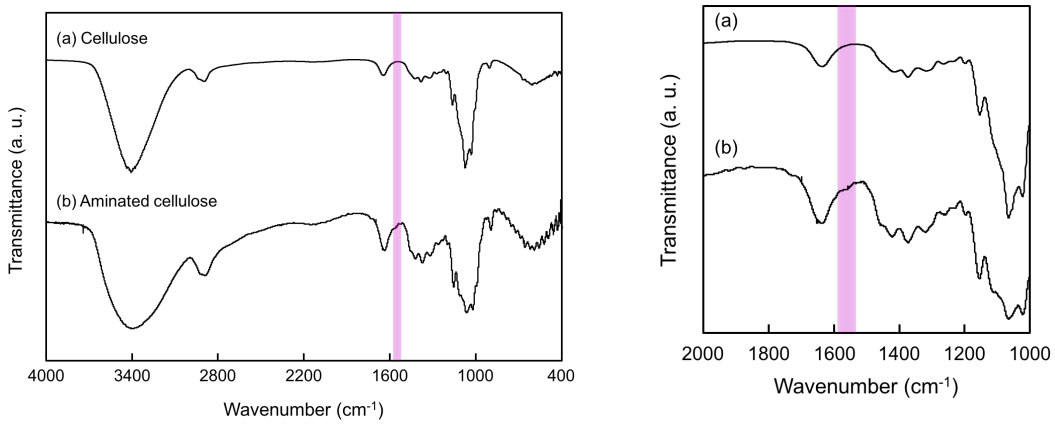


**Figure 2.** FT-IR spectra of cellulose particles before (a) and after (b) the amine functionalization.

***Preparation of Cellulose/Ag Composite Particles***

To prepare cellulose/Ag composite particles, aminated cellulose particles were immersed in an $AgNO_3$ aqueous solution for 1 h at room temperature upon stirring, where the Ag cations were coordinated to the amine groups on the cellulose particles. Reduction of the Ag cations was then conducted in the $AgNO_3$ aqueous solution for 2h at 80°C, in which the amine groups worked as a reducing agent; thus the molar ratio between amine groups and Ag cations should influence the resulting nanoparticles.[45, 46] In the case of $AgNO_3$/amine molar ratio of 0/10 (use of unmodified cellulose particles), the color of the cellulose particles changed

from whitish to light yellow and AgNPs were not observed in the solution and the wall of the vessel due to the intrinsic reducing character of cellulose[16, 47] (Figure 3a, d). The AgNPs content on the cellulose particles was measured by TGA analysis under a nitrogen atmosphere considering the possibility of the oxidation of AgNPs to $Ag_2O$ under an oxygen atmosphere.

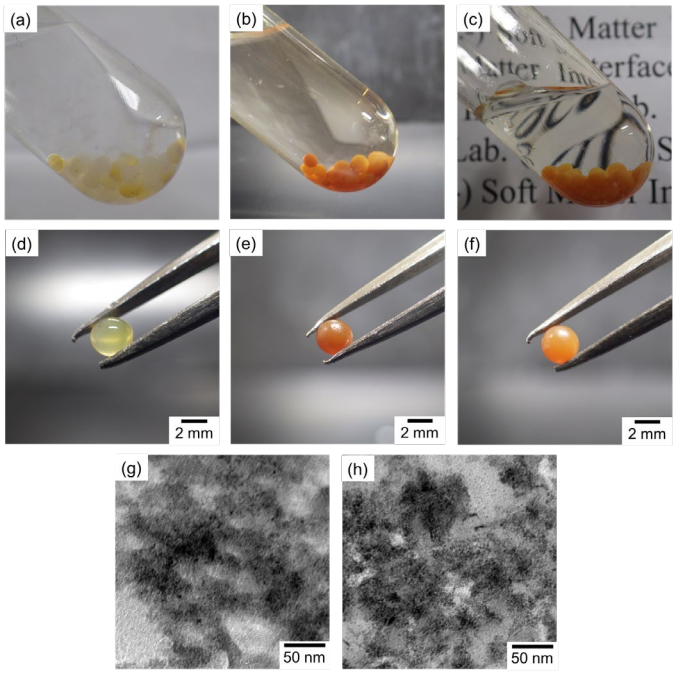


**Figure 3.** Photos of reaction vessels (a–c), composite cellulose/Ag particles (d–f), and TEM images of ultrathin cross sections (g, h) of the particles after the reduction of Ag cations in aqueous $AgNO_3$ solutions at different molar ratio between $AgNO_3$ and amine groups. $AgNO_3$/amine molar ratio: 10/0 (a, d); 10/1 (b, e, g); 1/1 (c, f, h).

Figure 4 shows TGA curves of the cellulose particles and cellulose/Ag composite particles. The amount of AgNPs was determined from the remaining weight considering the weight loss of cellulose at 900°C, and the result indicates that 34.9 mg of AgNPs were synthesized on 1 g of the cellulose particles. However, there was the variation in color change of the obtained particles, indicating that the reduction reaction of Ag cations differs depending on the cellulose

particles (Figure 3a). On the other hand, when aminated cellulose particles were used, the colors of all obtained particles change to yellow-brown, and the color became deeper increase in concentration of $AgNO_3$. The TEM images of the ultrathin cross sections at $AgNO_3$/amine molar ratios of 1/1 and 10/1 show that AgNPs with much higher contrast were supported on the porous structures of the obtained particles with lower contrast in each system although some aggregations of AgNPs were observed. The $D_n$ and $C_v$ of the AgNPs synthesized in each system were 6.4 nm (28.8%) and 9.1 nm (28.9%), respectively (Figure 3g, h). From the TGA results, the amounts of AgNPs synthesized at $AgNO_3$/amine molar ratios of 1/1 and 10/1 were 57.1 and 124.0 mg of 1 g of cellulose particles, respectively. These results indicate that the amine groups worked as a reducing agent for Ag cations and that the amount of AgNPs on cellulose particles could be controlled by changing the molar ratio of $AgNO_3$ and amine group.

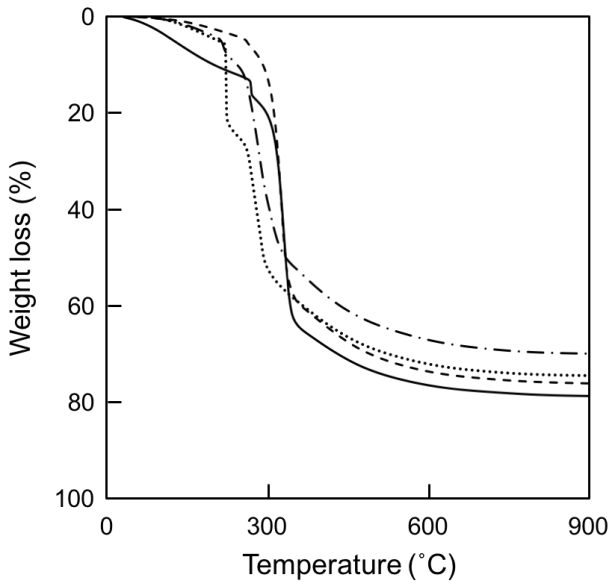


**Figure 4.** Thermal decomposition profiles (under $N_2$ atmosphere) of cellulose particles (solid line) and composite cellulose/Ag particles prepared with different $AgNO_3$/amine group (mol/mol): 10/0 (dashed line); 1/1 (dotted line); 10/1 (dash-dot line).

***Catalytic Properties of Cellulose/Ag Composite Particles***

The catalytic performance of the aminated cellulose/Ag particles was estimated by monitoring the reduction of 4-NP to 4-AP in the presence of $NaBH_4$ by UV–visible spectroscopy. In this reaction, 4-NP is firstly converted into 4-NP ion after adding $NaBH_4$, and then the 4-NP ion is reduced into 4-AP ion by $NaBH_4$ in the presence of a catalyst.[9] When the reduction reaction occurred, the intensity of the characteristic peak for the 4-NP ion (at 400 nm) decreased, whereas that of the peak for the 4-AP ion (at 300 nm) increased. If the concentration of $NaBH_4$ exceeds that of 4-NP largely, the reaction should be first order with regard to the 4-NP concentration; thus, the catalytic rate can be evaluated. In addition, the apparent kinetic rate constant $k_{app}$ is known to be proportional to the total surface area of AgNPs because the catalytic reduction proceeds on the surface of AgNPs.[9] We calculated the rate constant $k_1$ normalized to $S$, which is the surface area of all AgNPs normalized to the unit volume of the reaction system, defined by the following equation:

$$-\frac{dC_t}{dt} = k_{app}C_t = k_1 S C_t$$

where $C_t$ is concentration of 4-NP at time $t$. To calculate $S$, the bulk density of silver ($\rho = 10.5 \times 10^3$ kg m$^{-3}$) was used. The amount of AgNPs was estimated from TGA analysis and it was assumed not to change after the reduction of 4-NP. Moreover, the diameter of AgNPs was determined by the TEM results.

Figure 5 shows the relation between $\ln(C_t/C_0)$ and the reaction time for the composite cellulose/Ag particles prepared at different synthesis condition, $AgNO_3$/amine molar ratios of 1/1 and 10/1 during three runs, where $C_t$ is the concentration at determined given time and $C_0$ is the initial concentration at $t = 0$ of 4-NP. In both cases, a linear correlation was found between $\ln(C_t/C_0)$ and the reaction time, indicating that the catalytic reduction proceeded with first-order kinetics for 4-NP reduction. When the composite particles prepared in $AgNO_3$/amine molar ratios of 10/1 system were used as the catalyst in the reaction, $k_{app}$ and the reaction conversion

for 25 min were 2.41 × $10^{-3}$ $s^{-1}$ and almost 100%, respectively; however, when the reduction was conducted using the recycled particles recovered after the first reduction, the catalyst activity decreased remarkably (Figure 5) because the AgNPs were detached from the cellulose particles during the reaction and the washing step due to the presence of excess amount of AgNPs relative to amine group as a linkage between cellulose particles and AgNPs. On the other hand, in use of the particles prepared in in $AgNO_3$/amine molar ratios of 1/1 system, the catalytic activity of the composite particles was maintained during three cycles, and the conversion of 4-NP was almost same (approx. 100%) in each step. This indicates that the amine groups linked the cellulose particles with AgNPs effectively and they could prevent the AgNPs from detaching from the cellulose particles.

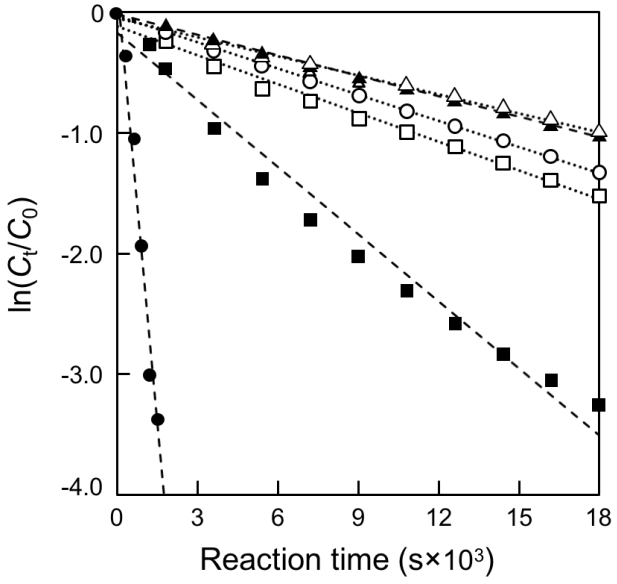


**Figure 5.** Relationships between $\ln(C_t/C_0)$ and time for the catalytic reduction of 4-nitrophenol using cellulose/Ag composite particles prepared with different $AgNO_3$/amine group (mol/mol): 10/1 (closed circles, squares, and triangles); 1/1 (open circles, squares, and triangles); first run (circles), second run (squares), and third run (triangles).

Moreover, we compared to the rate constant $k_1$ reported in the other system, summarized in Table 1 (the materials in other system can be used at least three times). From the table, the

catalytic activity of AgNPs in the cellulose particles in this work is comparable with the AgNPs-immobilized cellulose particles (in ***Chapter 5***) and those encapsulated in the bulk polymer hydrogel;[48] therefore, the aminated cellulose/Ag particles are the good recyclable catalyst.

Table 1. Catalytic activity of the silver nanoparticles for the reduction reaction of 4-nitrophenol.

| Samples | Carrier system | $D_n$ [nm][a)] | $k_1$ [$s^{-1}$ $m^{-2}$ L][b)] |
|---|---|---|---|
| Aminated Cellulose/Ag 1st run | Cellulose particles; this work | 6.4±1.6 | $2.85\times10^{-5}$ |
| Aminated Cellulose/Ag 3rd run | Cellulose particles; this work | 6.4±1.6 | $2.07\times10^{-5}$ |
| Cellulose-S-Ag 1st run | Cellulose particles; in ***Chapter 5*** | 8.6±2.8 | $2.75\times10^{-5}$ |
| Cellulose-S-Ag 3rd run | Cellulose particles in ***Chapter 5*** | 8.6±2.8 | $3.37\times10^{-5}$ |
| Ref 48 | PVA/PS-PEGMA hydrogel | 35±5 | $7.80\times10^{-5}$ |
| Ref 48 | PVA hydrogel | 45±5 | $7.31\times10^{-5}$ |

[a)] $D_n$, diameter of silver nanoparticles measured by TEM images
[b)] $k_1$, rate constant normalized to the total surface of the nanoparticles in the reduction system

## Conclusion

The composite cellulose/Ag particles have been successfully prepared by introducing amine groups into the porous structures of cellulose particles, which reduced Ag cations in the aqueous $AgNO_3$ solution and also worked as a linkage of cellulose and AgNPs. The amount of AgNPs could be controllable by changing the molar ratio of $AgNO_3$ and amine groups. The catalytic ability of the composite particles for the reduction of 4-NP to 4-AP increased with increase in the content of AgNPs; however, when the amount of AgNPs was much higher than that of amine groups, which were synthesized by the reduction at 10/1 ratio of $AgNO_3$ and amine groups, the catalytic efficiency decreased dramatically owing to the detachment of AgNPs from the cellulose particles. On the other hand, in use of the composite particles prepared by the reduction at the equal ratio to each other, the catalytic efficiency was maintained for at least three cycles without immobilizing treatment of AgNPs on the cellulose particles because of the amine groups as a linkage of cellulose particles and AgNPs. Moreover, the catalytic ability was comparable to the carboxylated cellulose particles with immobilization of AgNPs via Ag–sulfar bonds (in ***chapter 5***). The knowledge obtained in this study is readily available for the preparation of other metal nanoparticles on the cellulose particles and they can be to handled and recycled without complicated process and immobilization step of metal nanoparticles. Therefore, resulting materials have a great potential for catalyst applications. Moreover, for more improvement of catalytic efficiency, the amine content working as a reducing agent and a linkage would be needed to increase by adjusting a preparation condition in the future.

## References


1. I. Hussain, M. Brust, A. J. Papworth and A. I. Cooper, *Langmuir*, 2003, **19**, 4831-4835.
2. P. M. Tessier, O. D. Velev, A. T. Kalambur, J. F. Rabolt, A. M. Lenhoff and E. W. Kaler, *Journal of the American Chemical Society*, 2000, **122**, 9554-9555.
3. G. Schmid, *Chemical Reviews*, 1992, **92**, 1709-1727.
4. P. Dauthal and M. Mukhopadhyay, *Industrial & Engineering Chemistry Research*, 2016, **55**, 9557-9577.
5. Y. C. Cao, R. Jin and C. A. Mirkin, *Science*, 2002, **297**, 1536.
6. N. L. Rosi and C. A. Mirkin, *Chemical Reviews*, 2005, **105**, 1547-1562.
7. P. V. Kamat, *The Journal of Physical Chemistry B*, 2002, **106**, 7729-7744.
8. S. Link and M. A. El-Sayed, *The Journal of Physical Chemistry B*, 1999, **103**, 8410-8426.
9. N. Pradhan, A. Pal and T. Pal, *Colloids and Surfaces A: Physicochemical and Engineering Aspects*, 2002, **196**, 247-257.
10. K. Esumi, R. Isono and T. Yoshimura, *Langmuir*, 2004, **20**, 237-243.
11. V. K. Sharma, R. A. Yngard and Y. Lin, *Advances in Colloid and Interface Science*, 2009, **145**, 83-96.
12. S. Agnihotri, S. Mukherji and S. Mukherji, *RSC Advances*, 2014, **4**, 3974-3983.
13. M. V. Roldán, L. B. Scaffardi, O. de Sanctis and N. Pellegri, *Materials Chemistry and Physics*, 2008, **112**, 984-990.
14. C. Battocchio, C. Meneghini, I. Fratoddi, I. Venditti, M. V. Russo, G. Aquilanti, C. Maurizio, F. Bondino, R. Matassa, M. Rossi, S. Mobilio and G. Polzonetti, *The Journal of Physical Chemistry C*, 2012, **116**, 19571-19578.
15. K. Y. van Berkel and C. J. Hawker, *Journal of Polymer Science Part A: Polymer Chemistry*, 2010, **48**, 1594-1606.
16. J. Wu, N. Zhao, X. Zhang and J. Xu, *Cellulose*, 2012, **19**, 1239-1249.
17. Y. Lu, Y. Mei, M. Schrinner, M. Ballauff, M. W. Möller and J. Breu, *The Journal of Physical Chemistry C*, 2007, **111**, 7676-7681.
18. J. He, T. Kunitake and A. Nakao, *Chemistry of Materials*, 2003, **15**, 4401-4406.
19. D. Klemm, B. Heublein, H.-P. Fink and A. Bohn, *Angewandte Chemie International Edition*, 2005, **44**, 3358-3393.
20. J. Pérez, J. Muñoz-Dorado, T. de la Rubia and J. Martínez, *International Microbiology*, 2002, **5**, 53-63.
21. D. Pokhrel and T. Viraraghavan, *Science of The Total Environment*, 2004, **333**, 37-58.
22. M. Nogi, S. Iwamoto, A. N. Nakagaito and H. Yano, *Advanced Materials*, 2009, **21**, 1595-1598.
23. S. Wang, A. Lu and L. Zhang, *Progress in Polymer Science*, 2016, **53**, 169-206.
24. M. Gericke, J. Trygg and P. Fardim, *Chemical Reviews*, 2013, **113**, 4812-4836.
25. X. Luo and L. Zhang, *Journal of Hazardous Materials*, 2009, **171**, 340-347.
26. N. Li and R. Bai, *Separation and Purification Technology*, 2005, **42**, 237-247.

27. K.-F. Du, M. Yan, Q.-Y. Wang and H. Song, *Journal of Chromatography A*, 2010, **1217**, 1298-1304.
28. R. J. Moon, A. Martini, J. Nairn, J. Simonsen and J. Youngblood, *Chemical Society Reviews*, 2011, **40**, 3941-3994.
29. D. J. Gardner, G. S. Oporto, R. Mills and M. A. S. A. Samir, *Journal of Adhesion Science and Technology*, 2008, **22**, 545-567.
30. Y. Habibi, L. A. Lucia and O. J. Rojas, *Chemical Reviews*, 2010, **110**, 3479-3500.
31. R. P. Swatloski, S. K. Spear, J. D. Holbrey and R. D. Rogers, *Journal of the American Chemical Society*, 2002, **124**, 4974-4975.
32. R. D. Rogers and K. R. Seddon, *Science*, 2003, **302**, 792.
33. H. Wang, G. Gurau and R. D. Rogers, *Chemical Society Reviews*, 2012, **41**, 1519-1537.
34. M. Isik, H. Sardon and D. Mecerreyes, *International Journal of Molecular Sciences*, 2014, **15**.
35. A. Pinkert, K. N. Marsh, S. Pang and M. P. Staiger, *Chemical Reviews*, 2009, **109**, 6712-6728.
36. T. Suzuki, K. Kono, K. Shimomura and H. Minami, *Journal of Colloid and Interface Science*, 2014, **418**, 126-131.
37. M. Okubo, Y. Konishi, M. Takebe and H. Minami, *Colloid and Polymer Science*, 2000, **278**, 919-926.
38. M. Okubo, Y. Konishi, S. Sebki and H. Minami, *Colloid and Polymer Science*, 2002, **280**, 765-769.
39. T. Omura, K. Imagawa, K. Kono, T. Suzuki and H. Minami, *ACS Applied Materials & Interfaces*, 2017, **9**, 944-949.
40. T. Omura, K. Imagawa, T. Suzuki and H. Minami, *Langmuir*, 2018, **34**, 15490-15494.
41. K. Imagawa, T. Omura, Y. Ihara, K. Kono, T. Suzuki and H. Minami, *Cellulose*, 2017, **24**, 3111-3118.
42. S. P. Akhlaghi, M. Zaman, N. Mohammed, C. Brinatti, R. Batmaz, R. Berry, W. Loh and K. C. Tam, *Carbohydrate Research*, 2015, **409**, 48-55.
43. S. Dong and M. Roman, *Journal of the American Chemical Society*, 2007, **129**, 13810-13811.
44. J. Coates, *Encyclopedia of Analytical Chemistry*, 2006, DOI: doi:10.1002/9780470027318.a5606
45. A. Frattini, N. Pellegri, D. Nicastro and O. d. Sanctis, *Materials Chemistry and Physics*, 2005, **94**, 148-152.
46. J. Song, Y. Chu, Y. Liu, L. Li and W. Sun, *Chemical Communications*, 2008, DOI: 10.1039/B715884J, 1223-1225.
47. J. Cai, S. Kimura, M. Wada and S. Kuga, *Biomacromolecules*, 2009, **10**, 87-94.
48. Y. Lu, P. Spyra, Y. Mei, M. Ballauff and A. Pich, *Macromolecular Chemistry and Physics*, 2007, **208**, 254-261.

# *Chapter 7*

## Preparation of Cellulose/Silica Composite Particles by in Situ Sol-Gel Reaction

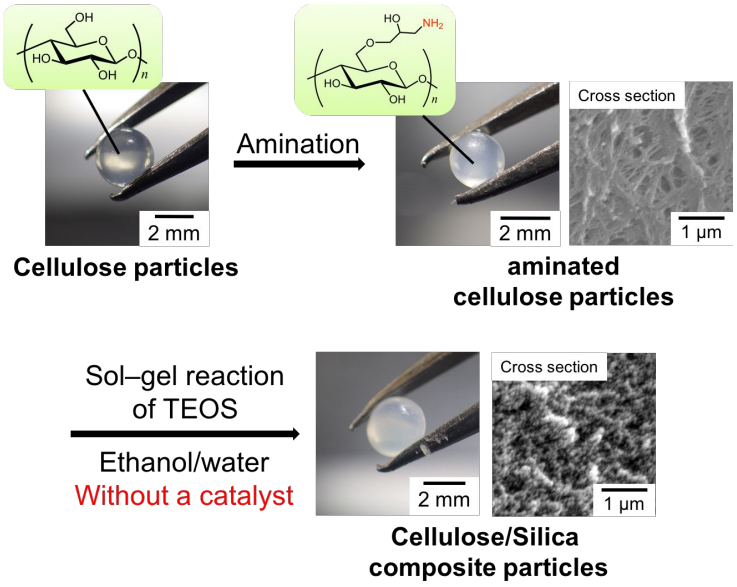


**Abstract:** Aminated cellulose particles, prepared via the SRM using [BmimCl] followed by introduction with primary amine groups, were used for the template to prepare cellulose/silica composite particles, in which sol–gel reaction of tetraethoxysilane induced by the amime groups as a catalyst in situ (only in the cellulose particles) to form silica nanoparticles. The microscopic morphologies (specific surface area, pore diameter, and pore volume) of the obtained composites were characterized by scanning electron microscope (SEM), nitrogen adsorption experiments, showing that the morphologies were affected by the silica nanoparticle content in the composites which could be controlled by the sol-gel reaction time. Moreover, thermal stabilities of the composite particles estimated by thermal gravimetric analysis were enhanced by the presence of silica nanoparticles.

## Introduction

Organic–inorganic materials have attracted a lot of attention as new attractive materials with interesting mechanical, optical, electrical, thermal properties. Therefore, they have been widely studied and developed not only in academic but also industrial world;[1-3] however, in recent year, since the concerns to the environment issues have been raised, it is necessary for development of more environmentally sustainable alternatives to synthetic materials.

Cellulose is the most abundant natural polymer on Earth, estimated to be produced globally $1.5\times10^{12}$ tons per year.[4] Since it has unique characteristics such as It is extensively used for thermal and chemical stability, nontoxicity, biocompatibility, and biodegradability,[4, 5] it has been widely used as pulp,[6] paper,[7] fiber, and membrane.[8] For utilizing their unique characteristics and enlarging the potential application of cellulose-based materials, cellulose/inorganic hybrids have been attractive attention. The presence of an inorganic phase can give new functionalities to the composite materials such as electric,[9, 10] magnetic,[11, 12] catalytic,[13, 14] and antibacterial[15] properties. One of the most studied cellulose–inorganic composites is cellulose/silica composite because the presence of silica can contribute the enhancement of thermal stability, hydrophobicity, and mechanical property without losing cellulose biocompatibility.[16-18] The sol-gel process with tetraethoxysilane (TEOS) as a precursor is in common use to prepare cellulose/silica composites, in which TEOS is catalyzed in acid or base conditions, resulting in formation of silica deposited on the surface of cellulose fiber/membrane as thin films or as nanoparticles.[19-21] These materials exhibit very attractive functionalities, including high mechanical properties,[22-26] thermal stability,[23, 24] excellent thermal insulation performance,[23, 25] oil-water separation property,[27] high hydrophobicity,[25, 28, 29] and molecular imprinting properties.[30] Cellulose/silica composite in a spherical state were

also reported and applied for chromatographic application;[31] however, the procedure of preparing the composite particles needed derivatization of the cellulose for following sol-gel reaction with a silica precursor. Moreover, the dissolution of cellulose was necessary for multi-step processes as cellulose is insoluble in most common solvents owing to its strong hydrogen bonding network and hydrophobic interactions.[32]

In 2002, Rogers et al.[33] found that some ionic liquids (ILs), such as 1-butyl-3-methylimidazolium chloride and bromide ([Bmim]Cl and [Bmim]Br), could dissolve cellulose under a mild condition. Thereafter, ILs have been attracting interest as new solvents for cellulose and utilized for synthesis of functional cellulose materials.[34-37] Using this knowledge, Minami et al.[38] reported the successful preparation of porous cellulose particles using a [Bmim]Cl as a solvent and by the solvent releasing method (SRM).[39, 40] The cellulose particles had a high specific surface area and the porous structure was filled with a surrounding medium.[41-43] In ***Chapter 6***, the composite cellulose/Ag particles with a recyclable catalytic ability were successfully prepared, without a linking agent of Ag nanoparticles with the cellulose particles, by introduction of primary amine groups, which worked both as a reducing agent for Ag cations and as a linkage between the cellulose and Ag nanoparticles.

In ***Chapter 7***, cellulose/silica composite particles were prepared via in situ sol–gel process using tetraethoxysilane (TEOS) as a precursor catalyzed by aminated cellulose particles. The obtained cellulose/silica composite particles were characterized in view point of microstructure and thermal stability.

# Experimental Section

## Materials

Microcrystalline cellulose (powder, derived from cotton linter) and [Bmim]Cl were used as received from Aldrich Chemical Co., Ltd. Acetone, 1-butanol, *N*,*N*-dimethylformamide (DMF), dimethyl sulfoxide (DMSO), ethanol, ammonium hydroxide (28% $NH_3$ in water), sodium hydrate (NaOH), and 2-chloromethyloxirane were used as received from Nacalai Tesque Inc. (Kyoto, Japan). Hydrochloric acid (HCl; Wako Pure Chemical Industries, Ltd.), and tributylamine (TBA; Tokyo Chemical Industry Co., Ltd.) were also used as received. All the water used in the experiments was purified in an ErixUV (Millipore, Japan) purification system and had a resistivity of 18.2 MΩ cm.

## Preparation of Cellulose Particles by the SRM

Cellulose particles were prepared by the SRM as mentioned in ***Chapter 6***. The obtained cellulose particles were reserved in DMSO.

## Preparation of Amino-Functionalized Porous Cellulose Particles

Amino functionalization of cellulose particles was carried out following the literature:[42, 43] 2-Chloromethyloxirane (0.44 g) was added to ammonium hydroxide (0.87 g) and heated at 65°C for 2 h. The obtained solution was added to DMSO solution (20.4 g) containing dissolved TBA (0.24 g), and then cellulose particles (70 mg) were immersed in this solution for 1 h upon stirring in a round-bottom Schlenk flask sealed off with a silicon rubber septum. Reaction was performed by stirring the mixture at 50°C for 3 h, and the obtained aminated cellulose particles were thoroughly washed with ethanol. The obtained cellulose particles were reserved in water.

**Preparation of Cellulose/Silica Composite Particles**

The untreated or aminated cellulose particles (35 mg) were subjected to medium exchange with a mixture of ethanol/water (5/1, w/w). Then, the particles were immersed in a mixture of TEOS (5 g), ethanol (8 g), and water (1.6 g), and sol–gel reaction was conducted in a vial bottle at room temperature upon stirring. In use of a catalyst, ammonium hydroxide was added to the above-mentioned mixture before immersing untreated cellulose particles in the reaction solution. After the sol–gel reaction for various reaction times, the resulting cellulose/silica particles were thoroughly washed with ethanol to remove the residual TEOS, and then were freeze-dried using a freeze-dryer (FDU-1200, Tokyo Rikakikai Co., Ltd.; Tokyo, Japan).

**Characterization**

The dried cellulose particles were observed using a scanning electron microscope (SEM, JSM-6510, JEOL, Tokyo, Japan) on an accelerating voltage 20 kV after platinum coating. Nitrogen adsorption measurements were performed using a Quantachrome NOVA 3200e instrument (USA). The Brunauer–Emmett–Teller (BET) specific surface area of the cellulose particles was assessed from the adsorption branch of the isotherm for a relative pressure of 0.05–0.3 at 77 K. The Barrett–Joyner–Halenda (BJH) pore distribution was determined from the desorption branch of the isotherm with the instrument software. The samples were degassed at room temperature for 3 h prior to the analysis. The products were qualitatively analyzed using a Fourier-transform infrared spectrometer (FT-IR, FT/IR-6200, JASCO, Tokyo, Japan) and the pressed KBr pellet technique. The electric conductivity titration method was applied to quantify the amine content in the cellulose particles. Briefly, dried cellulose particles (80 mg) were immersed in hydrochloric acid (15 mL, 0.01 M) and

disintegrated into a well-dispersed slurry by ultrasonication. Further, an aqueous NaOH solution (0.01 M) was added to the mixture at a rate of 0.4 mL/min while monitoring the electric conductivity of the system using a conductance meter (F-74, HORIBA Corp., Kyoto, Japan). The amount of silica in the composite particles was measured using a thermogravimetric analyzer (TGA, EXSTAR TG/DTA6200, SII Nano Technology Inc., Japan) at a heating rate of 10 °C $min^{-1}$ from 30 to 900°C under a nitrogen atmosphere.

## Results and Discussion

### *Preparation of Cellulose/Silica Composite Particles*

Cellulose particles were functionalized with primary amine groups according to the method as mentioned ***Chapter 6*** before sol-gel reaction. Figure 1 shows that amine-functionalized cellulose particles maintained their spherical shapes and porous structures. The specific surface area of the aminated cellulose particles was 105 $m^2$ $g^{-1}$ measured by BET method. In addition, the amine group amount in the cellulose particles was 0.37 mmol $g^{-1}$-cellulose measured by electric conductivity titration.

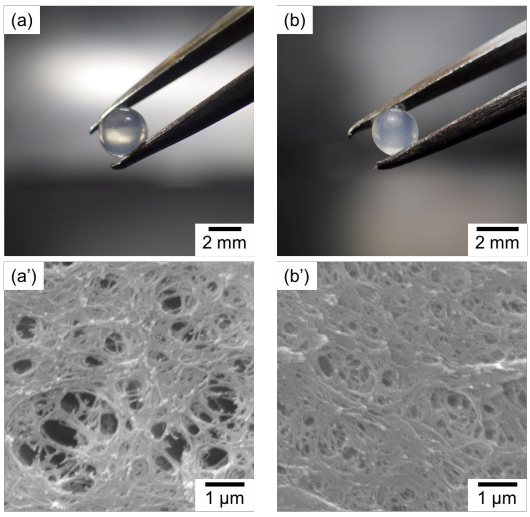


**Figure 1.** Photos of cellulose particles (a, b) and SEM images of the cross sections of freeze-dried cellulose particles (a', b') before (a, a') and after (b, b') amine-functionalization.

The aminated cellulose particles were dipped in TEOS solution comprising ethanol and water upon stirring to prepare cellulose/silica composite particles via the sol–gel reaction of TEOS. The FT-IR measurements were performed to investigate the chemical structure information about the particle before and after the reaction for 8 h, as shown in Figure 2. The cellulose particles after the reaction exhibited a new adsorption band at 800 $cm^{-1}$ and 450 $cm^{-1}$

corresponding to Si-O-Si bending and symmetric stretching vibration, respectively.[44, 45] Figure 3 shows the photos of the reaction vessels and the obtained particles after the sol–gel reaction using the untreated cellulose particles with and without an ammonia solution for 48 h (which is labeled as CP/silica), and using the aminated cellulose particles for 8, 24, and 48 h (which are labeled as ACP/silica-8, 24, and 48, respectively). The obtained particles in each system maintained their spherical shapes and sizes (Figure 3f–j). However, in use of ammonia solution, the reaction medium became turbid, indicating that silica generated not only in untreated cellulose particles but also in the reaction medium (Figure 3e). By contrast, silica neither appeared in solution nor deposited on the wall of vessels in the case of no ammonia solution (Figure 3a–d). The silica content in composite particles was 63.2 wt% for the ACP/silica-8, 67.3 wt% for ACP/silica-24, and 71.3 wt% for ACP/silica-48; while 4.9 wt% for CP/silica, determined by TGA considering the weight loss of cellulose at 900°C (Figure 6a). These results indicate that the sol–gel reaction of TEOS was effectively induced by amine group in aminated cellulose particles and that the silica content increased with increase in the reaction time.

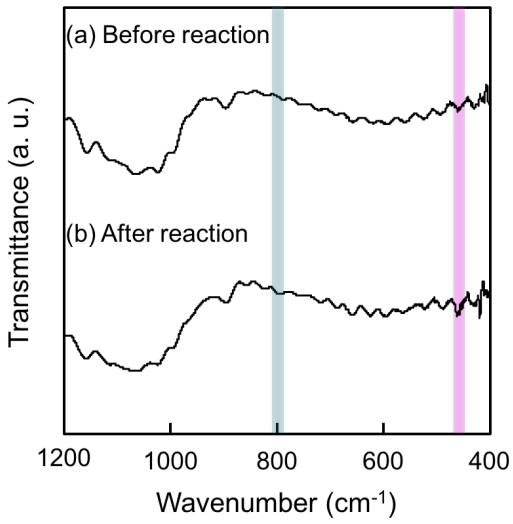


**Figure 2.** FT-IR spectra of cellulose particles before (a) and after (b) the sol–gel reaction of TEOS for 8 h.

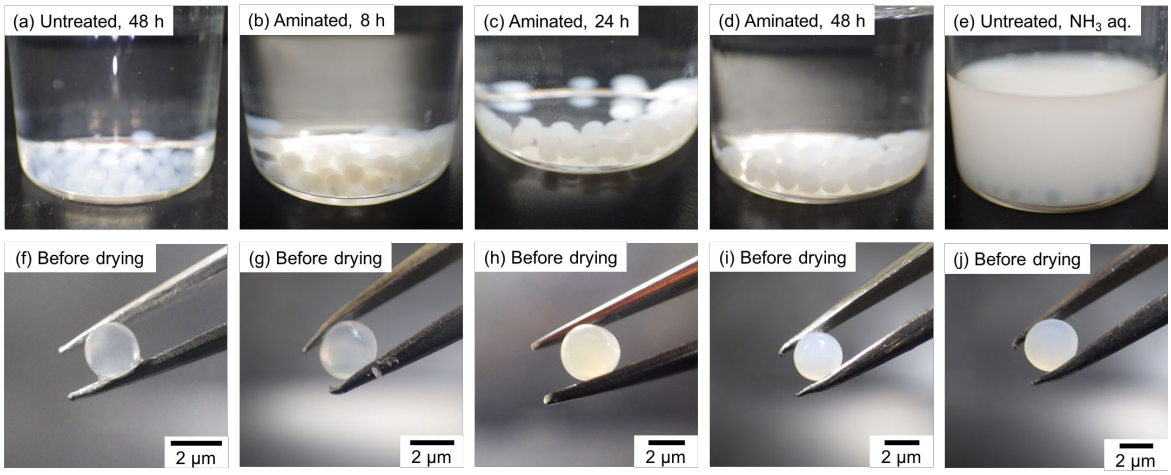


**Figure 3.** Photos of reaction vessels (a, b, c, d, e) and obtained particles (f, g, h, i, j), after the sol–gel reactions of TEOS for 8 h (b, g), 24 h (c, h), and 48 h (a, d, e, f, i, j) using aminated cellulose particles (b, c, d, g, h, i), or untreated cellulose particles with (a, f) and without ammonia solution (e, j)

Inner morphologies of the cellulose/silica composite particles were investigated by SEM. Figure 4 shows the SEM images of cross section of the ACP/silica-8, 24, 48, and CP/silica after freeze-drying. In the case of CP/silica, silica was not observed in the cellulose particles though silica concentration was 4.9 wt% in the composites (Figure 4a). On the other hand, using the aminated cellulose particles, silica nanoparticles deposited on the porous cellulose networks and were distributed uniformly (Figure 4b, c, d). The number of silica nanoparticles increased with increasing silica content, while the size of silica nanoparticles was larger in ACP/silica-48. Moreover, it is clear that the silica nanoparticles in ACP/silica-24 and 48 deposited on cellulose and filled the voids in the porous networks of cellulose homogeneously, compared with the silica nanoparticles depositing on the porous network of cellulose. To investigate the microscopic structures of the cellulose/silica composite particles, nitrogen adsorption/desorption experiments were carried out. Figure 5 shows nitrogen adsorption/desorption isotherms and BJH pore size distributions for the composites, which were

summarized in Table 1. The isotherm of ACP/silica-8 shows the significant different from other isotherms. The graph was categorized to type I according to IUPAC classification with a hysteresis loop, suggesting the presence of micropore structure beside mesopores. The pore size was approximately 1.5 nm from the BJH pore size distribution corresponding to the isotherm, although the BJH method is inadequate for micropore structures. On the other hand, isotherms of CP/silica, ACP/silica-24, and 48 show similar results categorized to type IV with a hysteresis loop (presence of mesoporous structures), which were in according to the BJH analysis results. Moreover, the peak of BJH pore distribution shifted to larger size range, and pore volume and BET surface area decreased with increase in silica content, except for CP/silica having a similar porous structure (Table 1). These results are attributed to high contents of silica nanoparticles filling the porous network of cellulose particles and to their aggregations. On the other hand, the pore sizes were approximately 2–6 nm and the pore size distributions were in the range between 2 to several nm. These results indicate that the microscopic morphology of cellulose/silica composite particle could be controlled by the sol–gel reaction time.

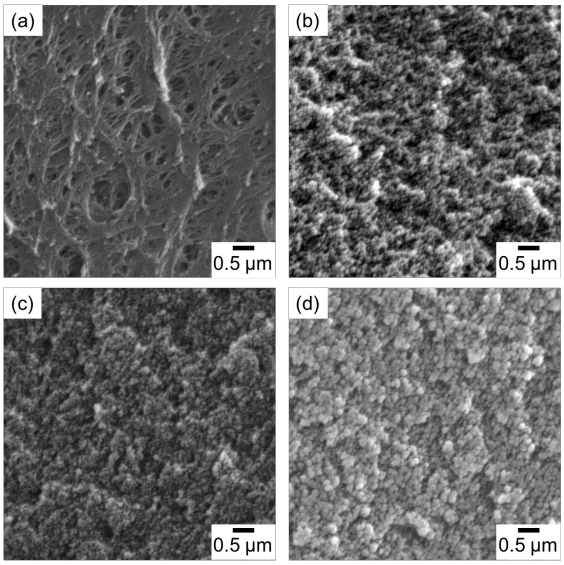


**Figure 4.** SEM images of cross sections of untreated cellulose/silica (a), aminated cellulose/silica-8 (b), 24 (c), and 48 (d) composite particles. All particles were freeze-dried before the observations.

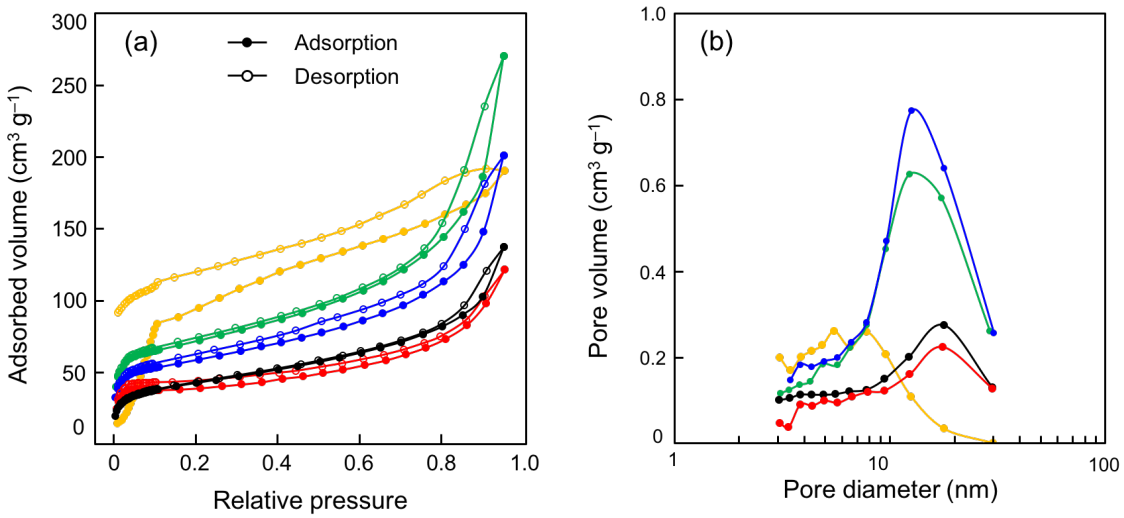


**Figure 5.** Nitrogen adsorption (close circles) and desorption (open circles) isotherms (a) and BJH pore size distribution (b) of cellulose particles (black), untreated cellulose/silica (red), aminated cellulose/silica-8 (orange), 24 (green), and 48 (blue) composite particles.

**Table 1.** Microscopic characteristics of cellulose particles and cellulose/silica composite particles.

| Samples | Pore volume [cm$^3$ g$^{-1}$] | $S_{BET}$ [m$^2$ g$^{-1}$] | Pore diameter [nm] | $SiO_2$ in composite [wt%] |
|---|---|---|---|---|
| CP | 0.18 | 112 | 1.5 | 0 |
| CP/silica | 0.15 | 122 | 1.9 | 4.9 |
| ACP/silica-8 | 0.14 | 400 | 1.5 | 63.2 |
| ACP/silica-24 | 0.46 | 216 | 4.9 | 67.3 |
| ACP/silica-48 | 0.41 | 189 | 6.3 | 71.8 |

***Thermal Properties of Cellulose/Silica Composite Particles***

Thermal stabilities of materials are important for practical use, therefore, we examined the thermal decomposition of obtained cellulose/silica composite particles by TGA in a nitrogen atmosphere. Figure 6 shows the TGA and DTG curves of the cellulose particles and cellulose/silica composite particles. The TGA curves exhibit that the cellulose particles without silica and the celluloses in the composites decomposed at 300°C–350°C, respectively (Figure 6a), which was unrelated to the composition of silica in the composite particles. However, compared with cellulose particles without silica, the DTA peak of shifted from 328°C to about 353°C, suggesting that the silica in composite has a thermal stabilizing effect on cellulose.

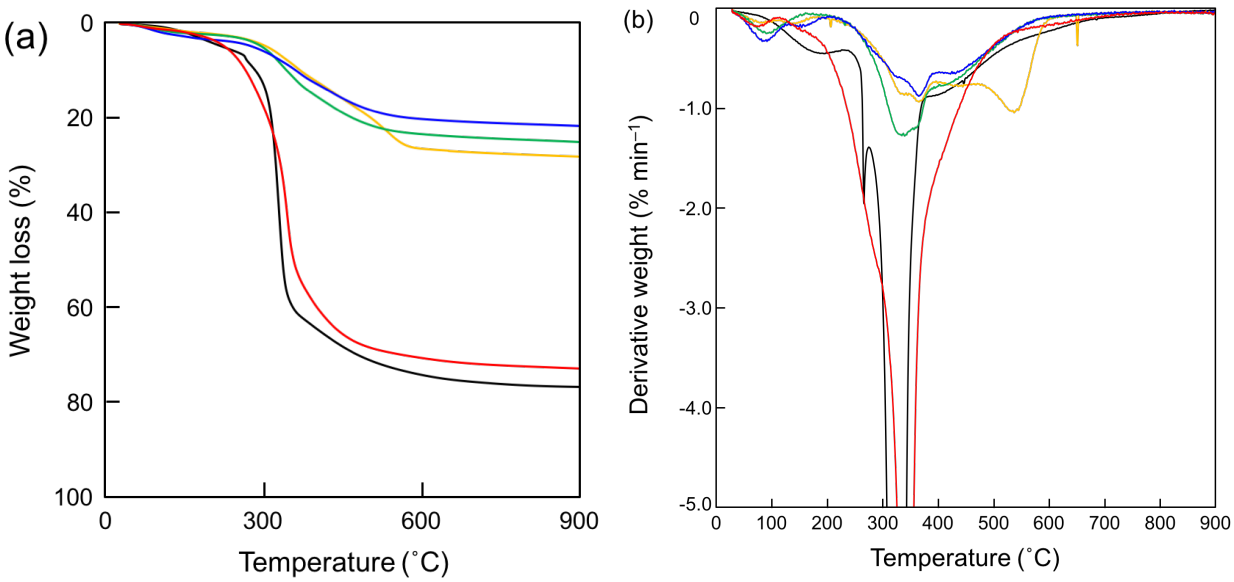


**Figure 6.** (a) Thermogravimetry analysis (TGA, 10 °C $min^{-1}$ heating, $N_2$ atmosphere) and (b) Derivative thermogravimetry (DTG) curves of cellulose particles (black), untreated cellulose/silica-48 (red), aminated cellulose/silica-8 (orange), 24 (green), and 48 (blue) composite particles.

## Conclusion

The aminated cellulose particles, prepared via the SRM using the ionic liquid followed by introduced with the primary amine groups, could serve the template to prepare the cellulose/silica composite particles by in situ sol–gel reaction of TEOS and by freeze-drying. The amine groups could work as a catalyst for the sol–gel reaction of TEOS and the obtained composites had the high specific surface area and the higher thermal stability than untreated cellulose particles, which were tunable by the sol–gel reaction time. This is first report to prepare these cellulose/silica composite particles and it is expected to form the foundation for the development of various cellulose composite particles.

## References


1. C. Sanchez, B. Julián, P. Belleville and M. Popall, *Journal of Materials Chemistry*, 2005, **15**, 3559-3592.
2. F. Hoffmann, M. Cornelius, J. Morell and M. Fröba, *Angewandte Chemie International Edition*, 2006, **45**, 3216-3251.
3. A. Dolbecq, E. Dumas, C. R. Mayer and P. Mialane, *Chem. Rev. (Washington, DC, U. S.)*, 2010, **110**, 6009-6048.
4. D. Klemm, B. Heublein, H.-P. Fink and A. Bohn, *Angewandte Chemie International Edition*, 2005, **44**, 3358-3393.
5. J. Pérez, J. Muñoz-Dorado, T. de la Rubia and J. Martínez, *International Microbiology*, 2002, **5**, 53-63.
6. D. Pokhrel and T. Viraraghavan, *Science of The Total Environment*, 2004, **333**, 37-58.
7. M. Nogi, S. Iwamoto, A. N. Nakagaito and H. Yano, *Advanced Materials*, 2009, **21**, 1595-1598.
8. S. Wang, A. Lu and L. Zhang, *Progress in Polymer Science*, 2016, **53**, 169-206.
9. H. Oh, S. S. Kwak, B. Kim, E. Han, G.-H. Lim, S.-W. Kim and B. Lim, *Advanced Functional Materials*, 2019, **29**, 1904066.
10. H. Koga, M. Nogi, N. Komoda, T. T. Nge, T. Sugahara and K. Suganuma, *NPG Asia Materials*, 2014, **6**, e93-e93.
11. N. Sun, R. P. Swatloski, M. L. Maxim, M. Rahman, A. G. Harland, A. Haque, S. K. Spear, D. T. Daly and R. D. Rogers, *Journal of Materials Chemistry*, 2008, **18**, 283-290.
12. R. Sescousse, R. Gavillon and T. Budtova, *Journal of Materials Science*, 2011, **46**, 759-765.
13. J. Wu, N. Zhao, X. Zhang and J. Xu, *Cellulose*, 2012, **19**, 1239-1249.
14. M. Kaushik and A. Moores, *Green Chemistry*, 2016, **18**, 622-637.
15. R. Xiong, C. Lu, W. Zhang, Z. Zhou and X. Zhang, *Carbohydrate Polymers*, 2013, **95**, 214-219.
16. I. I. Slowing, J. L. Vivero-Escoto, C.-W. Wu and V. S. Y. Lin, *Adv. Drug Delivery Rev.*, 2008, **60**, 1278-1288.
17. A. Stein, B. J. Melde and R. C. Schroden, *Advanced Materials*, 2000, **12**, 1403-1419.
18. S. Hribernik, M. S. Smole, K. S. Kleinschek, M. Bele, J. Jamnik and M. Gaberscek, *Polymer Degradation and Stability*, 2007, **92**, 1957-1965.
19. A. Demilecamps, C. Beauger, C. Hildenbrand, A. Rigacci and T. Budtova, *Carbohydrate Polymers*, 2015, **122**, 293-300.
20. A. Demilecamps, G. Reichenauer, A. Rigacci and T. Budtova, *Cellulose*, 2014, **21**, 2625-2636.
21. M. Litschauer, M.-A. Neouze, E. Haimer, U. Henniges, A. Potthast, T. Rosenau and F. Liebner, *Cellulose*, 2011, **18**, 143-149.
22. S. Liu, T. Yu, N. Hu, R. Liu and X. Liu, *Colloids and Surfaces A: Physicochemical and Engineering Aspects*, 2013, **439**, 159-166.
23. B. Yuan, J. Zhang, Q. Mi, J. Yu, R. Song and J. Zhang, *ACS Sustainable Chemistry & Engineering*, 2017, **5**, 11117-11123.

24. J. Cai, S. Liu, J. Feng, S. Kimura, M. Wada, S. Kuga and L. Zhang, *Angewandte Chemie International Edition*, 2012, **51**, 2076-2079.
25. G. Hayase, K. Kanamori, K. Abe, H. Yano, A. Maeno, H. Kaji and K. Nakanishi, *ACS Applied Materials & Interfaces*, 2014, **6**, 9466-9471.
26. J. Laskowski, B. Milow and L. Ratke, *The Journal of Supercritical Fluids*, 2015, **106**, 93-99.
27. G. Li, C. Zou, Y. Sun, W. Fan, X. Ma, J. Tao, P. Li and Y. Xu, *ACS Sustainable Chemistry & Engineering*, 2019, **7**, 14591-14600.
28. X. Chen, Y. Liu, H. Lu, H. Yang, X. Zhou and J. H. Xin, *Cellulose*, 2010, **17**, 1103-1113.
29. G. Gonçalves, P. A. A. P. Marques, T. Trindade, C. P. Neto and A. Gandini, *Journal of Colloid and Interface Science*, 2008, **324**, 42-46.
30. R. S. Gill, M. Marquez and G. Larsen, *Microporous and Mesoporous Materials*, 2005, **85**, 129-135.
31. X. Weng, Z. Bao, Z. Zhang, B. Su, H. Xing, Q. Yang, Y. Yang and Q. Ren, *Journal of Materials Chemistry B*, 2015, **3**, 620-628.
32. Y. Habibi, L. A. Lucia and O. J. Rojas, *Chemical Reviews*, 2010, **110**, 3479-3500.
33. R. P. Swatloski, S. K. Spear, J. D. Holbrey and R. D. Rogers, *Journal of the American Chemical Society*, 2002, **124**, 4974-4975.
34. R. D. Rogers and K. R. Seddon, *Science*, 2003, **302**, 792.
35. A. Pinkert, K. N. Marsh, S. Pang and M. P. Staiger, *Chemical Reviews*, 2009, **109**, 6712-6728.
36. H. Wang, G. Gurau and R. D. Rogers, *Chemical Society Reviews*, 2012, **41**, 1519-1537.
37. M. Isik, H. Sardon and D. Mecerreyes, *International Journal of Molecular Sciences*, 2014, **15**.
38. T. Suzuki, K. Kono, K. Shimomura and H. Minami, *Journal of Colloid and Interface Science*, 2014, **418**, 126-131.
39. M. Okubo, Y. Konishi, M. Takebe and H. Minami, *Colloid and Polymer Science*, 2000, **278**, 919-926.
40. M. Okubo, Y. Konishi, S. Sebki and H. Minami, *Colloid and Polymer Science*, 2002, **280**, 765-769.
41. K. Imagawa, T. Omura, Y. Ihara, K. Kono, T. Suzuki and H. Minami, *Cellulose*, 2017, **24**, 3111-3118.
42. T. Omura, K. Imagawa, K. Kono, T. Suzuki and H. Minami, *ACS Applied Materials & Interfaces*, 2017, **9**, 944-949.
43. T. Omura, K. Imagawa, T. Suzuki and H. Minami, *Langmuir*, 2018, **34**, 15490-15494.
44. N. Primeau, C. Vautey and M. Langlet, *Thin Solid Films*, 1997, **310**, 47-56.
45. S. A. Labib, A. M. Yousif, I. A. Ibrahim and A. A. Atia, *Journal of Porous Materials*, 2018, **25**, 383-396.

# Concluding remarks

Preparation of cellulose particles has been examined using solvent-releasing method (SRM) and ionic liquids. It is important for the morphology control of cellulose particles to establish the preparation conditions (affinity of ionic liquid with precipitant, phase separation rate) and the post-treatment methods (stirring rate/time, drying condition). In addition, it has been demonstrated that these cellulose particles could be applied to microcapsule materials, scaffolds for silver nanoparticles, and template for cellulose/silica composite particles.

In ***Chapter 1***, morphology of porous cellulose particles in a dry state prepared by the SRM could be controlled by changing a dispersion medium filling the inside of the particles at drying. When the dispersion medium having the lower surface tension was used, the particle's specific surface area increased, resulting in the formation of softer particles. This porosity control method is useful due to being without multi-step processes (freeze or $scCO_2$ drying) and can make us to control porous materials precisely at a dry state.

In ***Chapter 2***, disk-like cellulose particles were successfully prepared by stirring a dispersion of porous cellulose particles with a magnetic stir bar, in which the porous particles prepared by the SRM deformed by the grinding between the stir bar and the vail. Moreover, the number of disk-like particles and the degree of deformation increased as the stirring time, the stirring speed, and the contact area between the stir bar and the vials increased. This method to prepare disk-like cellulose particles is superior to conventional methods using pulverization aids.

In ***Chapter 3***, Cellulose particles with different morphologies were prepared by the solvent-releasing method (SRM) without a co-solvent; a dispersion consisting of 1-ethyl-3-methylimidazolium acetate ([Emim]Ac) droplets containing cellulose in hexane medium was added to large amounts of various solvents that acted as cellulose precipitants. Porous structures were obtained using precipitants with high affinity for [Emim]Ac, namely ethanol and t-butanol. On the contrary, the use of acetone and n-octanol, which have low affinity for [Emim]Ac, resulted in hollow structures. Moreover, the release rate of [Emim]Ac from the cellulose–[Emim]Ac solution into the solvent decreased with the precipitant's affinity for [Emim]Ac, contributing to the formation of such hollow structures.

In ***Chapter 4***, the encapsulation of the nonvolatile substance in porous cellulose particles (beads) prepared by the SRM was carried out by dispersing the particles in the solution containing the substance and drying the dispersion. Regardless of whether the substance was hydrophilic or hydrophobic, the encapsulation efficiency exceeded 80%. The maximum loading reflected the saturated solubility of substance in solution that filled the cellulose beads. Moreover, the encapsulated solute was released by dispersing the cellulose beads in the solution, and the rate of release of the encapsulated solute could be controlled by coating the cellulose beads with a conventional polymer.

In ***Chapter 5***, The composite cellulose/Ag particles have successfully prepared by introducing carboxylate groups into the porous structures of cellulose particles, which are used as a scaffold for the synthesis of Ag nanoparticles (AgNPs). The catalytic ability of the cellulose/Ag particles for the reduction of 4-nitrophenol to 4-aminophenol was much higher than that of cellulose-free AgNPs. Furthermore, when AgNPs were immobilized on the cellulose/Ag particles via Ag–sulfur bonds, the obtained immobilized particles maintained their

catalytic performance during three cycles. The knowledge obtained in this study is readily available for the preparation of other metal nanoparticles on the cellulose particles and they can be to handled and recycled without complicated process.

In ***Chapter 6***, The composite cellulose/Ag particles have been successfully prepared by introducing amine groups into the porous structures of cellulose particles, which reduced Ag cations in the aqueous $AgNO_3$ solution and also worked as a linkage of cellulose and AgNPs. The amount of AgNPs could be controllable by changing the molar ratio of $AgNO_3$ and amine groups. The catalytic ability of the composite particles for the reduction of 4-NP to 4-AP increased with increase in the content of AgNPs; however, when the amount of AgNPs was much higher than that of amine groups, which were synthesized by the reduction at 10/1 ratio of $AgNO_3$ and amine groups, the catalytic efficiency decreased dramatically owing to the detachment of AgNPs from the cellulose particles. On the other hand, in use of the composite particles prepared by the reduction at the equal ratio to each other, the catalytic efficiency was maintained for at least three cycles without immobilizing treatment of AgNPs on the cellulose particles because of the amine groups as a linkage of cellulose particles and AgNPs. Moreover, the catalytic ability was comparable to the carboxylated cellulose particles with immobilization of AgNPs via Ag–sulfur bonds (in ***Chapter 5***). The knowledge obtained in this study is useful because they can be to handled and recycled without complicated process and immobilization step of metal nanoparticles. Therefore, resulting materials have a great potential for catalyst applications. Moreover, for more improvement of catalytic efficiency, the amine content working as a reducing agent and a linkage would be needed to increase by adjusting a preparation condition in the future.

In ***Chapter 7***, The aminated cellulose particles, prepared via the SRM using the ionic liquid followed by introduced with the primary amine groups (according to the ***Chapter 6***), could serve the template to prepare the cellulose/silica composite particles by in situ sol–gel reaction of tetraethoxysilane (TEOS) and by freeze-drying. The amine groups could work as a catalyst for the sol–gel reaction of TEOS and the obtained composites had the high specific surface area and the higher thermal stability than untreated cellulose particles, which were tunable by the sol–gel reaction time. This is first report to prepare these cellulose/silica composite particles and it is expected to form the foundation for the development of various cellulose composite particles.

The basic and important knowledge on morphology control and functionalization of cellulose particles should be mentioned in this dissertation. The research field on cellulose is recent hot topic but there is a lot of things we don’t understand about the behavior of cellulose at interfaces. It has a high expectation of the further development on this field by more work.

# Publication List

## Chapter 1

"Morphology Control of Porous Cellulose Particles by Tuning the Surface Tension of Media during Drying"

T. Omura, K. Imagawa, T. Suzuki, H. Minami

*Langmuir*, **34**, 15490 (2018)

## Chapter 2

"Preparation of Disk-like Cellulose Particles"

K. Imagawa, T. Omura, Y. Ihara, K. Kono, T. Suzuki, H. Minami

*Cellulose*, **24**, 3111 (2017)

## Chapter 3

"Preparation of Cellulose Particles Having Hollow Structure"

T. Omura, T. Suzuki, H. Minami

*Langmuir*, **in revision**

## Chapter 4

"Encapsulation of Either Hydrophilic or Hydrophobic Substances in Spongy Cellulose Particles"

T. Omura, K. Imagawa, K. Kono, T. Suzuki, H. Minami

*ACS Appl. Mater. Interfaces*, **9**, 944 (2017)

## Chapter 5

"Preparation of Cellulose/Silver Composite Particles Having Recyclable Catalytic Property"

Y. Fujii, K. Imagawa, T. Omura, T. Suzuki, H. Minami

*ACS Omega*, **revised**

## Chapter 6

"Preparation of Amine-Functionalized Cellulose Particles with Catalytic Activity"

Y. Fujii, T. Omura, T. Suzuki, H. Minami

*In preparation*

## Chapter 7

"Preparation of Cellulose/Silica Composite Particles by in Situ Sol-Gel Reaction"

T. Omura, Y. Fujii, T. Suzuki, H. Minami

*In preparation*

## Related Publications

"Fluorescent Spherical Sponge Cellulose Sensors for Highly Selective and Semi-quantitative Visual Analysis: Detection of $Hg^{2+}$ and $Cu^{2+}$ ions"

S. Yu, W. Li, Y. Fujii, T. Omura, H. Minami

*ACS Sustainable Chemistry & Engineering*, **7**, 19157 (2019)

"Ambient Temperature Waterborne Polymer/rGO Nanocomposite Films: Effect of rGO Distribution on Electrical Conductivity"

Y. Fadil, L. N. M. Dinh, M. Yap, R. Kuchel, Y. Yao, T. Omura, U. A.-Robles, N. Song, S. Huang, F. Jasinski, S. Thickett, H. Minami, V. Agarwal, P. B. Zetterlund

*ACS Appl. Mater. Interfaces*, **11**, 48450 (2019)

## Review

"Recent Trend on Synthesis of Functional Polymer Particles"

T. Omura, H. Minami

*KOBUNSHI (in Japanese)*, **68**(8), 422 (2019)

Doctor Thesis, Kobe University
“Preparation of Functional Cellulose Particles”, 157 pages
Submitted on January, 21th, 2020
The date of publication is printed in cover of repository version published in Kobe University Repository Kernel.